การดัดแปรมอดีไนต์ และการใช้เป็นตัวรองรับเหล็กเพื่อเร่งปฏิกิริยาการเติมหมู่ไฮดรอกซิลบนฟีนอล

นายสิทธิชัย กุลวงค์

MORDENITE MODIFICATION AND UTILIZATION AS

SUPPORTS FOR IRON IN CATALYTIC PHENOL

HYDROXYLATION

Sittichai Kulawong

A Thesis Submitted in Partial Fulfillment of the Requirements for the

Degree of Doctor of Philosophy in Chemistry

Suranaree University of Technology

Academic Year 2012

MORDENITE MODIFICATION AND UTILIZATION AS SUPPORTS FOR IRON IN CATALYTIC PHENOL HYDROXYLATION

Suranaree University of Technology has approved this thesis submitted in partial fulfillment of the requirements for the Degree of Doctor of Philosophy.

Thesis Examining Committee

_____
(Asst. Prof. Dr. Sanchai Prayoonpokarach)

Chairperson

_____
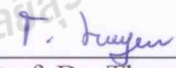(Assoc. Prof. Dr. Jatuporn Wittayakun)

Member (Thesis Advisor)

_____
(Asst. Prof. Dr. Kunwadee Rangsriwatananon)

Member

_____
(Asst. Prof. Dr. Thanaporn Manyum)

Member

_____
(Asst. Prof. Dr. Arthit Neramittagapong)

Member

_____   _____
(Prof. Dr. Sukit Limpijumnong)   (Assoc. Prof. Dr. Prapun Manyum)

Vice Rector for Academic Affairs   Dean of Institute of Science

สิทธิชัย กุลวงศ์ : การดัดแปรมอดีไนต์ และการใช้เป็นตัวรองรับเหล็กเพื่อเร่งปฏิกิริยาการเติม
หมู่ไฮดรอกซิลบนฟีนอล (MORDENITE MODIFICATION AND UTILIZATION AS
SUPPORTS FOR IRON IN CATALYTIC PHENOL HYDROXYLATION) อาจารย์ที่ปรึกษา :
รองศาสตราจารย์ ดร.จตุพร วิทยาคุณ, 114 หน้า.

วิทยานิพนธ์นี้มุ่งเน้น การดัดแปร ซีโอไลต์มอดีไนต์ (MOR) และการใช้เป็นตัวรองรับ ของเหล็ก
เพื่อเร่งปฏิกิริยาการเติมหมู่ไฮดรอกซิลบนฟีนอล การดัดแปร ทำให้มีเปลี่ยนแปลง อัตราส่วนโครง
ประกอบระหว่าง ซิลิคอน กับอะลูมิเนียม และสมบัติของรูพรุน เปลี่ยน ซึ่งจะ ส่งผลต่อการเร่งปฏิกิริยา ได้
วิทยานิพนธ์ นี้เริ่มต้นจาก การนำ ซิลิกาที่ได้จากแกลบข้าวมาสังเคราะห์ซีโอไลต์ มอดีไนต์ในรูป โซเดียม
(NaMOR) ด้วยวิธีไฮโดรเทอร์มัล และเปลี่ยนให้เป็นรูปโปรตอน (HMOR) จากนั้นดัดแปร ซีโอไลต์
NaMOR โดยการ กัดด้วยกรด (AMOR) ด้วยเบส (BMOR) และ ด้วยทั้งกรดและเบส (ABMOR) แล้ว
เปลี่ยนเป็นรูปโปรตอน นอกจากนี้ ยังได้ สังเคราะห์วัสดุคอมพอสิท ระหว่าง NaMOR และ MCM-41 โดย
ใช้ NaMOR เป็นแหล่งของซิลิกาและอลูมินา และใช้ ซีทิลไตรเมทิลแอมโมเนียมโบรไมด์ (CTAB) เป็น
สารอินทรีย์แม่แบบ จากนั้น ได้วิเคราะห์สมบัติทางกายภาพและเคมีของ ซีโอไลต์ทั้งหมด ที่สังเคราะห์และ
ดัดแปร ด้วยเทคนิคหลายชนิด ก่อนนำไป ใช้เป็นตัวรองรับเหล็ก ที่เตรียมด้วยวิธีการทำให้เอิบชุ่ม เพื่อเร่ง
ปฏิกิริยาการเติมหมู่ไฮดรอกซิลบนฟีนอล

จากการวิเคราะห์สมบัติทางกายภาพและเคมี ซีโอไลต์ที่ถูกดัดแปรยังรูปร่างของ MOR โดยมี
พื้นที่ผิวสูงกว่า NaMOR ต้นแบบและมีเพียง ABMOR เท่านั้น ที่แสดงให้เห็น การเปลี่ยนแปลงไอโซเทิร์ม
ของการดูดซับและการคายแก๊ส ไนโตรเจน อย่างมีนัยสำคัญ โดยเปลี่ยนจากชนิดที่หนึ่งไปเป็นชนิดที่สี่ ซึ่ง
เป็นลักษณะของวัสดุที่มีรูพรุน แบบมีโซพอร์ การมีลักษณะของรูพรุน แบบมีโซพอร์ ใน ABMOR ส่งผล
ให้มีสภาพ กรดเพิ่ม เพราะสารตั้งต้น เข้าถึง ตำแหน่งของการเร่งปฏิกิริยาดีขึ้น ในวัสดุคอมพอสิท ที่
ประกอบไปด้วย NaMOR และ MCM-41 พบว่าการเพิ่มพื้นที่ผิวและ ขนาดของรูพรุนขึ้นกับปริมาณของ
วัสดุ MCM-41 และพบว่าเหล็กในตัวเร่งปฏิกิริยาทุกตัวที่เตรียมอยู่ในรูป Fe_2O_3 เป็นหลัก

การเร่งปฏิกิริยาการเติมหมู่ไฮดรอกซิลบนฟีนอล เพื่อผลิตแคทีคอล (CE) และ ไฮโดรควิโนน
(HQ) ทดสอบที่อุณหภูมิ 70 °C โดยใช้น้ำเป็นตัวทำละลาย ใช้ไฮโดรเจนเปอร์ออกไซด์เป็น แหล่งอนุมูล
อิสระไฮดรอกซิล และใช้ฟีนอลต่อไฮโดรเจนเปอร์ออกไซด์ในอัตราส่วนโดยโมล 1:3 พบว่าการแปลงผัน
ของฟีนอลเร็วที่สุดและ สูงที่สุดเมื่อใช้ 5Fe/ABMOR เป็นตัวเร่งปฏิกิริยาให้ CE ต่อ HQ ในอัตราส่วนโดย
โมล 3:2 ซึ่งดีกว่าการเร่งปฏิกิริยา ของ 5Fe/NaMOR/MCM-41 ทั้งอัตราการ แปลงผันของฟีนอลและการ
คัดเลือกผลิตภัณฑ์ (อัตราส่วนโดยโมลของ CE:HQ = 1:1)

สาขาวิชาเคมี   ลายมือชื่อนักศึกษา_____
ปีการศึกษา 2555   ลายมือชื่ออาจารย์ที่ปรึกษา_____

SITTICHAI KULAWONG : MORDENITE MODIFICATION AND
UTILIZATION AS SUPPORTS FOR IRON IN CATALYTIC PHENOL
HYDROXYLATION. THESIS ADVISOR : ASSOC. PROF. JATUPRON
WITTAYAKUN, Ph.D. 114 PP.

MORDENITE MODIFICATION/MESOPOROUS ZEOLITE/IRON/PHENOL
HYDROXYLATION/RICE HUSK SILICA

This thesis focuses on modification of zeolite mordenite (MOR) and utilization as
supports for iron (Fe) catalysts in phenol hydroxylation. The modification changed the
framework Si/Al ratio and pore properties which could affect the catalyzed reaction. This
thesis began by utilization of silica from rice husk in the synthesis of mordenite in sodium
form (NaMOR) by hydrothermal method and transformed to proton form (HMOR). The
NaMOR was modified by leaching with acid (AMOR), base (BMOR), and acid-base
(ABMOR) before converting to proton form. In addition, a composite between NaMOR
and MCM-41 was synthesized by using parent NaMOR as a silica-alumina source and
cetyl trimethyl ammonium bromide (CTAB) as an organic template. Physicochemical
properties of all zeolites were analyzed by several methods before being used as supports
for Fe catalysts prepared by impregnation method for phenol hydroxylation.

From physicochemical characterization, the modified zeolite still exhibited MOR
phase with higher surface area than the parent NaMOR. Only the ABMOR sample showed
a significant change in nitrogen adsorption-desorption isotherm from type I to type IV, a
characteristic of mesoporous materials. The presence of mesopores in ABMOR could
therefore enhance acidity because the accessibility of reactants to active sites was
improved. In the NaMOR/MCM-41 composite zeolite, the increase in surface area and pore

size depended on the amount of MCM-41 materials. The major form of Fe in all catalysts was Fe_2O_3.

The catalytic phenol hydroxylation to produce catechol (CE) and hydroquinone (HQ) was tested at temperature of 70 °C using water as a solvent, H_2O_2 solution as a source for hydroxyl radical and the phenol:H_2O_2 mole ratio of 1:3. The fastest and highest phenol conversion was observed on 5Fe/ABMOR catalyst producing CE and HQ with mole ratio of CE and HQ equal to 3:2 showing the improvement in both rate conversion of phenol and selectivity of products compared to those on 5Fe/NaMOR/MCM-41 catalyst (CE:HQ = 1:1).

School of Chemistry   Student's Signature_____

Academic Year 2012   Advisor's Signature_____

ACKNOWLEDGEMENTS

Sittichai Kulawong

CONTENTS

Page

CONTENTS (Continued)

CONTENTS (Continued)

CONTENTS (Continued)

CONTENTS (Continued)

LIST OF FIGURES

LIST OF FIGURES (Continued)

LIST OF FIGURES (Continued)

LIST OF TABLES

LIST OF SCHEMES

CHAPTER I

INTRODUCTION

1.1 Aim of thesis

The aim of this thesis was to use rice husk silica (RHS) as a silica source for the synthesis of mordenite in sodium form (NaMOR). The zeolite was further modified by treatment with acid (AMOR), base (BMOR) and acid-base (ABMOR). In another synthesis, a NaMOR/MCM-41 composite was synthesized by using NaMOR as a silica-alumina source and cetyl trimethyl ammonium bromide (CTAB) as an organic template. The parent NaMOR, modified MOR and NaMOR/MCM-41 composite were characterized by using x-ray diffraction (XRD) to confirm MOR structure; nitrogen (N_2) adsorption-desorption to study the textural properties; transmission electron microscopy (TEM) to study the morphology; temperature programmed desorption of ammonia (NH_3-TPD) to determine the acid sites; ^{27}Al magic angle spinning nuclear magnetic resonance (^{27}Al MAS NMR) to investigate coordination state of Al in framework; and the conversion of methylbutynol or 2-methyl-3-butyn-2-ol (MBOH) as a probe reaction to study acidic, basic and amphoteric pathways on the surface of each zeolite sample. All of the zeolite samples were impregnated with iron (Fe) and characterized by XRD, TEM and x-ray absorption near edge structure (XANES) to understand the influence of metal forms and support types on the catalytic activity. Finally, all the supported Fe catalysts were tested for phenol hydroxylation in a batch-type setup.

1.2 Background of phenol hydroxylation

Phenol hydroxylation is an oxidation of phenol by hydrogen peroxide (H_2O_2) to produce catechol and hydroquinone (Scheme 1.1). Both products are widely used in industry, with their consumption in 2002 accounting in total for 77,000 tonnes/year worldwide (catechol 30,000 tonnes/year and hydroquinone 47,000 tonnes/year) (Bellussi and Perego, 2008).
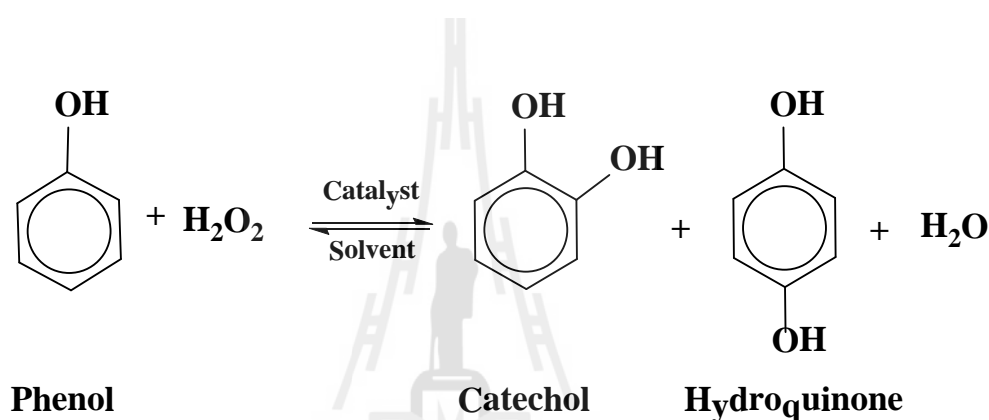
Scheme 1.1 Phenol hydroxylation.

Direct hydroxylation can be accomplished by free radical reagents, such as a mixture of H_2O_2 with a transition metal catalyst (Ti, Cu, Fe, Zr and V in various forms of oxides) and a redox buffer [i.e. Fe^{2+} + H_2O_2 (Fenton's reagent), Fe^{3+} + H_2O_2 + catechol (Hamilton's reagent)]. However, yields are usually poor, in the range of 5 - 20%, and there are significant amounts of coupling products (Rappoport, 2003). To increase catalytic performance, heterogeneous catalysts for phenol hydroxylation have been developed.

Among transition metals Fe has been most widely investigated for phenol hydroxylation. When supported on various zeolites including ZSM-5, NaY and MOR, the phenol conversions were less than 40% and only Fe/MOR gave 100% catechol selectivity (Preethi et al., 2008). This information inferred that the shape and size of pores of the supports had influences on product selectivity.

When Fe catalysts were supported on mesoporous materials such as MCM-41, Al-MCM-41 and MCM-48, the conversions were higher than those on zeolites mentioned above (Choi et al., 2006; Preethi et al., 2008; Zhao et al., 2001). The mesoporous materials may facilitate the diffusion of the reactants and products. The conversion of phenol hydroxylation on the Fe catalysts can be improved by using mesoporous supports and the selectivity can be improved by using MOR. In this thesis, Fe supported on MOR with mesopores was proposed to improve both conversion and selectivity.

1.3 Background of MOR

Mordenite (MOR) is a high silica zeolite with interconnected pore channels between 12-membered ring (6.7×7.0 Å) and 8-membered ring (3.4×4.8 Å). The framework structure of MOR represented linked SiO_4/AlO_4 tetrahedral is shown in Figure 1.1. Typical composition of unit cell is $Na_8[(AlO_2)_8(SiO_2)_{40}] \cdot 24H_2O$ and the SiO_2/Al_2O_3 ratio can be varied in the range of 9 - 35 depending on composition of the synthetic batch (Roland and Kleinschmit, 2003). Due to its high thermal and acid stability, the MOR has been used as a catalyst in various industrial processes including isomerization, cracking, alkylation, and oxidation (Viswanadham and Kumar, 2006; Katada et al., 2004; Groen et al., 2004; Preethi et al., 2008).
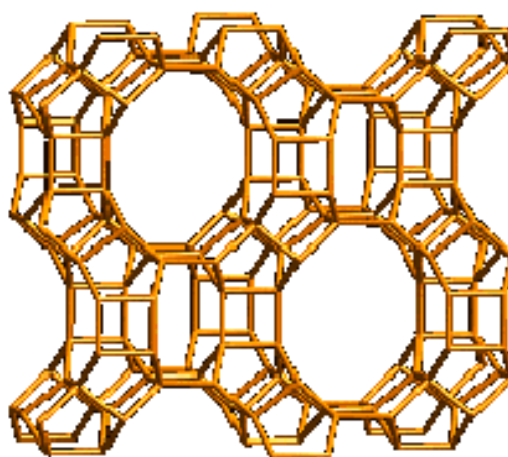
Figure 1.1 Framework structure of MOR represented linked SiO_4/AlO_4 tetrahedral.

1.4 Modification of zeolites

In general, the catalytic reactivity of zeolites of based on acid sites provided by hydroxyl groups (Brönsted acid site) and aluminum (Al) atoms in the framework (Lewis acid sites). Moreover, the uniform microporous framework structure plays an important role in terms of the shape selectivity. The small pore size restricts physical transport (diffusion) of molecules to and from active sites located in the micropores. Typical consequences of diffusion limitations are lower catalytic activities of catalyst and deactivation of carbonaceous deposition (coking). To improve the diffusion, the zeolite could be modified to cooperate pore size in mesoporous range (2-50 nm). The mesoporous materials generally provide satisfactory results for the catalytic conversion of bulky reactants. However, their low hydrothermal stability compared to microporous materials could hinder their applications. The relatively low catalytic activity and hydrothermal stability can be attributed to the amorphous nature of the mesoporous walls. Thus, the development of more open structures by creating additional porosity by combining micro- and mesopores, could lead to significant improvement in diffusional properties.

There are several strategies available for the preparation of materials with both micropores and mesopores. Three methods were used in this thesis. The details are as follows.

1.4.1 Generation of mesopores in zeolite by dealumination

Dealumination is removal of Al atoms in the zeolite framework without destroying the micropore structure. Dealumination can be achieved by acid leaching, steam treatment, or the use of complexing agents. These methods have been applied to alter the acidic or hydrothermal property of zeolites. Upon the removal of Al from the zeolite framework, mesoporosity could be generated at some extent depending on the amount of Al extracted away. At the same time, Lewis acidity was also created because the occurrence of extra framework Al. This method is practical for the zeolites with high

content of Al in the framework (low Si/Al ratio). However, for the zeolite with high content of Si (high Si/Al ratio), the formation of mesoporosity is relatively limited and the acidity were weakened. The dealumination has been successfully applied to create mesoporosity for the Al-rich zeolites Y (USY) and MOR (Datka et al., 1993; Segawa and Shimura, 2000).

1.4.2 Generation of mesopores in zeolite by desilication

Desilication is removal of Si atoms in the zeolite framework by alkaline treatment to generate mesoporosity. Because most of the zeolite frameworks contain a higher concentration of Si than Al, it is easy to achieve the formation of extra pores. In contrast to dealumination, the Si extraction has an impact to a smaller extent on the acidic properties. However, due to its novelty, only a few studies have been carried out on a well known high silica zeolites, namely, ZSM-5 (Ogura et al., 2000; Groen et al., 2004). Under optimum treatment conditions, mesopores with different volume were successfully created while the microporous structure of ZSM-5 was also preserved. Moreover, the acidity of ZSM-5 was not altered because the Al could be kept from extraction by using this method.

1.4.3 Synthesis of composite molecular sieves comprising of zeolite and mesopore materials

Composites containing both micropores in zeolite domains and mesopores in matrix are also interesting because they retain the zeolite properties including acidity and hydrothermal stability at high temperature and contain the mesopores that facilitate diffusion of large molecules. Wang et al. (2005) reported a new preparation method for composite between MOR and MCM-41 zeolite by using MOR as a silica-alumina source. The synthesis procedure involved the treatment of MOR with sodium hydroxide and a solution of hexadecyltrimethylammonium bromide (CTAB). After adjusting pH of the reaction mixture by addition of aqueous HCl, the mixture was hydrothermally treated at 100 °C for 24 h. The analysis results by N_2 adsorption-desorption isotherms showed that

the composite possessed a stepwise distributed pore structure. Compared with a corresponding mechanical mixture, the composite showed a higher catalytic activity. It was attributed to the existence of secondary building units characteristic of zeolite MOR in the composite mesopore walls which gave rise to the improved hydrothermal stability and acidity of the composite. This new synthesis method of the micro/mesoporous composite products might be useful for preparing various types of mesoporous molecular sieves with pore walls characteristic of zeolites.

1.5 Scope and limitations of the study

The RHS was prepared by a method from literature (Khemtong et al., 2007) and was used as a silica source for the synthesis of NaMOR. The NaMOR/MCM41 composite was prepared by using parent NaMOR as a silica-alumina source and CTAB as an organic template with a method from literature (Wang et al., 2005). Catalysts containing Fe was prepared by incipient wetness impregnation. The reaction was tested over all catalysts by fixing molar ratio between phenol and H_2O_2 to 1:3 and temperature of 70 °C. Products from phenol hydroxylation were determined by a gas chromatograph (Shimadzu 14A series) equipped with an ID-BP1 coated capillary column and a flame ionization detector.

1.6 References

Bellussi, G. and Perego, C. (2008). Phenol hydroxylation and related oxidations. Ertl, G., Knözinger, H., Schüth, F. and Weitkamp, J. (eds.). **Handbook of heterogeneous catalysis** (vol. 7). (2nd ed., pp. 3538-3539). Wiley-VCH Verlag GmbH, Weinheim.

Choi, J. S., Yoon, S. S., Jang, S. H. and Ahn, W. S. (2006). Phenol hydroxylation using Fe-MCM-41. **Catalysis Today**. 280: 111-287.

Datka, J., Kolidziejski, W., Klinowski, J. and Sulikowski., B. (1993). Dealumination of zeolite Y by H_4EDTA. **Catalysis Letters**. 19: 159-165.

Groen, J. C., Peffer, L. A. A., Moulijn, J. A. and Perez-Ramirez, J. (2004). Optimal aluminum-assisted mesoporosity development in MFI zeolites by desilication. **Colloids and Surfaces A: Physicochemical and Engineering Aspects**. 241 : 53-58.

Khemtong, P., Prayoonpokarach, S. and Wittayakun, J. (2007). Synthesis and characterization of zeolite LSX from rice husk silica. **Suranaree Journal of Science and Technology**. 14: 367-379.

Katada, N., Kanai, T. and Niwa, M. (2004). Dealumination of proton form mordenite with high aluminum content in atmosphere. **Microporous and Mesoporous Materials**. 75: 61-67.

Ogura, M., Shinomiya, S., Tateno, J., Nara, Y, Kikuchi, E. and Matsukata, M. (2000). Formation of uniform mesopores in ZSM-5 zeolite through treatment in alkaline solution. **Chemistry Letters**. 29: 882-883.

Preethi, M. E. L., Revathi, S., Sivakumar, T., Manikandan, D., Divakar, D., Rupa, A. V. and Palanichami, M. (2008). Phenol hydroxylation using Fe/Al-MCM-41. **Catalysis Letters**. 120: 56-64.

Rappoport, Z. (ed.). (2003). **The chemistry of phenols**. England: John Wiley & Sons.

Roland, E. and Kleinschmit, P. (2003). Zeolites. Bohnet, M., et al. (eds.). **Ullmann's encyclopedia of industrial chemistry** (vol. 39). (6th ed., pp. 625-655). Wiley-VCH Verlag GmbH, Weinheim.

Segawa, K. and Shimura, T. (2000). Effect of dealumination of mordenite by acid leaching for selective synthesis of ethylenediamine from ethanolamine. **Applied Catalysis A: General**. 194: 309-317.

Viswanadham, N. and Kumar, M. (2006). Effect of dealumination severity on the pore size distribution of mordenite. **Microporous and Mesoporous Materials**. 92: 31-37.

Wang, S., Dou, T., Li, Y., Zhang, Y., Li, X. and Yan, Z. (2005). A novel method for the preparation of MOR/MCM-41 composite molecular sieve. **Catalysis Communications**. 6: 87-91.

Zhao, W., Luo, Y., Deng, P. and Li, Q. (2001). Synthesis of Fe-MCM-48 and its catalytic performance in phenol hydroxylation. **Catalysis Letters**. 73: 199-202.

CHAPTER II

LITERATURE REVIEW

Phenol hydroxylation is an oxidation reaction between phenol and hydrogen peroxide (H_2O_2). The products are catechol (CE) and hydroquinone (HQ). The factors affecting efficiency and selectivity of reaction pathways depend on an oxidant, catalyst preparation, and solvent. In this thesis, effects of various reaction parameters will be mentioned in this chapter.

2.1 Choices of oxidant

Table 2.1 Potential oxygen donating species for selective hydrocarbon oxidations [a].

Potential oxidant	Active oxygen (Molecular weight %)	Phase	By-product of oxidation
Hydrogen peroxide, H_2O_2	47.0	Liquid	H_2O
Nitrous oxide, N_2O	36.4	Gas	N_2
Sodium chlorite, $NaClO_2$	35.6	Liquid	NaCl
Ozone, O_3	33.3	Gas	O_2
Nitric acid, HNO_3	25.4	Liquid	HNO_2
Sodium hypochlorite, NaClO	21.6	Liquid	NaCl
tert-Butylhydroperoxide, TBHP	17.8	Liquid	t-BuOH
Sodium bromate, $NaBrO_3$	13.4	Liquid	NaBr

[a] Reviewed by Burton, 2006.

The oxidant is important in mechanism of hydroxylation. Compared to other oxidants (Table 2.1), the H_2O_2 is a suitable source of oxygen for the hydroxylation because it has the highest available active oxygen content per molecular weight and it can be mixed with water in any proportion, thus making dilution to different concentrations uncomplicated. Moreover, H_2O_2 is an environmentally friendly oxidant because the only by-product from the reaction is water and any residual H_2O_2 is decomposed by UV light. In this thesis, the H_2O_2 was therefore used as an oxidizing reagent in the phenol hydroxylation reaction.

2.2 Catalyst preparation for phenol hydroxylation

Oxide of transition metal such as iron (Fe), copper (Cu), and cobalt (Co) on various support materials have been tested (Villa et al., 2005; Park et al., 2006; Preethi et al., 2008) and Fe has been most widely investigated (Table 2.2).

Park et al. (2006) prepared Co- and Fe-NaY catalysts by ion-exchange method. Their catalytic performances for the phenol hydroxylation were evaluated between 30 and 90 °C. The optimum temperature was found to be 70 ℃. The Fe-NaY catalyst exhibited catalytic activity in phenol hydroxylation using H_2O_2 as an oxidant, giving phenol conversion of 19.7% at 70 °C (phenol:H2O2 = 3:1, in water).

Villa et al. (2005) also prepared Cu- and Fe-ZSM-5 catalysts by hydrothermal synthesis. The Cu- and Fe-ZSM-5 catalysts were characterized by XRD, BET, FT-IR and UV-vis techniques. The Fe-ZSM-5 catalyst showed higher activity than Cu-ZSM-5 catalyst, giving phenol conversion of 32.9% at 80 °C (phenol:H_2O_2 = 3:1, in water).

Preethi et al. (2008) prepared 10Fe/MOR and 10Fe/Al-MCM-41 catalysts by impregnation method at 80 °C without stirring. The catalysts were characterized by XRD, N_2 adsorption-desorption, FT-IR, and UV-Vis techniques. The Fe supported on Al-MCM-41 (Fe/Al-MCM-41) was influenced by the support Si/Al ratio. At the lower ratio, the reaction rates were faster. The ratio between CE and HQ was about 1:2 at low Si/Al ratios

and about 1:1 at high Si/Al ratios. Fe supported on MOR zeollite (Fe/MOR) was reported to give 100% CE selectivity but the phenol conversion was only 21.0%.

Table 2.2 Transition metal oxides on various support materials for phenol hydroxylation.

Catalysts	Temperature, solvent and time	Phenol:H_2O_2 and catalyst amount	% Conversion of Phenol	% Selectivity				Reference
				CE	HQ	BQ	BPs	
2Fe/NaY	70 °C, water, 4 h	3:1, 2 g	19.7	39.5	16.9	17.0	26.6	Park et al., 2006
Fe/ZSM-5	80 °C, water, 4 h	3:1, 0.2 g	32.9	60.5	39.5	0.0	0.0	Villa et al., 2005
10Fe/MOR	40 °C, water, 4 h	1:3, 0.1 g	21.0	100.0	0.0	0.0	0.0	
10Fe/Al-MCM-41 (25)	40 °C, water, 4 h	1:3, 0.1 g	58.5	39.0	61.0	0.0	0.0	
10Fe/Al-MCM-41 (50)	40 °C, water, 4 h	1:3, 0.1 g	55.3	39.6	60.4	0.0	0.0	Preethi et al., 2008
10Fe/Al-MCM-41 (75)	40 °C, water, 4 h	1:3, 0.1 g	50.5	41.7	58.3	0.0	0.0	
10Fe/Al-MCM-41 (100)	40 °C, water, 4 h	1:3, 0.1 g	41.9	45.3	54.7	0.0	0.0	
4Fe/MCM-41	50 °C, water, 1 h	1:1, 0.03 g	60.0	68.0	32.0	0.0	0.0	Choi et al., 2006
0.153 Fe/MCM-48	60 °C, water, 4 h	1:1, 0.01 g	43.6	73.3	24.4	0.0	2.3	Zhao et al., 2001

CE : Catechol, HQ: Hydroquinone, BQ: Benzoquinone and BPs: By products.

Choi et al. (2006) prepared Fe-MCM-41 catalysts by hydrothermal synthesis and 0.5-4 Fe/Si mol% was loaded in a batch mixture. The Fe-MCM-41catalysts were characterized by XRD, SEM/TEM, EDS, N_2-sorption, and FT-IR and UV-vis techniques. The Fe-MCM-41 catalyst exhibited high catalytic activity in phenol hydroxylation using H_2O_2 as an oxidant, giving phenol conversion of 60.0% at 50 °C (phenol:H_2O_2 = 1:1, in water).

Zhao et al. (2001) prepared Fe-MCM-48 catalysts by similar method as Choi et al. (2006) and loading of Fe_2O_3/SiO_2 was 0.002 - 0.003 mol%. The Fe-MCM-48 catalysts were characterized by XRD, ^{29}Si-MAS NMR, ESR, and UV-Vis techniques. The Fe-MCM-48 catalyst exhibited catalytic activity in phenol hydroxylation using H_2O_2 as an oxidant, giving phenol conversion of 43.6% at 60 °C (phenol:H_2O_2 = 1:1, in water).

2.3 Solvent for phenol hydroxylation

The oxidation of phenol by H_2O_2 is a widely applied process in the chemical industry for the preparation of the dihydroxylated derivatives. The distribution of the dihydroxylated derivative products is affected by the nature of the solvent. The effect of various solvents on product selectivity is summarized in Table 2.3.

Table 2.3 The influence of solvent for phenol hydroxylation reaction.

Catalysts, phenol:H_2O_2, time, and temperature	Solvent	% Conversion of Phenol	%Selectivity				Reference
			CE	HQ	BQ	BPs	
Mn(IV)Mo, 1:1, 5 h, 70 °C	Acetone	2.6	0.0	2.6	0.0	-	Lin et al., 2000
	Dioxane	18.2	0.0	16.2	2.0	-	
	Methanol	45.0	0.0	38.6	2.1	-	
	Water	0.8	0.0	0.8	0.0	-	
V/FeAlPM (pillared montmorillonites), 1:5, 45 min, 80 °C	Acetone	5.5	69.0	31.1	-	-	Kurian and Sugunan, 2006
	Dioxan	4.9	36.3	63.7	-	-	
	Isopropanol	3.4	36.7	63.3	-	-	
	Water	77.2	64.1	35.9	-	-	
MFS-1.5 (mesoporous ferrosilicates), 1:1, 3 h, 50 °C	Acetone	0.0	0.0	0.0	-	-	Xin et al., 2008
	Acetonitrile	0.0	0.0	0.0	-	-	
	Ethanol	0.7	0.0	0.0	-	-	
	Water	56.0	69.0 (CE+HQ)		-	-	

2.4 Proposed mechanisms

Several reports have proposed hydroxylation mechanisms for phenol hydroxylation with H_2O_2 solution over homogeneous and heterogeneous catalysts. Thus, phenol hydroxylation mechanism over Fe supported MOR can be referred to those mechanisms.

2.4.1 Phenol hydroxylation with H_2O_2: Homogeneous catalysts

The oldest system used for the hydroxylation of phenol is known as the Fenton reaction, in which the catalyst is a soluble Co, Cu, and Fe salt. This reaction occurs via a

free-radical chain mechanism rather than an electrophilic mechanism, and it is therefore very fast.

In Fenton's reagent, the radical initiator is Fe^{2+} (a).

$$Fe^{2+} + H_2O_2 \longrightarrow Fe^{3+} + \cdot OH + OH^- \quad \text{.......................... (a)}$$
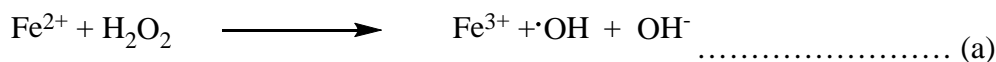
Phenol hydroxylation occurs via the steps shown in Scheme 2.1, with ferrous ions being consumed via the reaction (b) which breaks the redox chain. The catalyst used is a mixture of Fe^{3+} and Co^{2+} salts at a concentration level of a few parts per million.

$$Fe^{2+} + \cdot OH \longrightarrow Fe^{3+} + OH^- \quad \text{.......................... (b)}$$
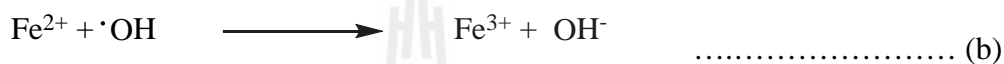
Initially, ferrocene was claimed to have good catalytic properties for this reaction, and the reaction was performed batchwise at 40 °C using 60 wt% aqueous H_2O_2. The main disadvantages were the low hydrogen peroxide selectivity, the formation of large quantities of tars, and most importantly the creation of only a small amount of resorcinol. Moreover, particular care had to be taken in order to prevent the accumulation of hydrogen peroxide. Consequently, CE and HQ were produced in ratio ranging from 2 to 2.3 (Bellussi and Perego, 2008).
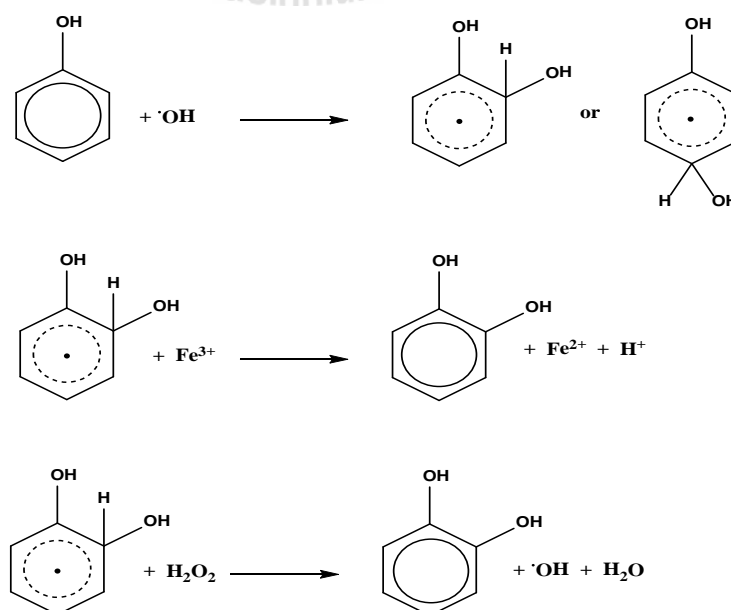
Scheme 2.1 Phenol hydroxylation via the Fenton's reagent.

2.4.2 Phenol hydroxylation with H_2O_2: Heterogeneous catalysts

As reported previously, one disadvantage of phenol hydroxylation using homogeneous catalyst is that the ortho/para-ratio exceeds 1.5. In an attempt to improve the existing technologies and to overcome this problem, several groups have used zeolite-based catalysts, taking advantage of their shape selectivity to favor the production of hydroquinone.

A mechanism for phenol hydroxylation with H_2O_2 solution over Fe/MCM-41 was proposed by Choi et al. (2006) as shown in Scheme 2.2. The Fe^{3+} sites reacted with H_2O_2 to form hydroxyl radicals which reacted with phenol to form CE and HQ.
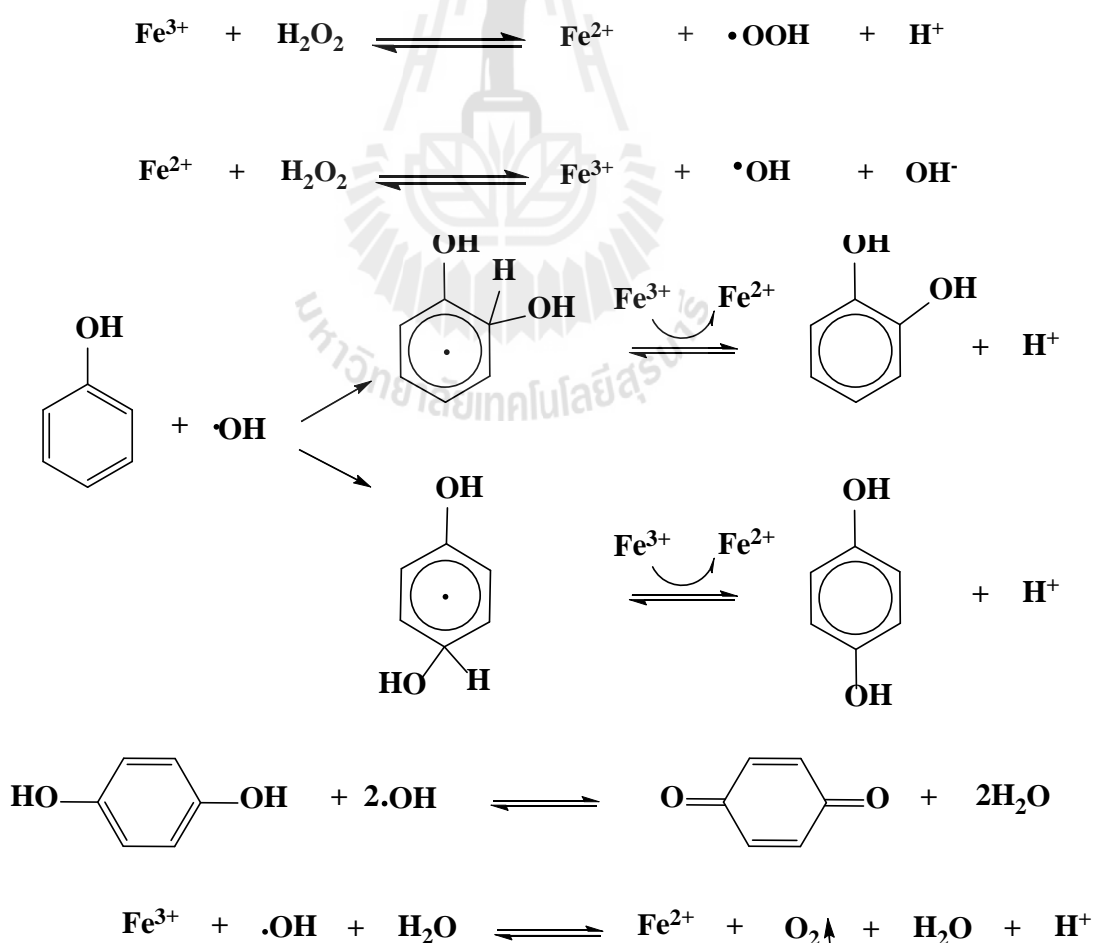
Scheme 2.2 Phenol hydroxylation pathway using Fe/MCM-41 (Choi et al., 2006).

Burton, (2006) proposed a mechanism for the formation of HQ in the hydroxylation of phenol via Ti-OOH active site coordinated to water or methanol molecues as shown in Scheme 2.3.
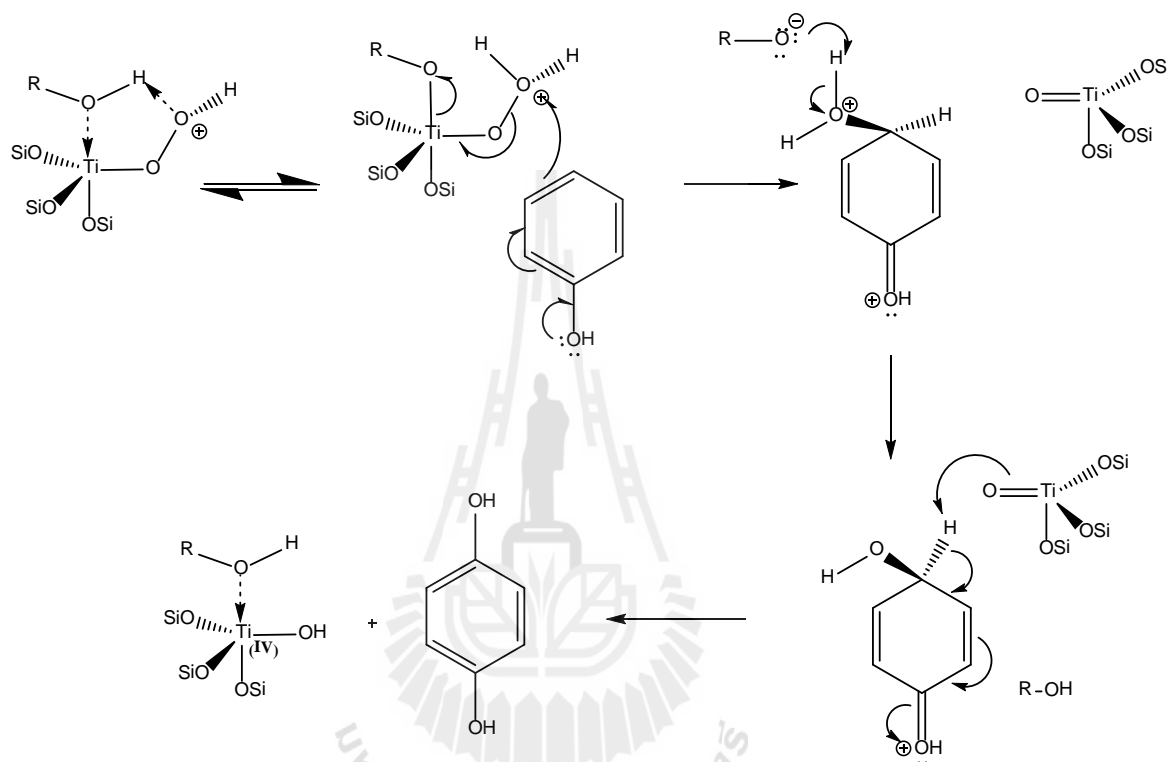
Scheme 2.3 Proposed reaction mechanism for the formation of HQ via methanol coordination to the Ti-OOH active site (R=H/CH$_3$).

2.5 References

Bellussi, G. and Perego, C. (2008). Phenol hydroxylation and related oxidations. Ertl, G., Knözinger, H., Schüth, F. and Weitkamp, J. (eds.). **Handbook of heterogeneous catalysis** (vol. 7). (2nd ed., pp. 3541-3542). Wiley-VCH Verlag GmbH, Weinheim.

Burton, R. M. (2006). **Oxidant concentration effects in the hydroxylation of phenol over titanium-based zeolites Al-free Ti-Beta and TS-1**. Ph. D Thesis, University of Stellenbosch, South Africa.

Choi, J. S., Yoon, S. S., Jang, S. H. and Ahn, W. S. (2006). Phenol hydroxylation using Fe-MCM-41. **Catalysis Today**. 280: 111-287.

Kurian, M. and Sugunan, S. (2006). Wet peroxide oxidation of phenol over mixed pillared montmorillonites. **Chemical Engineering Journal**. 115: 139-146.

Lin, S., Zhen, Y., Wang, S.-M. and Dai, Y. -M. (2000). Catalytic activity of $K_{0.5}(NH_4)_{5.5}[MnMo_9O_{32}]\cdot6H_2O$ in phenol hydroxylation with hydrogen peroxide. **Journal of Molecular Catalysis A: Chemical**. 156: 113-120.

Park, J. N., Wang, J., Choi, K. Y., Dong, W. Y., Hong, S. I., and Lee, C. W., (2006). Hydroxylation of phenol with H_2O_2 over Fe^{2+} and/or Co^{2+} ion-exchanged NaY catalyst in the fixed-bed flow reactor. **Journal of Molecular Catalysis A: Chemical**. 247: 73-79.

Preethi, M. E. L., Revathi, S., Sivakumar, T., Manikandan, D., Divakar, D., Rupa, A. V., and Palanichami, M. (2008). Phenol hydroxylation using Fe/Al-MCM-41. **Catalysis Letters**. 120: 56-64.

Villa, A. L., Caro, C. A. and de Correa, C. M. (2005). Cu- and Fe-ZSM-5 as Catalysts for phenol hydroxylation. **Journal of Molecular Catalysis A: Chemical**. 228: 233-240.

Xin, H., Liu, J., Fan, F., Feng, Z., Jia, G., Yang, Q., and Li, C. (2008). Mesoporous ferrosilicates ith high content of isolated iron species synthesized in mild buffer solution and their catalytic application. **Microporous and Mesoporous Materials**. 113: 231-239.

Zhao, W., Luo, Y., Deng, P. and Li, Q. (2001). Synthesis of Fe-MCM-48 and its catalytic performance in phenol hydroxylation. **Catalysis Letters**. 73: 199-202.

CHAPTER III

MORDENITE MODIFICATION AND UTILIZATION AS SUPPORTS FOR IRON CATALYST IN PHENOL HYDROXYLATION

Abstract

The goal of this work was to synthesize mordenite in sodium form (NaMOR) using rice husk silica; modify by treatment with acid, base or both; and use the obtained zeolites as supports for iron (Fe) catalysts for phenol hydroxylation. All MOR zeolites were characterized by x-ray diffraction (XRD) and nitrogen adsorption/desorption techniques and the Si/Al ratios were determined by inductively coupled plasma-mass spectrometry (ICP-MS). The influence of zeolite modification to the phenol hydroxylation was also studied. All modified zeolites still exhibited MOR phase with higher surface area than that of the parent NaMOR. Only the sample treated by acid and base (ABMOR) showed a significant change in adsorption-desorption isotherm from type I to type IV, a characteristic of mesoporous materials. The major forms of Fe (5 wt%) in all catalysts confirmed by XRD and x-ray absorption near edge structure (XANES) were Fe_2O_3. Because mesopores were generated in ABMOR to facilitate diffusion of reactants, the fastest reaction was obtained on Fe/ABMOR catalyst. The conversion was also highest on this catalyst probably because Fe was dispersed on the support with the highest surface area. However, the presence of mesopores did not improve the selectivity and the products observed were catechol and hydroquinone.

3.1 Introduction

Phenol hydroxylation is an oxidation of phenol (C_6H_5OH) by hydrogen peroxide (H_2O_2) to produce two benzenediols ($C_6H_4(OH)_2$) including catechol (IUPAC name: benzene-1,2-diol) and hydroquinone (IUPAC name: benzene-1,4-diol). The products are used in several applications as photographic chemicals, antioxidants, polymerization inhibitors, and others (Brook et al., 1982). They can be produced in industrial scales by using homogeneous acid catalysts at 40-90 °C (Knözinger and Kochloefl, 2003). However, the homogeneous catalysts are difficult to separate from the reaction mixture making their recovery and recycling almost impossible (Jeong et al., 2005).

To simplify the separation, several researchers have tried to develop heterogeneous catalysts for phenol hydroxylation. Oxides transition metals such as iron (Fe), copper (Cu) and cobalt (Co) on various support materials have been tested (Villa et al., 2005; Park et al., 2006; Preethi et al., 2008) and Fe has been most widely investigated. When supported on various zeolites including ZSM-5, NaY, and MOR, the phenol conversions were less than 40% in all Fe catalysts and only Fe/MOR gave 100% catechol selectivity (Preethi et al., 2008). This information inferred that the shape and size of pores of the supports had influences on product selectivity.

When Fe catalysts were supported on mesoporous materials such as MCM-41, Al-MCM-41 and MCM-48, the conversions were higher than those on zeolites mentioned above (Choi et al., 2006; Preethi et al., 2008; Zhao et al., 2001). Fe/MCM-41 was more active than Fe/MCM-48 at similar phenol/H_2O_2 ratio (1:1) using lower temperature and shorter reaction time. This information also indicated an influence from the pore dimension of mesoporous supports. The product selectivity in the reaction catalyzed by Fe/MCM-41 could be changed by changing the reaction conditions and support acidity (Choi et al., 2006; Preethi et al., 2008). Chumee et al. (2009) reported that catalysts supported on RH-MCM-41 provided a faster conversion than that supported on rice husk silica. The

mesoporous structure of MCM-41 may facilitate the diffusion of the reactants and products. Because the conversion of phenol hydroxylation on the Fe catalysts can be improved by using mesoporous supports and the selectivity can be improved by using MOR, we proposed that Fe supported on MOR with mesopores could improve both conversion and selectivity.

MOR, one of the high silica zeolites has two channel sizes (6.7 × 7.0 Å and 2.6 × 5.7 Å) (Meier and Kristallogr, 1961). Because it has the well-defined sizes of channels and cavities without interconnectivity, MOR has been explored as a catalyst and used as an adsorbent of saturated and unsaturated hydrocarbons (Pantu et al., 2007). In this work we synthesized MOR by using silica from rice husk and the resulting zeolite was modified to generate mesoporous structure by the methods from literatures (Viswanadham et al., 2006; Groen et al., 2004; Li et al., 2009). Acid treatment of the MOR by nitric acid removes aluminium atoms (dealumination) in the framework which are Lewis acid sites, and increases surface area and micropore volume (Li et al., 2009). Treatment of MOR with sodium hydroxide (NaOH) removes silicon atoms (desilication), opens up the structure and generates mesoporous structure (Li et al., 2009). Li et al. (2009) also produced mesoporous MOR by acid and base treatment.

This thesis involves the synthesis of MOR using rice husk silica and its modification by treatment with acid, base or both. The parent and modified MOR were characterized by x-ray diffraction (XRD) and nitrogen adsorption-desorption analysis to confirm the MOR structure and mesoporosity, respectively before utilization as supports for Fe catalysts. All the catalysts were characterized by XRD and x-ray absorption near edge structure (XANES) spectroscopy to determine the form of Fe before testing for phenol hydroxylation.

3.2 Experimental

3.2.1 Preparation and characterization of MOR supports

Rice husk silica was prepared by refluxing rice husk with HCl and calcination as described in the literature (Khemtong et al., 2007). The MOR in sodium form (NaMOR) was synthesized with a procedure similar to that in the literature (Kim and Ahn, 1991) by mixing a solution of rice husk silica in sodium hydroxide (Carlo Erba, 97%) and a solution of sodium aluminate (Riedel-de Haën®, 40-45% Na_2O, 50-60% Al_2O_3). An original gel with a molar composition of $2.5Na_2O : Al_2O_3 : 22SiO_2 : 518H_2O$ was prepared in a polypropylene bottle and kept understirring for 1 day to ensure the dissolution. Then the gel was transferred to a teflon-lined autoclave with 150 mL capacity for crystallization under autogeneous pressure at 170 °C without agitation. The crystallization time was varied from 24 to 96 h and only the condition producing NaMOR with the highest crystallinity was used for further synthesis.

The further synthesis was carried out using the autoclave with a volume of 250 mL. The product was separated by filtration, washed thoroughly with deionized water, dried at 80 °C overnight, and calcined in a muffle furnace at 500 °C for 3 h. The NaMOR was ion-exchanged with a 1.0 M NH_4NO_3 (Fluka, 99%) solution at 80 °C and calcined in air at 500 °C for 3 h to convert to proton form (HMOR).

The methods for modification of HMOR by acid and base treatment were modified from the literature (Li et al., 2009). In the base treatment (desilication), the NaMOR was refluxed with 0.2 M NaOH at 65 °C for 30 min, filtered, and washed with deionized water. The product was converted to proton form by ion-exchanged by the method mentioned above and referred to as BMOR. In the acid treatment (dealumination), the HMOR was refluxed with 2.0 M HNO_3 (Carlo Erba, 65%) at 100 °C for 4 h, washed with deionized water, dried at 80 °C for 10 h and calcined at 500 °C for 3 h. This product was referred to as AMOR. Finally, the AMOR was refluxed again with 0.2 M NaOH at 65

°C for 30 min, filtered, washed with deionized water, and ion-exchanged with the 1.0 M

NH_4NO_3 solution to convert to proton form. After calcination this acid-base treated sample

was referred to as ABMOR.

The parent NaMOR and all modified MOR were characterized by XRD (Bruker

AXS diffractometer D5005) using Cu Kα radiation to confirm the MOR structure. Their

surface area, pore volumes and pore sizes were determined by nitrogen adsorption-

desorption analysis (Micromeritics ASAP 2010). Each sample was degassed at 300 °C

before the measurement. The bulk Si/Al ratios of the dealuminated MOR were determined

by inductively coupled plasma-mass spectrometry (ICP-MS) on a Agilent 7500CE series

instrument.

3.2.2 Preparation and characterization of supported Fe catalysts

Supported catalysts with 5 wt.% Fe loading were prepared by incipient wetness

impregnation with a solution of $Fe(NO_3)_3 \cdot 9H_2O$ (QRëC) on the parent NaMOR and the

modified MOR. The catalysts were dried overnight at 105 °C, calcined at 500 °C for 3 h,

and characterized by XRD to observe any changes in the MOR structure and to determine

the form of Fe.

Forms of Fe supported on the parent NaMOR and modified MOR were also

analyzed by XANES at beamline 8 of the synchrotron light research institute, Thailand.

The XANES spectra of Fe K-edge were calibrated by a Fe foil at 7112 eV and recorded at

room temperature in transmission mode. Each sample was pressed into a frame covered by

a kapton tape and mounted onto a sample holder. The quantity of each Fe form was

computed by a linear combination fitting tool in ATHENA program (Ravel and Newville,

2005) from normalized XANES spectra of FeO, Fe_2O_3 and Fe_3O_4 in the energy range from

20.00 eV before and 40.00 eV after the Fe K-edge.

3.2.3 Performance of the supported Fe catalysts for phenol hydroxylation

The performance of Fe catalysts supported on NaMOR and modified MOR for phenol hydroxylation was studied by using an apparatus setup and condition similar to those in the literature (Chumee et al., 2009). Briefly, each reaction was carried out in a 50 mL three-neck round bottom flask fitted with a reflux condenser, a thermometer and a septum for sampling purpose. A mixture containing catalyst powder (0.05 g) suspended in an aqueous solution of phenol (0.8 g, 0.34 M) was magnetically stirred and heated to 70 °C for 30 min before an addition a 2.0 mL of hydrogen peroxide solution (H_2O_2, 30% W/V, Ajax). The mixture was sampled every hour and analyzed by a gas chromatograph (SHIMADZU 14A series) equipped with an ID-BP1 coated capillary column and a flame ionization detector. The reaction condition included phenol to H_2O_2 mole ratio of 1:3 and temperature of 70 °C.

3.3 Results and discussion

3.3.1 Characterization of parent NaMOR and modified MOR

The XRD patterns of zeolite products synthesized with rice husk silica from crystallization time of 24, 48, 72 and 96 h are shown in Figure 3.1a. In the product crystallized for 24 h, the characteristic peaks of MOR framework was not observed and only 2 broad bands were observed at about 13 and 25 degrees indicating amorphous phase. In the sample with crystallization time of 48 h, both broad bands were still observed along with MOR characteristic peaks at 25.5, 9.6, 22.1, and 26.2 degrees (Kim and Ahn, 1991; Zhang et al., 2009). The results indicated that 24 h was not long enough to complete the MOR crystallization. In the samples crystallized for 72 and 96 h, the broad bands were no longer observed. Both samples gave XRD patterns with peak positions similar to those of MOR in the literatures (Kim and Ahn, 1991; Zhang et al., 2009) indicating that the MOR synthesis using rice husk silica were accomplished by both conditions. However, the sample crystallized for 96 h gave XRD peaks with higher intensities indicating a higher

crystallinity. Consequently, the crystallization time of 96 h was used in the further MOR synthesis in a larger scale. Zhang et al. also reported that the crystallization time of MOR from silica gel was complete after 96 h (Zhang et al., 2009).

Figure 3.1b shows XRD patterns of the parent NaMOR from the larger scale synthesis and the products from modification including proton form (HMOR), base treated (desilicated) in proton form (BMOR), acid treated (dealuminated) in proton form (AMOR) and acid-based treated in proton form (ABMOR). The diffraction peak positions of all samples were similar to the MOR pattern reported in the literature (Kim and Ahn, 1991; Zhang et al., 2009) confirming that the modification did not significantly change the MOR framework. However, intensities of the major peaks were not identical probably from the difference in Si/Al ratio.

When the size of autoclave was changed from 150 to 250 mL, the XRD patterns of NaMOR in Figure 3.1a and 3.1b were slightly affected. In general, there are several parameters that have influence on the zeolite synthesis, for example, synthesis gel composition, temperature, and pressure (Bekkum et al., 2001). With the containers with different sizes, effects could arise from differences in the heating profile of the gel and in pressure increment during hydrothermal condition. Such parameters could affect the crystallization and result in different XRD intensity.
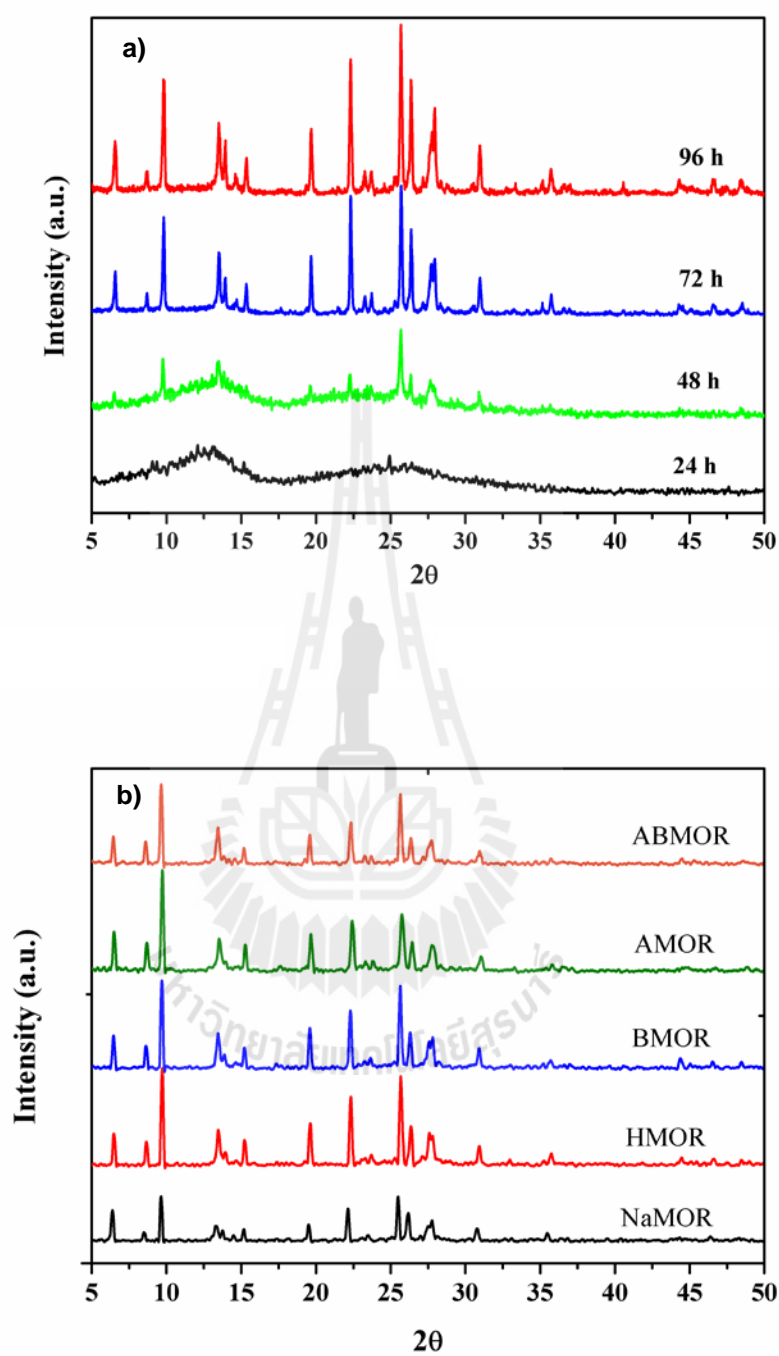
Figure 3.1 a) XRD patterns of zeolite products synthesized with rice husk silica from crystallization time of 24, 48, 72 and 96 h at 170 °C; b), XRD patterns of NaMOR, HMOR, BMOR, AMOR and ABMOR.

The nitrogen adsorption-desorption isotherm of the NaMOR, HMOR, BMOR, AMOR, and ABMOR are shown in Figure 3.2. The isotherm of NaMOR was type I, a characteristic of microporous materials in which the amount of adsorbed N_2 increased quickly at low relative pressure due to an adsorption on micropores and external surface. After that the adsorbed volume remained flat throughout the pressure range indicating monolayer adsorption. The isotherm of HMOR was also type I with a higher volume adsorbed indicating that the transformation caused an increase of micropore volume. In the BMOR which was obtained from treatment HMOR with base, the isotherm was similar to that of the HMOR indicating that desilication only occurred slightly. In the AMOR which was obtained by treatment HMOR with acid, the volume adsorbed was higher than those in HMOR and BMOR indicating higher micropore volume and external surface. Viswanadham and Kumar reported that acid treatment opened the side pocket of HMOR resulted in an increase of micropore surface area (Groen et al., 2007).

In the ABMOR which was treated by acid followed by base, the amount of N_2 uptake was the highest and the isotherm changed to type IV. The acid treatment increased micropore surface area and seemed to increase the efficiency of desilication by base to open up the MOR structure to generate mesopores. This result was similar to that in the literature (Li et al., 2009). A narrow hysteresis from mesopores was observed at the relative pressure above 0.4 indicating a formation of mesopores H4 type which is slit-like pore (Rouquerol, 1999).
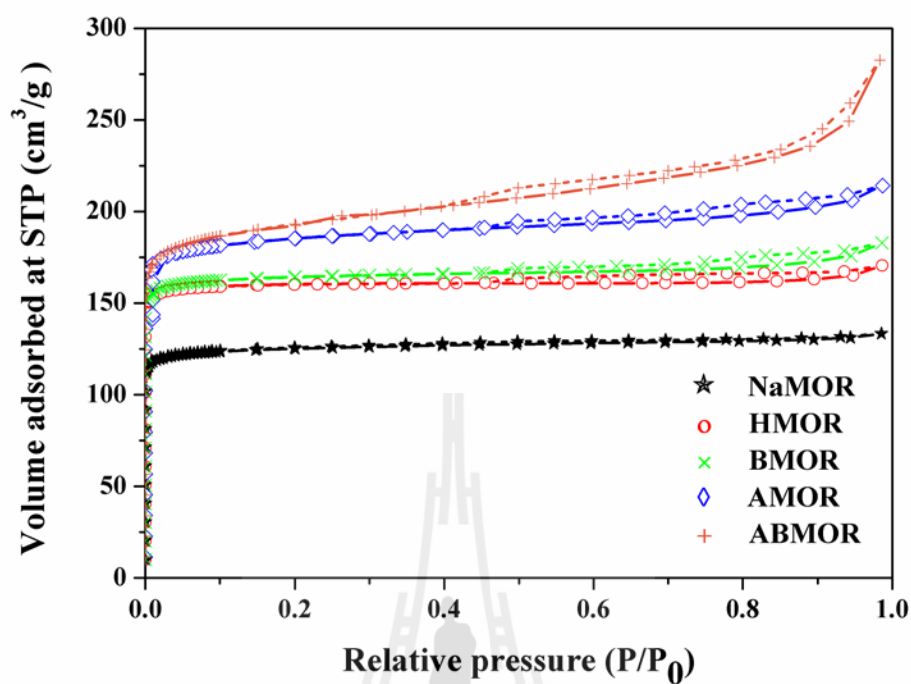
Figure 3.2 Nitrogen adsorption-desorption isotherm of the parent NaMOR and modified

MOR.

Table 3.1 Results from nitrogen adsorption-desorption and ICP-MS.

Samples	Surface area[a] (m²/g)	Micropore volume[b] (cm³/g)	External Surface Area[b] (m²/g)	Si/Al ratio[c]
NaMOR	414	0.18	36	11.0
HMOR	531	0.24	24	10.5
BMOR	545	0.24	38	9.5
AMOR	612	0.25	83	35.5
ABMOR	632	0.26	75	27.8

[a] BET method, [b] t-Plot method and [c] ICP-MS.
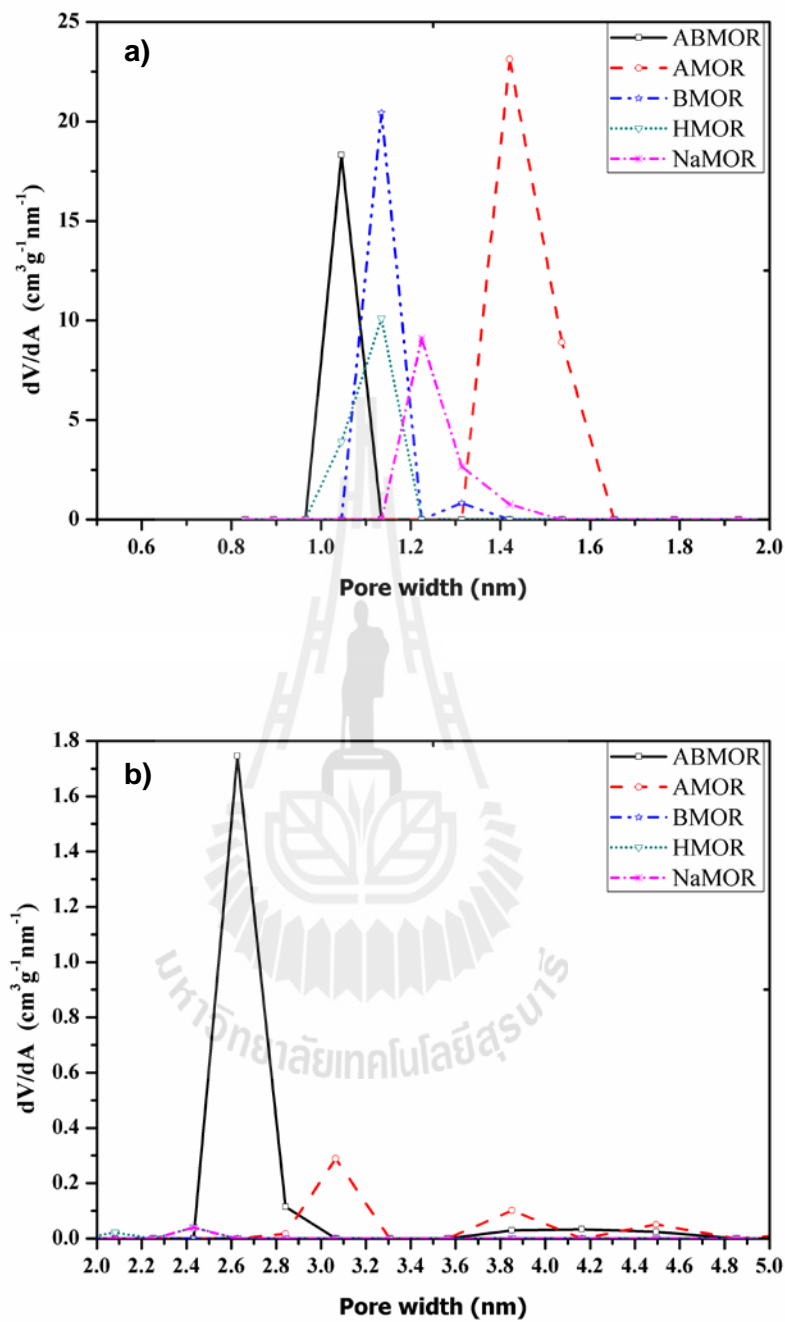
Figure 3.3 a) Pore size distribution at micropore range and b) mesopore range of the parent

NaMOR and modified MOR including HMOR, BMOR, AMOR and ABMOR

by BJH method.

The pore size distribution of the parent NaMOR and modified MOR calculated by Barrett-Joyner-Halenda (BJH) method are presented in Figure 3.3. The pore distributions in the micropore range are shown in Figure 3.3a. The largest size was observed in AMOR plausibly due to the opening of micropores from acid treatment. The pore distributions in the mesopore range are shown in Figure 3.3b. The ABMOR showed the most significant mesopore feature with average diameter of 2.7 nm. In addition, the AMOR showed some extent of mesopores with pore diameter of 3.1 nm. Table 3.1 shows surface areas and micropore volume of the parent NaMOR and modified MOR. High surface area of ABMOR was contributed from the presence of mesopores whereas high surface area of AMOR was from the increase of micropore volume and the presence of mesopores. The higher surface area of the modified MOR could lead to a better dispersion of metal catalysts which could improve the catalytic performance.

The Si/Al ratio of the parent NaMOR and the modified MOR determined by ICP-MS are shown in Table 3.1. After the NaMOR was transformed to the HMOR, the Si/Al ratio slightly decreased probably because of structural rearrangement during liquid-solid equilibrium. After a base treatment, the ratio decreased by desilication but the change was not as dramatic as the sample treated by acid in which the Si/Al ratio increased significantly by dealumination. Further desilication of AMOR to produce ABMOR generated mesopores and decreased the Si/Al.

3.3.2 Characterization of supported Fe catalysts

The XRD patterns of all Fe catalysts supported on MOR samples are shown in Figure 3.4a. The peaks of all MOR samples were not changed after metal loading. However, there was an increase of intensity of a peak at 33.5 degree which could be from the formation of Fe_2O_3. Because not all the characteristic peaks of Fe_2O_3 from JCPDS database at 33.5, 36.0, 49.8 and 54.2 degrees (JCPDS, 1998) were observed, it was necessary to confirm the form of Fe by another technique. In the case of 5Fe/ABMOR, the

peak at 33.5 degree was not observed indicating that particles of the Fe species were well dispersed on the support. In general, a good dispersion would lead to a high catalytic activity.

Table 3.2 Results from linear combination fitting of XANES spectra of Fe supported on the parent NaMOR and modified MOR.

Iron component	5Fe/NaMOR	5Fe/HMOR	5Fe/BMOR	5Fe/AMOR	5Fe/ABMOR
FeO (%)	0.0	0.0	4.9	0.0	0.0
Fe_2O_3 (%)	93.9	93.9	95.1	89.3	93.9
Fe_3O_4 (%)	6.1	6.1	0.0	10.7	6.1

The XANES spectra of all supported Fe catalysts were similar to that of the Fe_2O_3 standard indicating that Fe had oxidation state of +3. The composition of Fe phases in all catalysts could be calculated from the XANES spectra by the linear combination fitting tool. An example of the XANES spectrum and linear combination fitting results is shown in Figure 3.4b. Although the XRD peaks of Fe in 5Fe/ABMOR were not observed, the linear combination fitting suggested Fe_2O_3 to be a major component (93.9 wt%). Results from linear combination fitting of iron in all catalysts are shown in Table 3.2. The major Fe components in all catalysts were Fe_2O_3. This form has been reported to be an active form for phenol hydroxylation in several reports (Jia et al., 2007; Liu et al., 2006; Liu et al., 2001; Wang et al., 1998; Suja et al., 2003; Yang et al., 2009).

3.3.3 Phenol hydroxylation

The results from catalytic testing for phenol hydroxylation on supported Fe catalysts including phenol conversion and product selectivity are shown in Figure 3.5 and Table 3.3, respectively. The fastest conversion was observed on 5Fe/ABMOR which

reached equilibrium within one hour. Because HMOR has mono-dimensional pore structure, the adsorption of the first phenol molecule on the mouth of pore possibly limits the diffusion of other molecules (Amin et al., 2010). The presence of mesopores could facilitate diffusion of the reactants to the Fe active sites. At the first hour, the phenol conversion was in the following order: 5Fe/ABMOR > 5Fe/BMOR > 5Fe/NaMOR> 5Fe/HMOR $\cong$ 5Fe/AMOR. The results implied that the reaction was sensitive to the structure and properties of the support. Reaction on other Fe catalysts on supports without mesopores took a longer time to reach equilibrium. In our previous work, the catalyst supported on mesoporous MCM-41 showed a faster reaction rate than that supported on silica (Chumee et al., 2009). At the fourth hour, the conversions on 5Fe/BMOR, 5Fe/NaMOR and 5Fe/HMOR were similar at about 50% whereas the conversion on 5Fe/AMOR remained the lowest at about 20% throughout. Treatment the MOR with acid removed aluminium sites, Lewis acid sites, which could be adsorption sites for the reactants, phenol and H_2O_2. Bahranowski et al. (2001) reported that the decomposition of H_2O_2 was accelerated by strong Brönsted acid sites that have significantly competitive reaction of this process.

In addition, the conversion on 5Fe/ABMOR was the highest probably because the active metal was deposited on the support with the highest surface area, producing the highest dispersion. Although changing Si/Al ratio of zeolite could affect several reactions (Nawaz et al., 2010), the role of the mordenite in this reaction was mainly to disperse active metal species. Phenol adsorption was negligible in H-mordenite due to its hydrophilic nature, low SiO_2/Al_2O_3 ratio and smaller ring dimension (0.26 nm $\times$ 0.57 nm) (Amin et al., 2010). We conducted experiments on the zeolites to confirm that the reaction did not occur when the Fe was absent. The reaction mechanism has been proposed by Choi et al. (2006) involving the decomposition of H_2O_2 on Fe (III)/Fe (II) sites to produce $\cdot OOH$, $\cdot OH$, OH^- and H^+. Then the $\cdot OH$ reacts with phenol to produce catechol and

hydroquinone. In addition, the ·OH can react with hydroquinone to produce benzoquinone (Choi et al., 2006).

Table 3.3 Product selectivity of 5Fe supported on the parent NaMOR and modified MOR.

Catalyst	Time (h)	% Selectivity		
		Catechol	Hydroquinone	Benzoquinone
5Fe/NaMOR	1.0	0.0	0.0	100.0
	2.0	0.0	0.0	100.0
	3.0	29.4	0.0	70.6
	4.0	59.2	27.3	13.5
5Fe/HMOR	1.0	0.0	0.0	100.0
	2.0	35.5	0.0	64.5
	3.0	58.6	27.7	13.7
	4.0	60.0	37.8	2.2
5Fe/BMOR	1.0	44.1	0.0	55.9
	2.0	62.0	34.0	4.0
	3.0	64.1	34.2	1.7
	4.0	68.0	30.5	1.5
5Fe/AMOR	1.0	45.0	0.0	55.0
	2.0	55.5	38.8	5.7
	3.0	57.7	37.7	4.6
	4.0	53.7	43.6	2.7
5Fe/ABMOR	1.0	57.5	42.5	0.0
	2.0	58.3	41.7	0.0
	3.0	61.0	39.0	0.0
	4.0	56.3	43.7	0.0
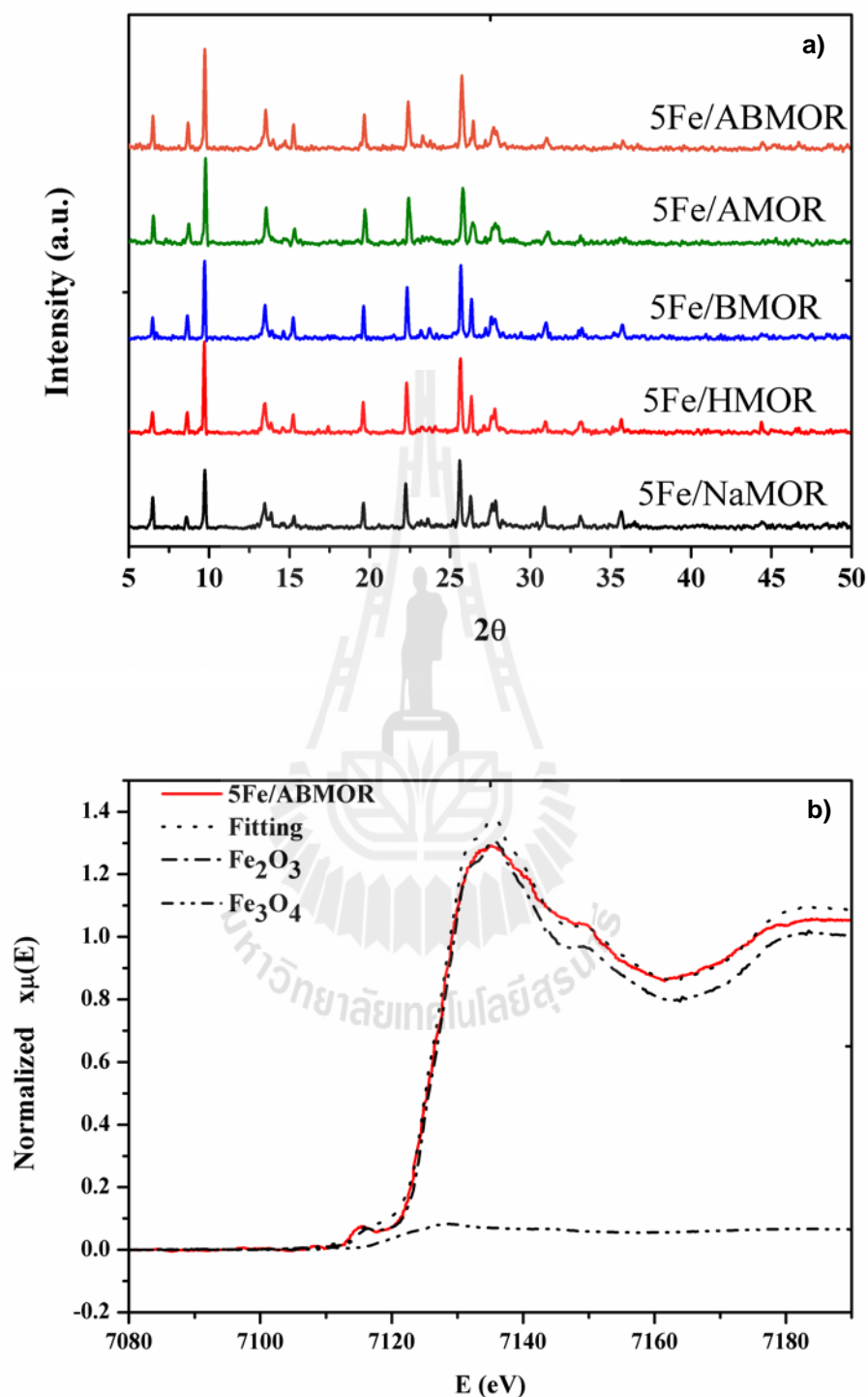
Figure 3.4 a) XRD patterns of supported Fe catalysts; b) XANES spectra and linear combination fitting of 5Fe/ABMOR showing forms of Fe as Fe_2O_3 and Fe_3O_4.
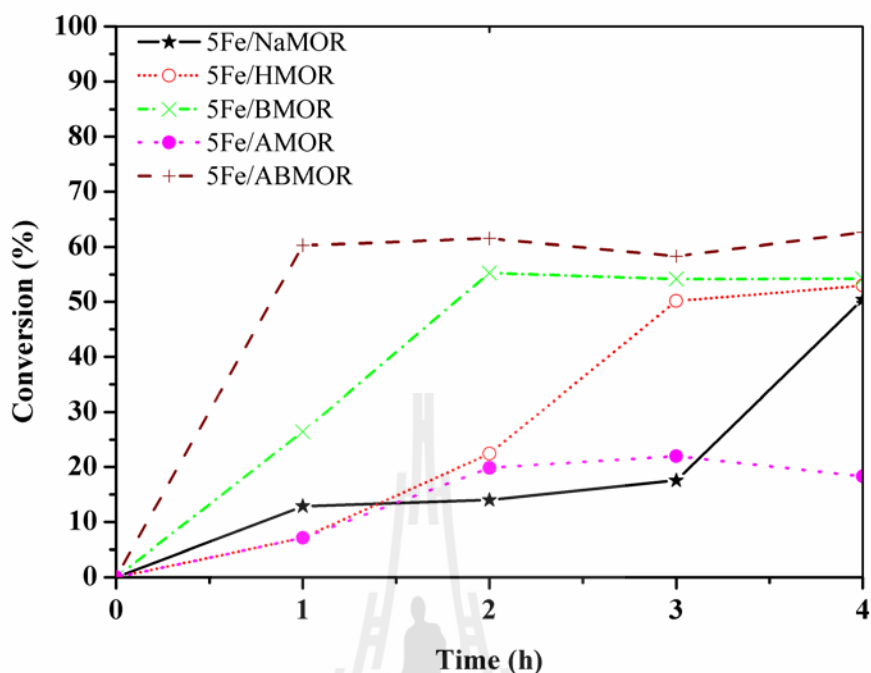
Figure 3.5 Phenol conversions of 5Fe supported on the parent NaMOR and modified

MOR.

Table 3.3 shows product selectivity from phenol hydroxylation on supported Fe

catalysts. Benzoquinone was observed at earlier stage in all catalysts except 5Fe/ABMOR.

Mechanism of phenol hydroxylation in the presence of Fe-containing acid sites involving

an electrophilic substitution (Zhao et al., 2001). The ortho- or para-positions of phenol are

preferable for substitution by $\cdot$OH according to resonance structure (McMurry, 1996). The

benzoquinone was produced by over-oxidation of hydroquinone when the amount of $\cdot$OH

was excess. The selectivity for benzoquinone decreased as the conversion increased. The

selectivity of catechol was higher than that of hydroquinone because the reaction could

occur over the active sites on external and internal surface (Wilkenhöner et al., 2001).
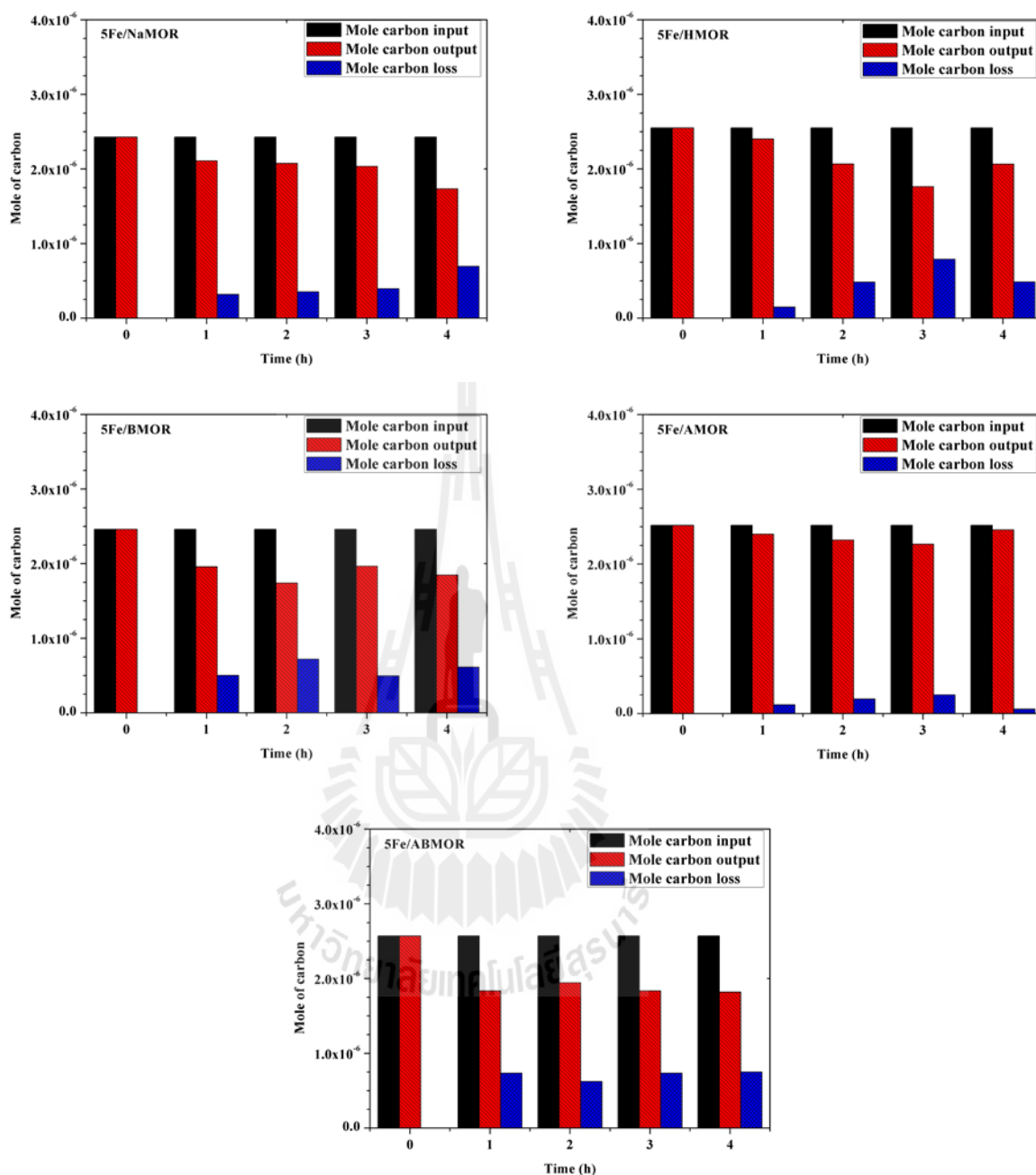
Figure 3.6 Mole carbon balance for phenol hydroxylation of 5Fe supported on the parent

NaMOR and modified MOR.

Mole of carbon balance for phenol hydroxylation of 5Fe supported on the parent

NaMOR and modified MOR were calculated at 0, 1, 2, 3 and 4 h and shown in Figure 3.6.

The carbon balance calculation is quite accurate if by-products are not present in the

reaction. Although the modified MOR was improved the rate conversion of phenol it

wasn't improved the product selectivities. The by-products, black tarry materials are

formed when the reaction took a longer time and that by-products were inferred to amount carbon loss. According to the amount carbon loss in the 1 h was in the following order: 5Fe/ABMOR > 5Fe/BMOR > 5Fe/NaMOR > 5Fe/HMOR > 5Fe/AMOR.

3.4 Conclusions

Zeolite NaMOR was synthesized by using rice husk silica, transformed to proton form (HMOR). The NaMOR was modified by treatment with acid, base, or both. The produced AMOR, BMOR and ABMOR, respectively had higher surface areas than the parent NaMOR. The MOR crystal structure was not destroyed in all modified samples and mesopores were generated significantly on ABMOR with average diameter of 2.7 nm. When loaded on NaMOR, HMOR, AMOR, BMOR and ABMOR, the major form of Fe active in all catalysts was Fe_2O_3. When the supported catalysts were tested for phenol hydroxylation, the fastest reaction rate and highest phenol conversion was obtained on 5Fe/ABMOR likely due to the presence of mesopores that facilitate Fe dispersion and the diffusion of reactants. However, the selectivity was not much improved and the products were mainly catechol and hydroquinone.

3.5 References

Amin, N. A. S., Akhtar, J. and Rai, H. K. (2010). Screening of combined zeolite-ozone system for phenol and COD removal. **Chemical Engineering Journal**. 158: 520-527.

Bahranowski, K., Dula, R., Gasior, M., Labanowska, M., Michalik, A., Vartikian, L. A. and Serwicka, E. M. (2001). Oxidation of aromatic-hydrocarbons with hydrogen-peroxide over Zn, Cu, Al layered double hydroxides. **Applied Clay Science**. 18: 93-101.

Bekkum, van H., Flanigen, E. M., Jacobs, P. A. and Jansen, J.C. (eds.). (2001). **Studies in surface science and catalysis** (vol. 137). (rev. 2nd ed.), Amsterdam: Elsevier.

Brook, M. A., Gatle, L. and Lindsay, I. R. (1982). Aromatic hydroxylation, part 7, oxidation of some benzenoid compounds by iron compounds and hydrogen peroxide with the aromatic compound acting as substrate and solvent. **Journal of the American Chemical Society**. 2: 687.

Choi, J. S., Yoon, S. S., Jang, S. H. and Ahn, W. S. (2006). Phenol hydroxylation using Fe-MCM-41. **Catalysis Today**. 280: 111-287.

Chumee, J., Grisdanurak, N., Neramittagapong, A. and Wittayakun, J. (2009). Characterization of platinum-iron catalysts supported on MCM-41 synthesized with rice husk silica and their performance for phenol hydroxylation. **Science and Technology of Advanced Materials**.10: 015006.

Groen, J. C., Peffer, L. A. A., Moulijn, J. A. and Perez-Ramirez, J. (2004). Optimal aluminum-assisted mesoporosity development in MFI zeolites by desilication. **Colloids and Surfaces A: Physicochemical and Engineering Aspects**. 241 : 53-58.

JCPDS, Joint Committee on Powder Diffraction Standards. (1998). International centre for diffraction data. Sets 1-48: 374.

Jeong, H. C., Shim, I. W., Choi, K. Y., Lee, J. K., Park, J. N. and Lee, C. W. (2005). Hydroxylation of phenol with H_2O_2 over transition metal containing nano-sized hollow core mesoporous shell carbon catalyst. **Korean Journal of Chemical Engineering**. 22: 657-660.

Jia, Y., Han, W., Xiong, G. and Yang, W. (2007). Diatomite as high performance and environmental friendly catalysts for phenol hydroxylation with H_2O_2. **Science and Technology of Advanced Materials**. 8: 106-109.

Khemtong, P., Prayoonpokarach, S. and Wittayakun, J. (2007). Synthesis and characterization of zeolite LSX from rice husk silica. **Suranaree Journal of Science and Technology**. 14: 367-379.

Kim, G. J. and Ahn, W. S. (1991). Direct synthesis and characterization of high-SiO_2-content mordenites. **Zeolites**. 11: 745-750.

Li, X., Prins, R. and van Bokhoven, J. A. (2009). Synthesis and characterization of mesoporous mordenite **Journal of Catalysis**. 262: 257-265.

Liu, H., Lu, G., Guo, Y., Guo, Y. and Wang, J. (2006). Synthesis of framework-substituted Fe-HMS and its catalytic performance for phenol hydroxylation. **Nanotechnology**. 17: 997-1003.

Liu, Q., Yu, J., Wang, Z., Yang, P. and Wu, T. (2001). Preparation, characterization and catalytic properties of α-Fe_2O_3/SiO_2 catalyst in phenol hydroxylation with hydrogen peroxide. **Reaction Kinetics and Catalysis Letters**. 73: 179-186.

McMurry, J. (ed.). (1996). **Organic Chemistry**. (4th ed.). California: Brooks/Cole Publishing Company Press.

Meier, W. M. (1961). The crystal structure of mordenite (ptilolite), **Z. Kristallogr**. 115: 439-450.

Nawaz, Z., Qing, S., Jixian, G., Tang, X. and Wei, F. (2010). Effect of Si/Al ratio on performance of Pt-Sn-based catalyst supported on ZSM-5 zeolite for n-butane conversion to light olefins. **Journal of Industrial and Engineering Chemistry**. 16: 57-62.

Pantu, P., Boekfa, B. and Limtrakul, J. (2007). Adsorption of saturated and unsaturated hydrocarbons on nanostructured zeolites (H-MOR and H-FAU): an ONIOM study, **Journal of Molecular Catalysis A: Chemical**. 277: 171-179.

Park, J. N., Wang, J., Choi, K. Y., Dong, W. Y., Hong, S. I. and Lee, C. W. (2006). Hydroxylation of phenol with H_2O_2 over Fe^{2+} and/or Co^{2+} ion-exchanged NaY catalyst in the fixed-bed flow reactor. **Journal of Molecular Catalysis A: Chemical**. 247: 73-79.

Preethi, M. E. L., Revathi, S., Sivakumar, T., Manikandan, D., Divakar, D., Rupa, A. V. and Palanichami, M. (2008). Phenol hydroxylation using Fe/Al-MCM-41. **Catalysis Letters**. 120: 56-64.

Ravel, B. and Newville, M. (2005). ATHENA, ARTEMIS, HEPHAESTUS: data analysis for x-ray absorption spectroscopy using IFEFFIT. **Journal of Synchrotron Radiation**. 12: 537-541.

Rouquerol, F., Rouquerol, J. and Sing, K. (eds.). (1999). **Adsorption by powders and porous solids**. San Diego, California: Academic Press.

Suja, H. and Sugunan, S. (2003). Iron promoted sulphated zirconia systems as efficient catalysts for phenol hydroxylation. **Bulletin of the Catalysis Society of India**. 2: 194-203.

Knözinger, H. and Kochloefl, K. (2003). Heterogeneous catalysis and solid catalysts. Bohnet, et al. (eds.). **Ullmann's encyclopedia of industrial chemistry** (vol. 16). (6th ed., pp. 315-431). Wiley-VCH Verlag GmbH, Weinheim.

Villa, A. L., Caro, C. A. and de Correa, C. M. (2005). Cu- and Fe-ZSM-5 as Catalysts for phenol hydroxylation. **Journal of Molecular Catalysis A: Chemical**. 228: 233-240.

Viswanadham, N. and Kumar, M. (2006). Effect of dealumination severity on the pore size distribution of mordenite. **Microporous and Mesoporous Materials**. 92: 31-37.

Wang, S., Dou, T., Li, Y., Zhang, Y., Li, X. and Yan, Z. (2005). A novel method for the preparation of MOR/MCM-41 composite molecular sieve. **Catalysis Communications**. 6: 87-91.

Wilkenhöner, U., Langhendries, G., van Laar, F., Baron, G. V., Gammon, D. W., Jacobs, P. A. and van Steen, E. (2001). Influence of pore and crystal size of crystalline titanosilicates on phenol hydroxylation in different solvents. **Journal of Catalysis**. 203: 201-212

Yang, X. Y., Li, Y., Tendeloo, G. V., Xiao, F. S. and Su, B. L. (2009). One-pot synthesis of catalytically stable and active nanoreactors: encapsulation of size-controlled nanoparticles within a hierarchically macroporous core@ordered mesoporous shell system. **Advanced Materials**. 21: 1368-1372.

Zhang, L., van Laak, A. N. C., de Jongh, P. E. and de Jong, K. P. (2009). Synthesis of large mordenite crystals with different aspect ratios. **Microporous and Mesoporous Materials**. 126: 115-124.

Zhao, W., Luo, Y., Deng, P. and Li, Q. (2001). Synthesis of Fe-MCM-48 and its catalytic performance in phenol hydroxylation. **Catalysis Letters**. 73: 199-202.
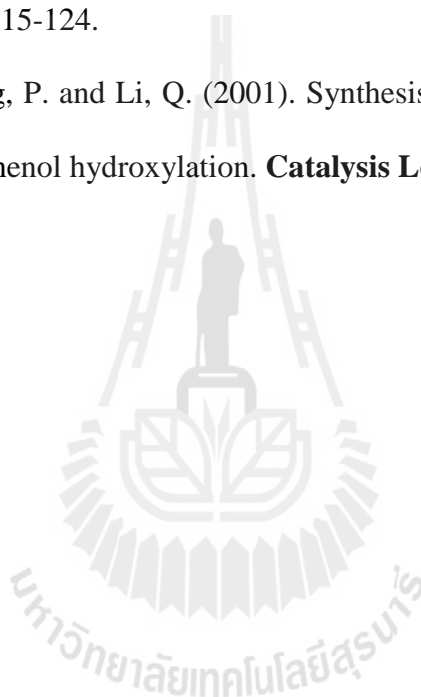
CHAPTER IV

ACID AND BASE PROPERTIES OF MODIFIED

MORDENITES STUDIED BY ^{27}Al MAS NMR, NH$_3$-TPD AND

METHYLBUTYNOL TEST REACTION

Abstract

This chapter reports changes in acid-base properties of mordenite (MOR) after modification by treatment with acid (AMOR), base (BMOR) and both acid-base (ABMOR) by ^{27}Al magic angle spinning nuclear magnetic resonance (^{27}Al MAS NMR), temperature-programmed desorption of ammonia (NH$_3$-TPD) and methylbutynol (MBOH) test reaction. The NMR results suggested concentration of framework aluminum in the order: HMOR $\approx$ BMOR > AMOR $\approx$ ABMOR and concentration of extraframework Al of in the order: HMOR > BMOR > ABMOR >AMOR. The NH$_3$-TPD results suggested amount of strong acid sites of HMOR > BMOR > ABMOR > AMOR. From the MBOH test reaction, the ABMOR gave highest MBOH conversion and product mainly from acid site pathway which could be contributed from accessibility to acid sites by the presence of mesopores.

4.1 Introduction

Mordenite (MOR) is a high silica zeolite with interconnected pore channels between 12-membered ring (6.7×7.0 Å) and 8-membered ring (3.4×4.8 Å) (Roland and Kleinschmit, 2003). The Si/Al ratio of MOR framework is generally between 5 and 12 depending on composition of the synthetic batch (Hincapie et al., 2009). In addition, the Si/Al ratio of 15 was reported in MOR nanocrystals. Because MOR is thermally stable and could be used in acidic conditions, it has been used as a catalyst in various industrial processes including isomerization, cracking, alkylation, and oxidation (Viswanadham and Kumar, 2006; Katada et al., 2004; Groen et al., 2007; Preethi et al., 2008).

For zeolites including MOR which are microporous materials, a major drawback is a problem in accessibility to active sites in the pores and diffusion limitation for large molecules. Several researchers have devoted to MOR modification to incorporate large pore size to the micropores. The attempts were either post-synthetic methods such as steam treatment (González et al., 2009; Hong and Fripiat, 1995), desilication by base, dealumination by acid (González et al., 2009; Hong and Fripiat, 1995) and templating methods with both organic and inorganic templates (Zamaro et al., 2006; Wang et al., 2005). Li et al. (2009) reported that mesopores can be generated effectively in HMOR after a sequential dealumination and desilication. First, the dealumination of HMOR by leaching with 2 M HNO_3 increased the Si/Al ratio from 15 to 25 and surface area from 384 to 455 m^2/g without changing much in the N_2 adsorption isotherm, and a slight decrease of extraframework Al. Further desilication of the acid-treated HMOR by 0.2 M NaOH generated mesoporous mordenite with the Si/Al ratio of 21-23 and surface area of 524-530 m^2/g and decreased extraframework Al. The mesoporous mordenite was active as a catalyst in alkylation of benzene with benzyl alcohol.

In chapter III synthesis of NaMOR by using silica from rice husk and modification of HMOR by acid, base and both acid-base were reported. The modified zeolites were used as supports of iron catalyst in phenol hydroxylation and the improvement in the reaction rate was observed. The modification changed the framework Si/Al ratio and pore properties which could affect the catalyzed reaction. However, changes in acid-base properties after the MOR modification were not clearly understood. Thus, the acid-base properties of the modified MOR were investigated in this chapter by ^{27}Al magic angle spinning nuclear magnetic resonance (^{27}Al MAS NMR), temperature-programmed desorption of ammonia (NH$_3$-TPD) and catalytic decomposition of methylbutynol (2-methyl-3-butyn-2-ol or MBOH).

In general, ^{27}Al MAS NMR can be used to differentiate framework aluminum which has tetrahedral coordination with oxygen atoms (namely, AlO$_4$ and referred to as Al$_{F-td}$) from the non-framework (extraframework) aluminum which has octahedral structure (namely, AlO$_6$ and referred to as Al$_{EF-oh}$) (Chester and Derouane, 2009). Hayashi and Kojima (2011) used ^{27}Al MAS NMR with ^{1}H high power decoupling during acquisition (HD) to investigate HMOR with Si/Al ratio of 7.5, 9.0 and 11.5. They reported broad signals at 53, 25 and -3 ppm corresponding to framework AlO$_4$, distorted AlO$_4$ or penta-coordinated AlO$_5$ and extraframework AlO$_6$, respectively. The signals became sharper when the HMOR samples were hydrated upon an exposure to ambient atmosphere. The signal of the extra-framework Al increased with Al content and the samples with high Al content showed more dealumination during the calcination. Li et al. (2009) used ^{27}Al MAS NMR to characterized HMOR with Si/Al ratio of 15 and assigned a strong peak at 54 ppm to Al$_{F-td}$ and a peak at -1 ppm to Al$_{EF-oh}$. The peak of Al$_{EF-oh}$ decreased due to the removal of aluminum after acid and base leaching.

Amount of acid sites in zeolites can be estimated by the NH_3-TPD technique. The amount of NH_3 adsorbed could be directly correlated to the number of acid sites and the desorption temperatures correspond to the adsorption strength (Chester and Derouane, 2009). For HMOR with Si/Al ratio = 7.5, its NH_3-TPD profile showed a low temperature (LT) peak at around 200 °C and high temperature (HT) peak at 450 °C. The LT peak does not give any information on the acidic properties of the solid because it could be found even on a Na form zeolite. Thus, it corresponds to adsorption on non-acidic sites and it could be easily replaced by water zeolites (Chester and Derouane, 2009). The HT peak is directly related to number of aluminum atoms in the zeolite (Chester and Derouane, 2009). A problem with NH_3-TPD method is that it can differentiate sites only by adsorption strength, but not Lewis from Brönsted sites. Thus, no information on the structure of the acid site is available and another method is needed.

The last method to study the acid and base properties of the zeolites was model reaction of catalytic decomposition of methylbutynol (2-methyl-3-butyn-2-ol, MBOH) which could be used on several materials (Lauron-Pernot et al., 1991) (Scheme 4.1). The conversion of MBOH on acid sites produces 2-methyl-1-butene-3-yne (MBYNE) by dehydration and 3-methyl-2-butenal (prenal) by intramolecular rearrangements. The conversion on basic sites produces acetone and acetylene by cleavage of C-C bond. Moreover, the reaction on defect sites generates 3-hydroxyl-3methyl-2-butanone (HMB) and 3-methyl-2-butyne-2-one (MIKP) by dehydrated product. The advantage is that MBOH is sensitive to reactive sites and the operating conditions such as temperature and flow rate can be adjusted to study the samples with small number of active sites (Lauron-Pernot, 2006). Other model reactions employing 1-phenylethanol and 2-propanol have been reported by Aramendia et al. (1999) but they gave less products, and thus, not as comprehensive as MBOH.

In this work, the ^{27}Al MAS NMR, NH$_3$-TPD and MBOH test reaction were used. The combined result of three techniques could lead to a clear understanding on acid and base properties of the parent NaMOR and modified MOR.
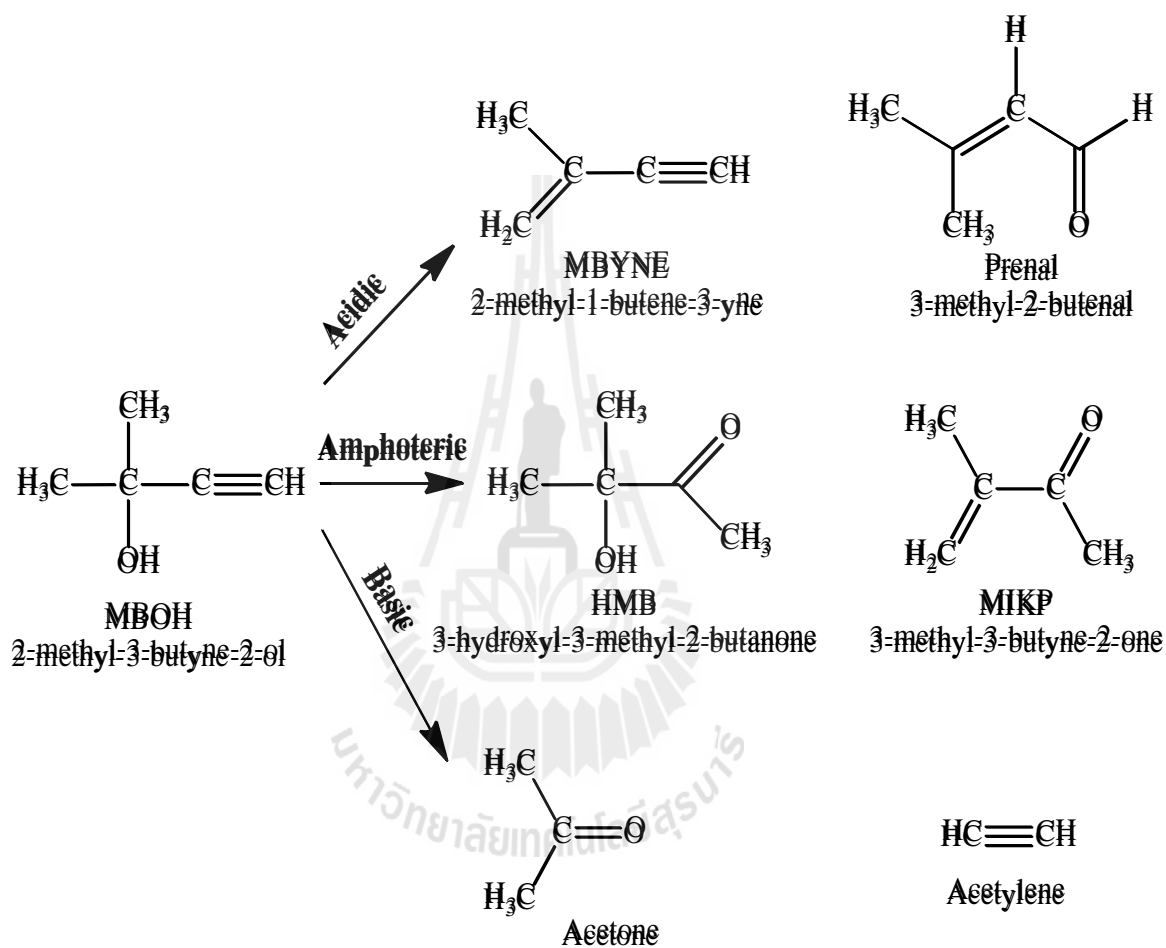
Scheme 4.1 Reaction pathways of MBOH conversion (Lauron-Pernot et al., 1991).

4.2 Experimental

4.2.1 Synthesis and modification of MOR

Rice husk silica (RHS) was prepared from rice husk (RH) (Khemtong et al., 2007). The RH was washed with water, dried at 100 °C overnight, refluxed with 3 M HCl at 100 °C for 3 h, washed repeatedly with water until the filtrate was neutral, dried again at 100 °C overnight, and calcined in a furnace at 550 °C for 6 h. The obtain RHS was used as a silica source for MOR synthesis.

MOR in sodium form (NaMOR) was synthesized with a procedure modified from Kim and Ahn (1991). A silicate solution prepared from RHS in NaOH was mixed with a solution of $NaAlO_2$ to give a gel with a molar composition of 2.5 Na_2O: Al_2O_3: 22 SiO_2: 518 H_2O in a polypropylene bottle, kept under stirring for 1 day and crystalized in a teflon-lined autoclave at 170 °C without agitation. The resulting NaMOR was filtered, washed thoroughly with deionized water, dried at 80 °C overnight, calcined in a muffle furnace at 500 °C for 3 h. The NaMOR was converted to proton form (HMOR) by ion-exchange with a 1.0 M NH_4NO_3 solution at 80 °C and calcination in air at 500 °C for 3 h.

HMOR was modified by acid and base treatment as described in the chapter III. In base treatment (desilication), the NaMOR was refluxed with 0.2 M NaOH at 65 °C for 30 min, filtered, washed with deionized water, and ion-exchanged with a 1.0 M NH_4NO_3 solution under stirring for 10 h at 80 °C, dried at 80 °C for 10 h, and calcined at 500 °C for 3 h. This base-treated MOR was notated as BMOR. In acid treatment (dealumination), the HMOR was refluxed with 2.0 M HNO_3 at 100 °C for 4 h, washed with deionized water, dried at 80 °C for 10 h, and calcined at 500 °C for 3 h. This acid-treated MOR is referred to as AMOR. Finally, the AMOR was refluxed with 0.2 M NaOH at 65 °C for 30 min, filtered, washed with deionized water, ion-exchanged with a 1.0 M NH_4NO_3 solution at 80 °C, dried at 80 °C for 10 h, and calcined at 500 °C for 3 h. This acid-base treated sample was referred to as ABMOR.

After modification, XRD characterization indicated that the MOR structure of all samples was still retained. Results from N_2 adsorption-desorption confirmed the presence of mesopores (Kulawong et al., 2011). BET surface area and Si/Al ratios from ICP-MS analysis are shown in Table 4.1.

Table 4.1 Results from N_2 adsorption-desorption [a], ICP-MS [b], and ^{27}Al MAS NMR [c].

Samples	BET surface area (m^2/g) [a]	Si/Al Ratio from ICP [b]	Chemical shift at 56 ppm		Chemical shift at 1 ppm		Area ratio of Al_{F-td}/Al_{EF-oh} [c]
			Area	Relative intensity	area	Relative intensity	
NaMOR	414	11.0	9.49E+14	100.0	-	-	-
HMOR	531	10.5	4.20E+14	44.3	3.17E+13	100.0	13.2
BMOR	545	9.5	3.88E+14	40.9	7.23E+12	22.8	53.7
AMOR	612	35.5	1.73E+14	18.2	3.92E+12	12.4	44.1
ABMOR	632	27.8	1.98E+14	20.9	7.08E+12	22.3	28.0

4.2.2 Characterization of MOR samples

The coordination state of Al in all zeolite samples were determined by ^{27}Al MAS NMR (500 MHz Varian INOVA) using a 4 mm probe with resonance frequencies of 130.32 MHz. The spectra were obtained with small flip angles of approximately 9° and with a recycle delay of 1 s. The ^{27}Al chemical shift was referenced to 1 M $Al(NO_3)_3$ in H_2O.

The natures of acid sites were determined by NH_3-TPD in a Raczek Analysentechnik equipped with a thermal conductivity detector. A sample amount of 300 mg was packed in a tubular U-shaped quartz cell, and degassed at 500 °C with a heating rate of 10 °C/min for 1 h in a He flow (49.8 mL/min), and cooled down to 70 °C. Then, the sample was exposed to a stream of 5 vol. % NH_3/Ar gas mixture at flow rate of 50 mL/min

for 30 min. Then, the sample was heated to 130 °C with a heating rate of 10 °C/min and held for 17 h to remove physisorbed species. The NH_3-TPD measurements was performed from 130 to 650 °C with a heating rate of 20 °C/min with He as a carrier gas.

The conversion of MBOH was carried out in a fixed-bed reactor. The MOR samples were pressed and sieved to 200 - 315 μm mesh size. One hundred milligrams of sample was packed in the center of a quartz tubular reactor, activated under air flow by heating to 400 °C with a rate of 8 °C/min and holding for 4 h to remove water and CO_2 adsorbed on the surface, and kept under to N_2 flow at this temperature for 4 h. After the activation, the reactor was cooled to the reaction temperature (180 °C). N_2 was flowed over a storage vessel containing a mixture of MBOH and toluene (95:5 v/v) cooled at 13 °C before entering the reactor. Toluene was used as an internal standard because it was not converted over the catalysts. The reaction products were analyzed by a gas chromatograph (Hewlett Packard HP 5890 Series II).

4.3 Results and discussion

4.3.1 Characterization by ^{27}Al MAS NMR

^{27}Al MAS NMR profiles of the parent NaMOR and modified MOR are shown in Figure 4.1(a). Comparisons of intensities of the position at ca. 56 and 1 ppm are provided in Figure 4.1(b) and (c), respectively. The parent NaMOR showed only one peak at 56 ppm which is a characteristic of framework tetrahedral coordinated AlO_4 (Al_{F-td}) in the zeolite (van Laak et al., 2010). In HMOR and modified MOR, the intensity of Al_{F-td} decreased in the following order: NaMOR > HMOR > BMOR > ABMOR > AMOR. The relative quantity based on the peak area is tabulated in Table 4.1. The peak at 1 ppm, characteristic of extraframework octahedral coordinated AlO_6 (Al_{EF-oh}) was also observed. The intensity was also in the same order, namely, HMOR > BMOR > ABMOR > AMOR. In addition,

area ratios of Al_{F-td}/Al_{EF-oh} are shown in Table 4.1. The order was in the order: BMOR > AMOR > ABMOR > HMOR.

In HMOR, some Al_{F-td} atoms were converted to Al_{EF-oh} (O'Donovan et al., 1995). The Al_{F-td}/Al_{EF-oh} ratio in HMOR was the lowest compared to all modified MOR. Thus, it had the highest amount of extraframework Al. In BMOR, the intensity of Al_{F-td} peak was slightly lower than that of HMOR but the Al_{F-td}/Al_{EF-oh} ratio was much higher, suggesting that BMOR had much less amount of extraframework Al. Thus, some extraframework Al was removed during desilication by alkaline solution. This could open up the zeolite structure and enhance the accessibility to the Lewis acid sites in the framework. In a work by van Laak et al. (2010) on a commercial MOR with Si/Al ratio of 5.7, the peak intensity of Al_{F-td} decreased and a new peak corresponding to Al_{EF-oh} was observed when NaMOR was transformed to HMOR. Both Al peaks were observed after the HMOR was desilicated by 1.0 M NaOH for 15 min and exchanged to proton form.

In AMOR, the intensity of Al_{F-td} and Al_{EF-oh} peaks significantly decreased compared to those of HMOR (Table 4.1). It was previously reported that Al_{EF-oh} which are Lewis acid sites could be removed from the lattice by dealumination (van Laak et al., 2010). An increase in Si/Al ratio of HMOR from 15 to 25 and decrease in the intensity of Al_{F-td} peak by dealumination with a condition similar to us was reported (Li et al., 2009). In ABMOR which was obtained by desilication of AMOR, peaks of Al_{F-td} and Al_{EF-oh} were higher than those of AMOR. The results suggested that desilication of dealuminated mordernite did not further remove Al but mainly remove Si resulting in lower Si/Al ratio and higher surfacearea. The Al_{F-td}/Al_{EF-oh} ratio of ABMOR was lower than that of BMOR and AMOR (Table 4.1) suggesting more extraframework Al.
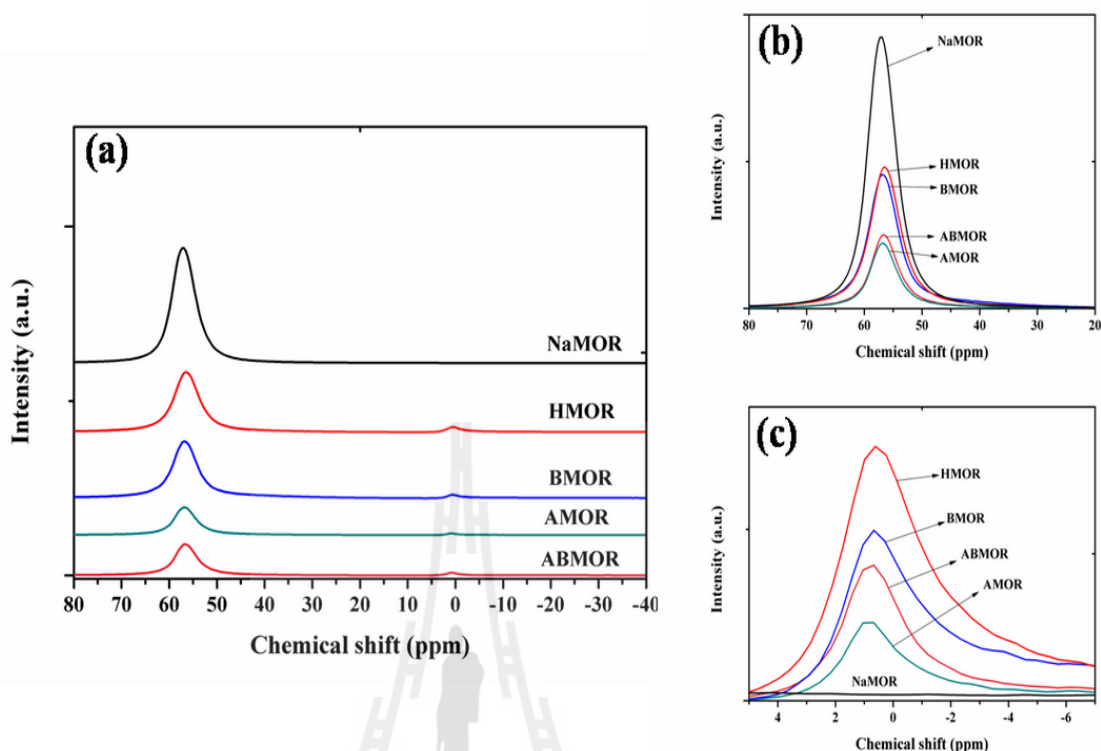
Figure 4.1 (a) ^{27}Al MAS NMR spectra of NaMOR, HMOR, BMOR, AMOR, and
ABMOR, (b) comparison of the chemical shift peaks at 56 ppm, and (c)
comparison of the chemical shift peaks at 1 ppm.

4.3.2 Acid-base properties characterized by NH₃-TPD

NH₃-TPD profiles of the parent NaMOR, HMOR and modified MOR from 130
to 650 °C are shown in Figure 4.2. All samples showed desorption peaks in two regions:
low-temperature (LT, lower than 400 °C) and high-temperature (HT, higher than 400 °C)
corresponding to weakly and strongly adsorbed NH₃, respectively. The peaks of weakly
adsorbed ammonia were observed in all samples because they were treated at only 130 °C
after the adsorption. These LT bands would decrease if the samples were treated at higher
temperatures (Lonyi and Valyon, 2001).

The NH₃-TPD profile of the parent NaMOR consisted of two intensive LT peaks
at 270 and 330 °C and a broad peak of lower intensity HT peak at 550 °C. The LT peaks
correspond to the adsorption on sodium ions (Na⁺) on isolated silanol groups (weak

Brönsted acid sites), and on NH_4^+ formed by prior adsorption of ammonia on the Brönsted acid sites Lonyi and Valyon, 2001; Chester and Derouane, 2009). These peaks do not give any information on the Brönsted acidic properties of the NaMOR. The HT band corresponds to the adsorption on Al_{F-td} (strong Lewis acid sites). Moradi et al. (2010) observed a single, broad LT peak on commercial NaMOR with Si/Al ratio ~ 8 in the temperature range of 180 to 450 °C. The intensity of the HT band of NaMOR was low because the Al sites were blocked by the charge balancing sodium ion. After the NaMOR was converted to HMOR, the intensity of LT bands decreased and that of the HT bands increased. All modified MOR (also in proton form) gave a broad HT band with higher intensity than the parent NaMOR. The broadening could be explained in term of re-adsorption of ammonia in the narrow channels of mordenite.

The HT band of BMOR was slightly lower than that of HMOR indicating lower Lewis acid sites. These results were consistent with the ^{27}Al MAS NMR that the areas of peaks corresponding to Al_{F-td} and Al_{EF-oh} of BMOR were second to those of HMOR. Thus, the base treatment of NaMOR followed by transformation to proton form did not to improve the acidity. Groen et al. (2007) reported similar NH_3-TPD results from a different NH_3-TPD procedure that the HT bands were not enhanced significantly after the alkaline treatment. In contrast, the HT bands of the AMOR and ABMOR were lower than those of HMOR and BMOR because some Al atoms were removed by the acid treatment. When the AMOR was further desilicated by NaOH, the structure became more open and the accessibility to the remaining Lewis acid sites was enhanced. Consequently, the HT band of ABMOR was higher than that of AMOR. These results were also consistent with the NMR results (see Table 4.1).

Comparing the HT area in NH_3-TPD profile, the strong acidity of modified MOR decreased in the following order: HMOR > BMOR > ABMOR > AMOR. However, when these zeolites were used as support materials for Fe in phenol hydroxylation, the fastest

reaction was observed on Fe/ABMOR (Kulawong et al., 2011). Such result could be attributed to combination of acidity and accessibility of large molecules to catalyst on mesoporous support.
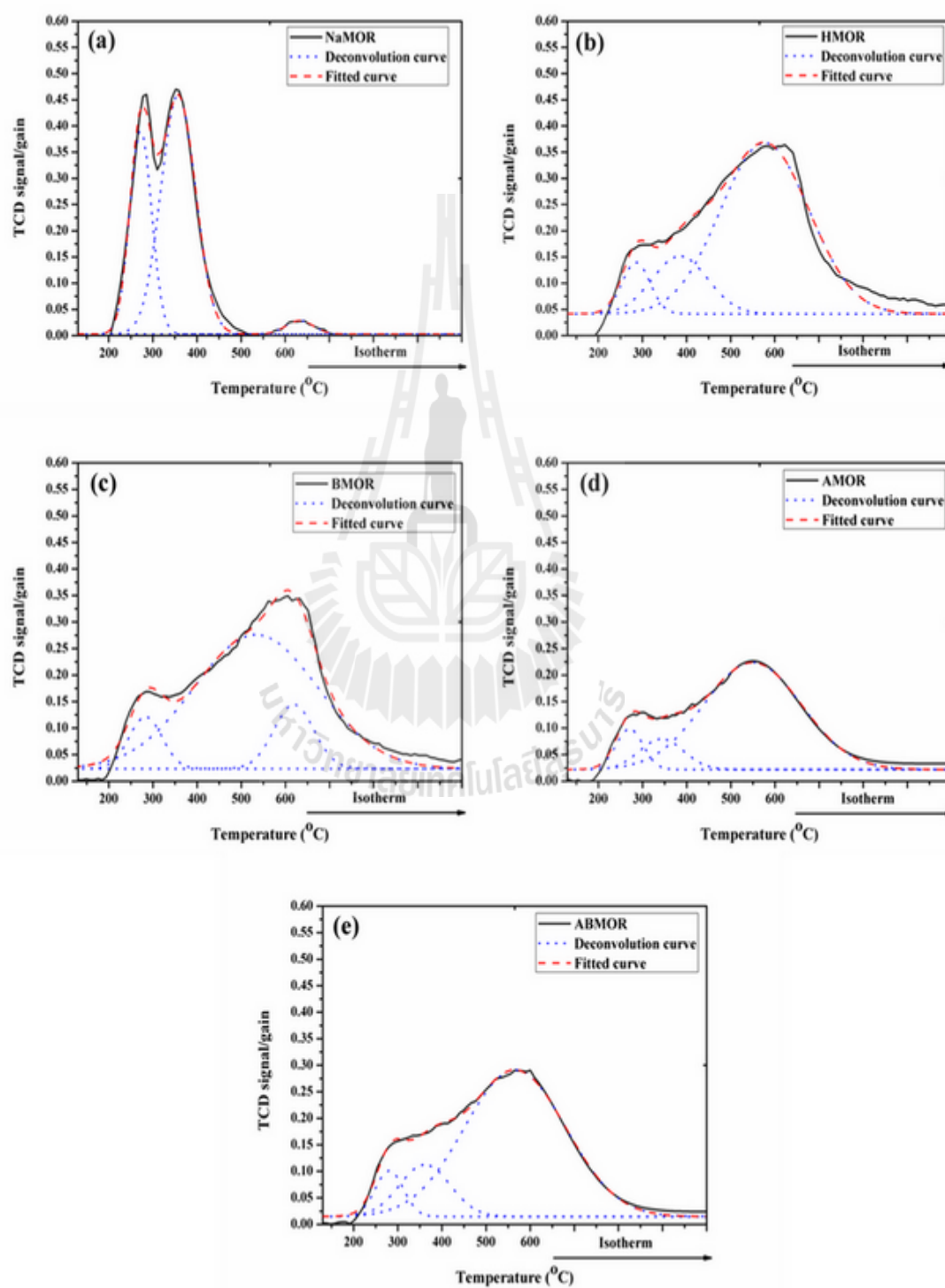
Figure 4.2 NH$_3$-TPD profiles, deconvolution, and fitted curves of (a) NaMOR, (b) HMOR, (c) BMOR, (d) AMOR, and (e) ABMOR.

4.3.3 Nature of acid and base sites investigated by MBOH test reaction

The results from decomposition of MBOH over parent NaMOR and modified MOR including conversions and product selectivities are shown in Figure 4.3. The initial MBOH conversions (Figure 4.3(a)) were in the following order: of ABMOR (90%) > BMOR (35%) > AMOR (16%) ≈ HMOR (15%) ≈ NaMOR (13%). The conversion was highest on ABMOR although it was not the sample with highest acidity suggested by NMR and NH_3-TPD. This could be attributed to the presence of mesopores which improve diffusion of reactants to active sites. After that the conversion over all samples decreased gradually and became nearly steady after 120 min. The order was still similar to the initial conversion, namely, ABMOR (27%) > BMOR (11%) > AMOR (8%) ≈ HMOR (8%) ≈ NaMOR (7%).

The decrease in MBOH conversion is typical for amorphous silica-alumina which is an acidic material. Alsawalha and Roessner (2008) reported that the MBOH conversion on silica-alumina at T=120 °C increased with increased with Si/Al ratio. However, more decrease in conversion was observed in the sample with higher Si/Al ratio. The decrease in conversion was attributed to strong adsorption of products. When they raised the reaction temperature to 180 °C, the conversion increased with less deactivation. The decrease of MBOH conversion was also reported previously by Huang and Kaliaguine (1993) who tested the reaction on NaMOR (Si/Al= 5.7) in a continuous flow reactor operated at atmospheric pressure at 180 °C with different activation procedure and amount of sample. Their MBOH conversion decreased from 22.5% in the first 5 min to 4.6% in 55 min. They also found that the more decrease in activity was observed in the sample with higher Si/Al ration. Decrease in conversion without change in selectivity was also reported on silica-alumina (Si/Al =18) tested for MBOH decomposition in a pulse reactor system, possibly due to strong product adsorption or secondary reactions leading to coke production on acidic sites (Katada and Niwa, 2004).

Figure 4.3(b)-(f) shows product selectivities on the parent NaMOR and all modified MOR. The selectivity of acetone and acetylene, the products formed on basic sites, was in the following order: NaMOR > HMOR > BMOR ≈ AMOR > ABMOR. The selectivities of both products on NaMOR agreed with the report of Huang and Kaliaguine (1993). The reaction on Na-exchanged zeolites only produced acetone and acetylene. In basic zeolites like NaMOR, the framework negative charge is compensated by sodium cation which has low electronegativity and then the charge on framework oxygen creates basic properties (Barthomeuf, 1996). Because proton has higher electronegativity than sodium (Shriver and Atkins, 1999), thus, the basicity decreased when NaMOR was transformed to HMOR. In addition, the selectivity for MBYNE, product from acid sites on HMOR was higher than that on NaMOR suggesting higher acidity. These results were consistent with NH_3-TPD results that area of HT band from HMOR was significantly higher than that from NaMOR.

On BMOR, the selectivity for MBYNE was higher than on HMOR and NaMOR because desilication removed some framework silicate and thus, increased silanol groups which are Brönsted acid sites. Desilication also improved accessibility to Al atoms which are Lewis acid sites. Thus, product from acid sites was dominant in BMOR. On AMOR, the product selectivities in average were slightly lower than that of HMOR. Dealumination removed some framework Al atoms resulting in decrease in framework charge and thus, basicity. Although dealumination also decrease Lewis acid sites, Brönsted acid sites were also generated.

According to the production of MBYNE, the product from acid sites, the acidity can be ranged in the following order: ABMOR > BMOR > AMOR > HMOR > NaMOR. The reaction occurred by an addition of proton to hydroxyl of MBOH. After elimination of water the acid site was regenerated and MBYNE desorbed from the surface (Alsawalha and Roessner, 2008). The selectivity of MBYNE was the highest on ABMOR because

treatment with both acid and base caused the structure to be more open, resulting in an increase in accessibility to Lewis acid sites. The treatment also increased Brönsted acid sites.
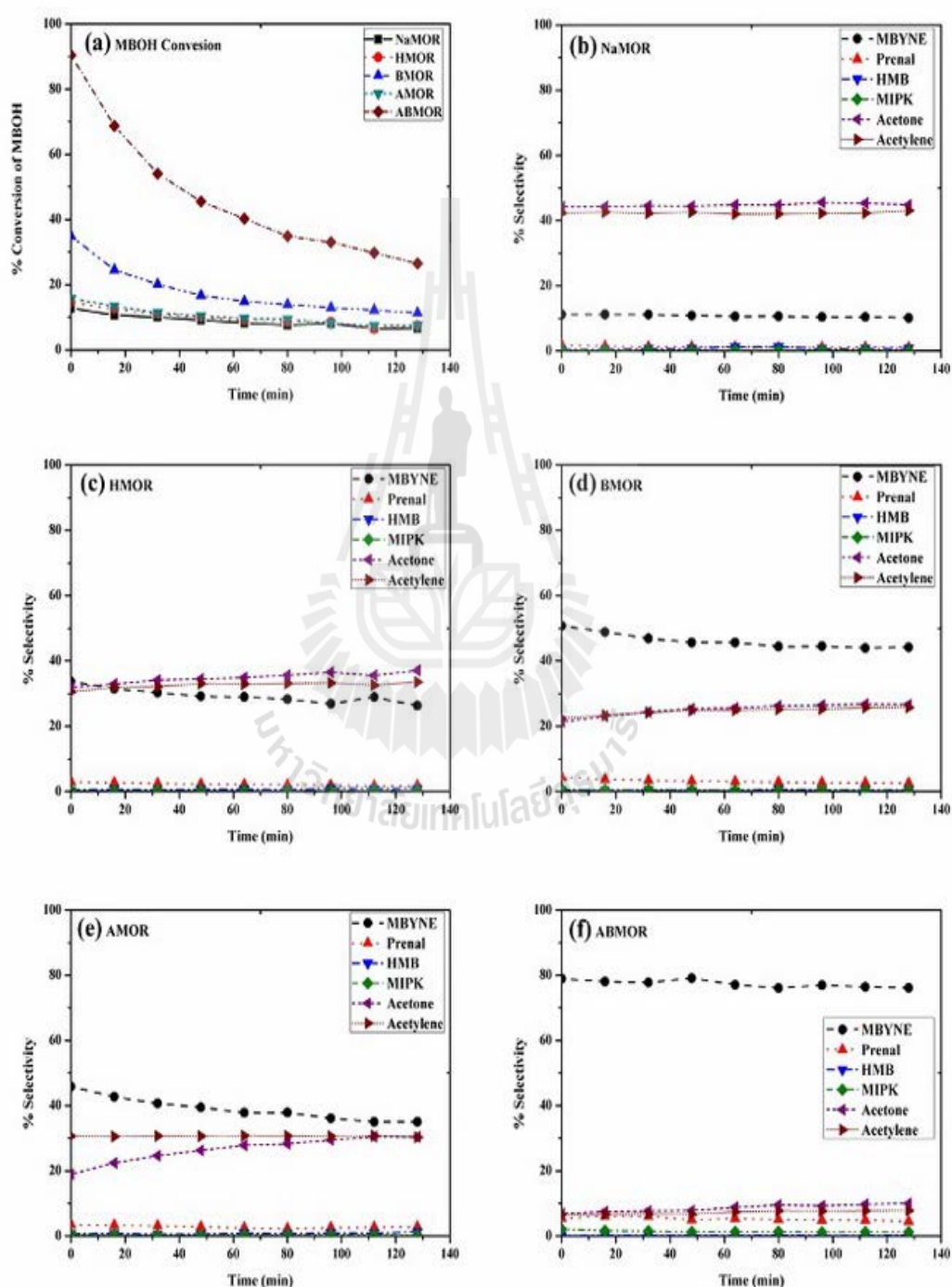
Figure 4.3 (a) % Conversion of the MBOH on MOR zeolites, (b) - (f) product selectivities

on NaMOR, HMOR, BMOR, AMOR, and ABMOR.

4.4 Conclusions

Changes in acid-base properties of MOR after modification by treatment with acid, base and both were investigated. From ^{27}Al MAS NMR, the amount of framework Al and extraframework Al was highest in HMOR. Both types of Al were decreased by desilication and dealumination. From NH$_3$-TPD, strong acid sites were highest on HMOR > BMOR > ABMOR > AMOR, consistent with the NMR results. In the MBOH test reaction, the highest MBOH conversion and highest selectivity to product from acid sites was on ABMOR attributing to an improvement in accessibility to acid sites and increase Brönsted acid sites from the presence of mesopores.

4.5 References

Alsawalha, M. and Roessner, F. (2008). Insight into the reaction mechanism of the conversion of methylbutynol on silica-alumina. **Reaction Kinetics and Catalysis Letters**. 9: 63-69.

Aramendia, M. A., Boráu, V., García, L. M., Jiménez, C., Marinas, A., Marinas, J. M., Porras, A. and Urbano, F. J. (1999). Dehydration-dehydrogenation of 1-phenylethanol over acid-basic catalysts**. Reaction Kinetics and Catalysis Letters**. 66: 343-350.

Barthomeuf, D. (1996). Basic zeolite: Characterization and uses in adsorption and catalysis. **Catalysis Reviews: Science and Engineering**. 38: 512.

Boveri, M., Márquez-Álvarez, C., Laborde, M. A. and Sastre, E. (2006). Steam and acid dealumination of mordenite: characterization and influence on the catalytic performance in linear alkylbenzene synthesis. **Catalysis Today**. 114: 217-225.

Čejka, J., Žilková, N. and Nachtigall, P. (eds.). (2005). **Studies in surface science and catalysis** (vol. 158). Elsevier, Amsterdam.

Chester, A. W. and Derouane, E. G. (eds.). (2009). **Zeolite characterization and catalysis a tutorial**. (1st ed., pp. 107). New York: Springer Press.

González, M. D., Cesteros , Y., Salagre , P., Medina, F. and Sueiras, J. E. (2009). Effect of microwaves in the dealumination of mordenite on its surface and acidic properties. **Microporous and Mesoporous Materials**. 118: 341-347.

Groen, J. C., Moulijn, J. A. and Perez-Ramirez, J. (2006). Desilication: on the controlled generation of mesoporosity in MFI Zeolites. **Journal of Materials Chemistry**. 16: 2121-2131.

Groen, J. C., Sano, T., Moulijn, J. A. and Pérez-Ramírez, J. (2007). Alkaline-mediated mesoporous mordenite for acid-catalyzed conversions. **Journal of Catalysis**. 251: 21-27.

Hayashi, S. and Kojima, N. (2011). Acid properties of H-type mordenite studied by solid-state NMR. **Microporous and Mesoporous Materials**. 141: 49-55.

Hincapie, B. O., Garces, L. J., Zhang, Q., Sacco, A. and Suib, S. L. (2004). Synthesis of mordenite nanocrystals. **Microporous and Mesoporous Materials**. 67: 19-26.

Hong, Y. and Fripiat, J. J. (1995). Microporous characteristics of H-Y, H-ZSM-5 and H-mordenite dealuminated by calcination. **Microporous Materials**. 4: 323-334.

Huang, M. and Kaliaguine, S. (1993). Reactions of methylbutynol on alkali-exchanged zeolites. A Lewis acid-base selectivity study. **Catalysis Letters**. 18: 373-389.

Katada, N., Kanai, T. and Niwa, M. (2004). Dealumination of proton form mordenite with high aluminum content in atmosphere. **Microporous and Mesoporous Materials**. 75: 61-67.

Khemtong, P., Prayoonpokarach, S. and Wittayakun, J. (2007). Synthesis and characterization of zeolite LSX from rice husk silica. **Suranaree Journal of Science and Technology**. 14: 367-379.

Kim, G. J. and Ahn, W. S. (1991). Direct synthesis and characterization of high-SiO$_2$-content mordenites. **Zeolites**. 11: 745-750.

Lauron-Pernot, H. (2006). Evaluation of surface acido-basic properties of inorganic-based solids by model catalytic alcohol reaction networks. **Catalysis Reviews**. 48: 315-361.

Lauron-Pernot, H., Luck, F. and Popa, J. M. (1991). Methylbutynol: A new and simple diagnostic tool for acidic and basic sites of solids. **Applied Catalysis**. 78: 213-225.

Li, X., Prins, R. and van Bokhoven, J. A. (2009). Synthesis and characterization of mesoporous mordenite**. Journal of Catalysis**. 262: 257-265.

Lónyi, F. and Valyon, J. (2001b). On the interpretation of the NH$_3$-TPD patterns of H-ZSM-5 and H-mordenite. **Microporous and Mesoporous Materials**. 47: 293-301.

Meyer, U. and Hoelderich, W. F. (1999). Application of basic zeolites in the decomposition reaction of 2-methyl-3-butyn-2-ol and the isomerization of 3-carene. **Journal of Molecular Catalysis A: Chemical**. 142: 213-222.

O'Donovan, A. W., O'Connor. C. T. and Koch, K. R. (1995). Effect of acid and steam treatment of Na- and H-mordenite on their structural, acidic and catalytic properties. **Microporous Materials**. 5: 185-202.

Pamba, M., Maurin, G., Devautour, S., Vanderschueren, J., Giuntini, J. C., Renzoc, F. D., Hamidid, F. (2000). Influence of framework Si/Al ratio on the Na$^+$/mordenite interaction energy. **Physical Chemistry Chemical Physics**. 22: 2027-2031.

Preethi, M. E. L., Revathi, S., Sivakumar, T., Manikandan, D., Divakar, D., Rupa, A. V. and Palanichami, M. (2008). Phenol hydroxylation using Fe/Al-MCM-41. **Catalysis Letters**. 120: 56-64.

Rodríguez-González, L., Hermes, F., Bertmer, M., Rodríguez-Castellón, E., Jiménez-López, A. and Simon, U. (2007). The acid properties of H-ZSM-5 as studied by NH_3-TPD and ^{27}Al-MAS-NMR spectroscopy. **Applied Catalysis A: General**. 328: 174-182.

Roland, E. and Kleinschmit, P. (2003). Zeolites. Bohnet, M., et al. (eds.). **Ullmann's encyclopedia of industrial chemistry** (vol. 39). (6th ed., pp 625-655). Wiley-VCH Verlag GmbH, Weinheim.

Shriver, D. F. and Atkins, P. W. (eds.). (1999). **Inorganic Chemistry**. (3rd ed.) New York: W. H. Freeman.

van Laak, A. N. C., Gosselink, R. W., Sagala, S. L., Meeldijk, J. D., de Jongh, P. E. and de Jong, K. P. (2010). Alkaline treatment on commercially available aluminum rich mordenite. **Applied Catalysis A: General**. 382: 65-72.

Viswanadham, N. and Kumar, M. (2006). Effect of dealumination severity on the pore size distribution of mordenite. **Microporous and Mesoporous Materials**. 92: 31-37.

Wang, S., Dou, T., Li, Y., Zhang, Y., Li, X. and Yan, Z. (2005). A novel method for the preparation of MOR/MCM-41 composite molecular sieve. **Catalysis Communications**. 6: 87-91.

Zamaro, J. M., Ulla, M. A. and Miroí, E. E. (2006). Growth of mordenite on monoliths by secondary synthesis: effects of the substrate on the coating structure and catalytic activity. **Applied Catalysis A: General**. 314: 101-113.

CHAPTER V

CHARACTERIZATION OF NaMOR/MCM-41 COMPOSITES AND UTILIZATION AS SUPPORTS FOR IRON CATALYSTS IN PHENOL HYDROXYLATION

Abstract

Composites of NaMOR and MCM-41 were prepared from silica-alumina source obtained from alkaline-treated NaMOR and cetyltrimethylammonium bromide (CTAB) surfactant under hydrothermal condition. Characterization of the composites by XRD, TEM and N_2 adsorption-desorption confirmed their crystal phases, morphology and textural properties including surface area, micro- and mesopores volume, respectively. Further analysis by ^{27}Al MAS NMR revealed that only tetrahedral coordinated Al (Al_{F-td}) were present in the MOR framework of the composites; results from NH_3-TPDshowed change in acidities of the composites with NaOH concentration. Moreover, the composites were tested for decomposition of methylbutynol (MBOH) and the results suggested the dominance of acid sites, different from the parent NaMOR. Finally, the composites were used as supports for Fe catalysts. From catalysts characterization, the support features were retained and Fe was in 3+ oxidation state. Catalytic testing of Fe supported on the composites for phenol hydroxylation showed improvement giving conversions in the range of 65-70% and catechol:hydroquinone ratio of 1:1.

5.1 Introduction

Zeolites are microporous minerals composed of SiO_4 and AlO_4 tetrahedra linked to each other by sharing oxygen atoms (Roland and Kleinschmit, 2003). Zeolites are important as heterogeneous catalysts or support materials because they have high surface area, acidity, and stability (Knözinger and Kochloefl, 2003). They have cavities and channels with uniform shape and size that make them catalytically selective to shape and size of organic compounds. However, the pores could be too small for bulky molecules and cause difficulty in diffusion to active sites. Moreover, strongly acidic zeolites as hydrocarbon transformation catalysts could lead to fast deactivation (O'Donovan et al., 1995).

In phenol hydroxylation which is an oxidation of phenol with hydrogen peroxide (H_2O_2) to produce catechol and hydroquinone, Fe supported on mordenite zeolite (Fe/MOR) was reported to give 100% catechol selectivity but the phenol conversion was only 20% (Preethi et al., 2008). In chapter III when Fe was loaded on MOR modified by treatment with acid, base or both, the phenol conversion and rate was improved. However, the product selectivity decreased; catechol was the major product and hydroquinone was also produced (Chapter III). This chapter reports another attempt to improve the catalytic performance for phenol hydroxylation by using Fe supported on composites of MOR and mesoporous MCM-41.

There were reports about the influence from the pore size and acidity of mesoporous supports on reaction rates and product selectivity of phenol hydroxylation. When Fe was supported on MCM-41, Al-MCM-41 and MCM-48, the reaction rates were fast (Zhao et al., 2001; Choi et al., 2006; Preethi et al., 2008). Preethi et al. (2008) reported that the reaction rates and product selectivity of phenol hydroxylation on Fe supported on Al-MCM-41 were influenced by the support Si/Al ratio. At the low ratio, the reaction rates

were fast. In term of selectivity, the ratios between catechol (CE) and hydroquinone (HQ) was about 1:2 at the low Si/Al ratios and about 1:1 at high Si/Al ratios.

When compared to zeolites, mesoporous materials have lower hydrothermal stability and their structure could change in the presence of water vapor (Wang et al., 2004; Zhang et al., 2008). The zeolite hydrothermal stability allows the utilization for reactions under harsh conditions because the structure could be retained. For examples, fluidized cracking catalysts (FCC), consisting of zeolite Y, can be used in processes where stream is used to strip off adhering hydrocarbons. The same factors that affect thermal stability also influence hydrothermal stability (Roland and Kleinschmit, 2003). Thus, preparation of new materials that combine advantages of zeolites and mesoporous materials could improve catalyst stability, selectivity and reaction rate.

In this chapter, zeolite composite was synthesized by partially dissolve MOR zeolite in NaOH solution to generate silica-alumina source and mixing with cetyltrimethylammonium bromide (CTAB) as an organic template for MCM-41 formation. This method could generate MCM-41 containing MOR on the wall of mesopores (Wang et al., 2004; Wang et al., 2005; Ivanova et al., 2011). The composites were characterized by X-ray diffraction (XRD) and nitrogen adsorption-desorption analysis to confirm the phase crystals and mesoporosity, respectively, before utilization as supports for Fe catalysts. To understanding their roles in catalytic reactions, the composites were analyzed by ^{27}Al magic angle spinning nuclear magnetic resonance (^{27}Al MAS NMR), temperature-programmed desorption of ammonia (NH$_3$-TPD) and decomposition of methylbutynol or 2-methyl-3-butyn-2-ol (MBOH). After impregnation with Fe, the resulting catalysts were characterized by XRD, X-ray absorption near edge structure (XANES) spectroscopy to determine the form of Fe, and transmission electron microscopy (TEM) to observe the mesoporosity and particles of Fe species. Finally, Fe supported on the composites were tested for phenol hydroxylation.

5.2 Experimental

5.2.1 Preparation of NaMOR/MCM-41 composites

The NaMOR/MCM-41 composites were prepared by using NaMOR as a silica-alumina source with a method modified from a literature (Wang et al., 2005). The NaMOR (4.5 g) was dispersed in 25 mL of 1 M, 2 M, and 3 M of NaOH solutions and stirred for 30 min at room temperature and added with 60 mL solution of CTAB (9.6 g CTAB dissolved with 60 mL H_2O). After additional stirring for about 30 min, the mixture was loaded in a stainless steel teflon-lined autoclave, heated at 100 °C for 24 h, cooled down to room temperature, adjusted pH to 8.5 by addition of 2.5 M H_2SO_4 solution dropwise under vigorous stirring at room temperature and heated at 100 °C for 24 h under an autogenous pressure. The resultant solid product was recovered by filtration, washed with distilled water, and dried at 80 °C overnight. In order to remove the organic template in the mesopores, the synthesized product was calcined at 500 °C for 3 h. The composites were denoted as NaMOR/MCM-41(xM) where x is 1, 2 and 3 according to the concentration of the employed NaOH solution.

5.2.2 Characterization of NaMOR/MCM-41 composites

The crystal phases of all NaMOR/MCM-41 composites were confirmed by XRD. Surface areas were calculated by Brunauer-Emmett-Teller (BET) method; the micropore (less than 2 nm) size distributions were calculated by Horvath-Kawazoe (HK) method; and mesopore (range 2-50 nm) size distributions were calculated by Barret-Joyner-Halenda (BJH) method. The morphology was investigated by TEM (JEOL JSM 6400). Specimens for TEM studies were dispersed in absolute ethanol, dropped on a copper holey carbon grid and dried at room temperature. The coordination states of Al in all zeolite samples were determined by ^{27}Al MAS NMR.

The natures of acid sites were determined by NH_3-TPD in a RaczekAnalysentechnik equipped with thermal conductivity detector. Three hundred

milligrams of sample was packed in a tubular U-shaped quartz cell, and degassed at 500°C with a heating rate of 10 °C/min for 1 h in a He flow (49.8 mL/min), and cooled down to 70 °C for NH_3 adsorption. In this process, the sample is exposed to a steam of 5 vol.% NH_3/Ar gas mixture at rate of (50 mL/min) for 30 min. Then, the sample was heated to 130 °C with a heating rate of 10 °C/min and kept for 17 h to remove physisorbed NH_3. The NH_3-TPD measurements was performed from 130 to 650 °C with a heating rate of 20 °C/min, with He as a carrier gas.

5.2.3 Decomposition of MBOH on NaMOR/MCM-41 composites

The conversion of MBOH was carried out in a fixed-bed reactor. The NaMOR/MCM-41(xM) composites were pressed and sieved to 200-315 μm mesh size. One hundred milligrams of sample was packed in the centre of a quartz tubular reactor, activated by heating to 400 °C with a rate of 8 °C/min and holding for 4 h under air gas flow and kept under N_2 flow at this temperature for 4 h. After the activation, the reactor was cooled to the reaction temperature of 180 °C. N_2 was flowed over a storage vessel containing mixture of MBOH and toluene (95:5 V/V) cooled at 13 °C before entering the reactor. Toluene was used as an internal standard because it was not converted over the catalysts. The reaction products were analyzed by using a gas chromatograph (Hewlett Packard HP 5890 Series II).

5.2.4 Preparation and characterization of supported Fe catalysts

5.2.4.1 Preparation of supported Fe/NaMOR/MCM-41(xM) catalysts by impregnation (IMP) method

All NaMOR/MCM-41(xM) composites were impregnated with a solution of $Fe(NO_3)_3 \cdot 9H_2O$ (QRëC) containing 5 wt.% of Fe, dried overnight at 80 °C overnight, calcined at 500 °C for 3 h. The catalysts were characterized by XRD and TEM and XANES and TEM to observe change of the support structure, forms of Fe and morphology, respectively.

Species of Fe supported on the NaMOR/MCM-41(xM) composites were further analyzed by XANES at Beamline 8 of the Synchrotron Light Research Institute, Thailand. The XANES spectra of Fe K-edge were calibrated by a Fe foil at 7112 eV and recorded at room temperature in transmission mode. Each sample was pressed into a frame covered by Kapton® tape and mounted onto a sample holder. The quantity of each Fe species were computed by Linear Combination Fitting tool in ATHENA program (Ravel and Newville, 2005) from normalized XANES spectra of FeO, Fe_2O_3 and Fe_3O_4 in the energy range from 20.00 eV before and 40.00 eV after the Fe K-edge.

5.2.4.2 Preparation of supported Fe/ABMOR catalysts by ion-exchanged (IE) method

First, the NaMOR was refluxed with 2.0 M HNO_3 (Carlo ERBA, 65%) at 100 °C for 4 h, washed with deionized water, filtered, dried at 80 °C overnight and calcined at 500 °C for 3 h. This acid-treated MOR was referred to as AMOR. Second, the AMOR was refluxed with 0.2 M NaOH at 65 °C for 30 min, washed with deionized water, filtered, dried at 80 °C overnight and calcined at 500 °C for 3 h. This acid-base treated sample was referred to as ABMOR. Third, the ABMOR was ion-exchanged with a 1.0 M NH_4NO_3 solution under stirring for 10 h at 80 °C, washed with deionized water, filtered, and dried at 80 °C overnight. This NH_4NO_3 ion-exchanged ABMOR was referred to as NH_4ABMOR. Fourth, 1 g of the NH_4ABMOR was ion-exchanged with 50 mL of 0.1 M Fe $Fe(NO_3)_3 \cdot 9H_2O$ solution for 14 h at 80 °C, washed with deionized water, filtered, dried at 80 °C overnight and calcined at 500 °C for 3 h. The catalyst was designated as Fe/ABMOR IE. The Fe/ABMOR IE was characterized by XRD to observe any changes.

5.2.4.3 Preparation of Fe/NaMOR/MCM-41(2M) IE catalysts by immobilization of Fe on support

First, the composite catalyst was prepared by using Fe/HMOR IE (prepared by ion-exchanged method) as a catalyst and using SiO_2 as a silica source. The

SiO_2 (2.5 g) was dispersed in 25 mL of 2 M of NaOH solutions and stirred for 30 min at room temperature and added with 60 mL solution of CTAB (9.6 g CTAB dissolved with 60 mL H_2O). After additional stirring for about 30 min, the mixture was loaded in a teflon-lined autoclave, heated at 100 °C for 24 h, cooled down to room temperature, adjusted pH to 8.5 by addition of 2.5 M H_2SO_4 solution dropwise under vigorous stirring at room temperature, then slowly added 2 g of Fe/HMOR IE catalyst, stirred for 2 h to homogenize and heated at 100 °C for 24 h under an autogenous pressure. The resultant solid product was recovered by filtration, washed with distilled water, and dried at 80 °C overnight.

Second, the composite catalyst was prepared by using Fe/HMOR IE as both catalyst and silica-alumina sources. The Fe/HMOR IE (4.5 g) was dispersed in 25 mL of 2 M of NaOH solutions and stirred for 30 min at room temperature and added with 60 mL solution of CTAB (9.6 g CTAB dissolved with 60 mL H_2O). After additional stirring for about 30 min, the mixture was loaded in a teflon-lined autoclave, heated at 100 °C for 24 h, cooled down to room temperature, adjusted pH to 8.5 by addition of 2.5 M H_2SO_4 solution dropwise under vigorous stirring at room temperature and heated at 100 °C for 24 h under an autogenous pressure. The resultant solid product was recovered by filtration, washed with distilled water, and dried at 80 °C overnight.

In order to remove the organic template, the synthesized products were calcined at 500 °C for 3 h. The composites catalysts are designated as Fe/NaMOR/MCM-41(2M) IE1 and Fe/NaMOR/MCM-41(2M) IE2, respectively.

5.2.5 Phenol hydroxylation on Fe supported on NaMOR/MCM-41 composites

The performance of Fe catalysts supported on the ABMOR and the NaMOR/MCM-41 composite zeolites for phenol hydroxylation were studied by using an apparatus setup and condition similar tochapter III. Each reaction was carried out in a 50 mL three-neck round bottom flask fitted with a reflux condenser, a thermometer and a septum for sampling purpose. A mixture containing catalyst powder (0.05 g) suspended in

an aqueous solution of phenol (0.8 g, 0.34 M) was magnetically stirred and heated to 70 °C for 30 min before an addition a 2.0 mL of hydrogen peroxide solution (H_2O_2, 30% W/V, Ajax). The mixture was sampled and analyzed by a gas chromatograph (SHIMADZU 14A series) equipped with an ID-BP1 coated capillary column and a flame ionization detector. The reaction was done at 70 °C with fixed phenol:H_2O_2 mole ratio of 1:3.

5.3 Results and discussion

5.3.1 Characterization of NaMOR/MCM-41 composites

The XRD patterns of the NaMOR and NaMOR/MCM-41 composites at low and high 2θ region are shown in Figure 5.1. The patterns at the low 2θ region are characteristic of MCM-41 mesoporous structure (Park et al., 2002) and those at high 2θ region are characteristic of NaMOR (Kim and Ahn, 1991). All the NaMOR/MCM-41 composites displayed both MCM-41 and MOR characteristics. For NaMOR/MCM-41(1M), the MCM-41 peaks were barely observed and the MOR peaks were not changed significantly. The result suggested that the NaOH concentration of 1 M was too low to dissolve the NaMOR to generate sufficient silicate species for the formation of MCM-41 structure. Because the first peak of MCM-41 of NaMOR/MCM-41(2M) was more intense than those of the other samples, the NaOH concentration of 2 M was considered to be optimum for preparation of NaMOR/MCM-41 composite. Besides, the peak intensities of MOR in NaMOR/MCM-41(3M) decreased more severely than in the other samples. Our results were slightly different the work by Wang et al. (2005) in which the highest MCM-41 peak was observed in the composite (in proton form) prepared from using 3 M of NaOH. The difference could be caused by several possibilities, for example, different Si/Al ratio (11 (ours) vs. 18), form of MOR (Na (ours) vs. Al), volume of the final solution caused by using different acid in pH adjustment.
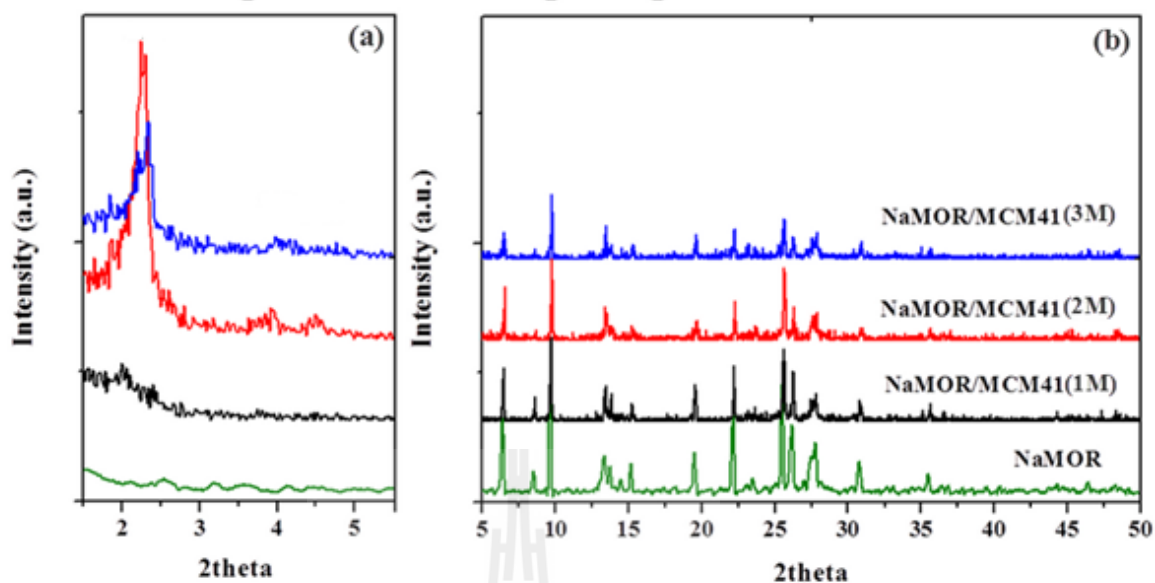
Figure 5.1 XRD profiles of the NaMOR, NaMOR/MCM-41(1M), NaMOR/MCM-41(2M) and NaMOR/MCM-41(3M) composite zeoiltes at low 2θregion (a) and high 2θ region (b).

The N_2 adsorption-desorption isotherm of the NaMOR/MCM-41 composites are shown in Figure 5.2. According to IUPAC classification, the isotherms were mixed type between type I and type IV which are characteristic of micropores and mesoporous materials, respectively (Rouquerol et al., 1999). For type I, the adsorbed volume increases rapidly at the beginning due to the adsorption on micropores and external surface area, then concave to the relative pressure (P/P_0) axis and became a plateau corresponding to formation of monolayer. For type IV, the beginning is similar to type I but the adsorbed volume is lower and the shape of isotherm is different at high relative pressure. The adsorbed volume increases with pressure corresponding to multilayer adsorption and a hysteresis, caused by filling and emptying mesopores, is formed.
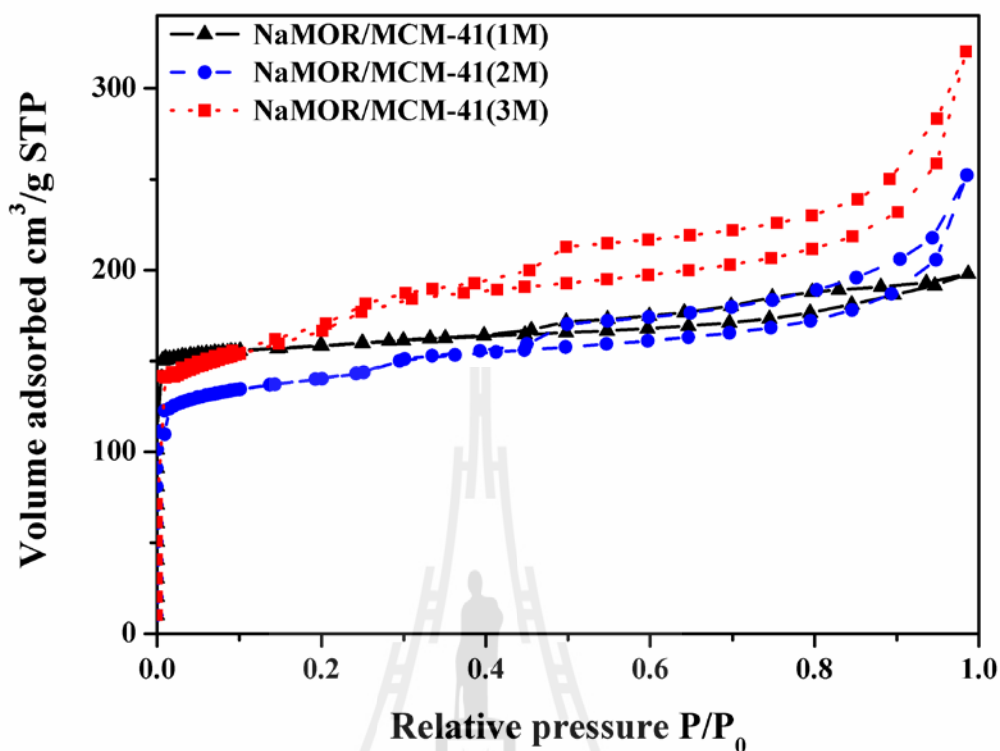
Figure 5.2 Nitrogen adsorption-desorption isotherm of the NaMOR/MCM-41(1M), NaMOR/MCM-41(2M) and NaMOR/MCM-41(3M) composite zeolites.

Among the three samples, the isotherm of NaMOR/MCM-41(1M) was the most similar to type I; the adsorbed volume at the beginning was higher than the other samples and there was not much change at higher pressures. The isotherm of NaMOR/MCM-41(2M) and NaMOR/MCM-41(3M) showed more character of type IV with multilayer adsorption after the adsorbed volume concaved to the P/P_0 axis. However, there were two types of mesopores in these samples because there was an increase of adsorbed volume at P/P_0 about 0.25 in the isotherm of NaMOR/MCM-41(2M) and a small hysteresis loop in the P/P_0 range of 0.12-0.45 in the isotherm of NaMOR/MCM-41(3M). The isotherms of all samples consisted a broad hysteresis loop in the P/P_0 range of 0.43-1.0 which can be classified as type H4 corresponding to slit-shaped pore shape but the pore size distribution

is mainly in the micropore range (Rouquerol et al., 1999). The loop volume increased as the following order: NaMOR/MCM-41(1M) < NaMOR/MCM-41(2M) < NaMOR/MCM-41(3M) suggesting that the extent of mesopores depended on the amount of dissolved MOR by NaOH solution. Our result of NaMOR/MCM-41(2M) was similar to the composite obtained from Wang et al. (2005) except that the volume after P/P_0 of 0.9 was lower.

The pore size distribution of NaMOR/MCM-41 composites in micropore range (less than 2 nm) and mesopore size (range 2-50 nm) calculated by HK and BJH method (Kurdi and Tremblay, 2002; Ou and Chevalier, 2002; Groen et al., 2003; Musa et al., 2011; Wang et al., 2011) are shown in Figure 5.3(a) and (b), respectively. By HK method, the distribution in the range of micropores was observed in all composites. The NaMOR/MCM-41(1M) showed only one range but both NaMOR/MCM-41(2M) and NaMOR/MCM-41(3M) showed two ranges suggesting more opening of micropores with higher concentration of NaOH. By BJH method, the distribution in the range of mesopores was also observed in all composites. The mesopore size distribution was the most uniform in the NaMOR/MCM-41(3M) whereas NaMOR/MCM-41(1M) and NaMOR/MCM-41(2M) produce a broad range distribution.

Figure 5.3 Pore size distribution of micropore size by HK mothod (a) and of mesopore
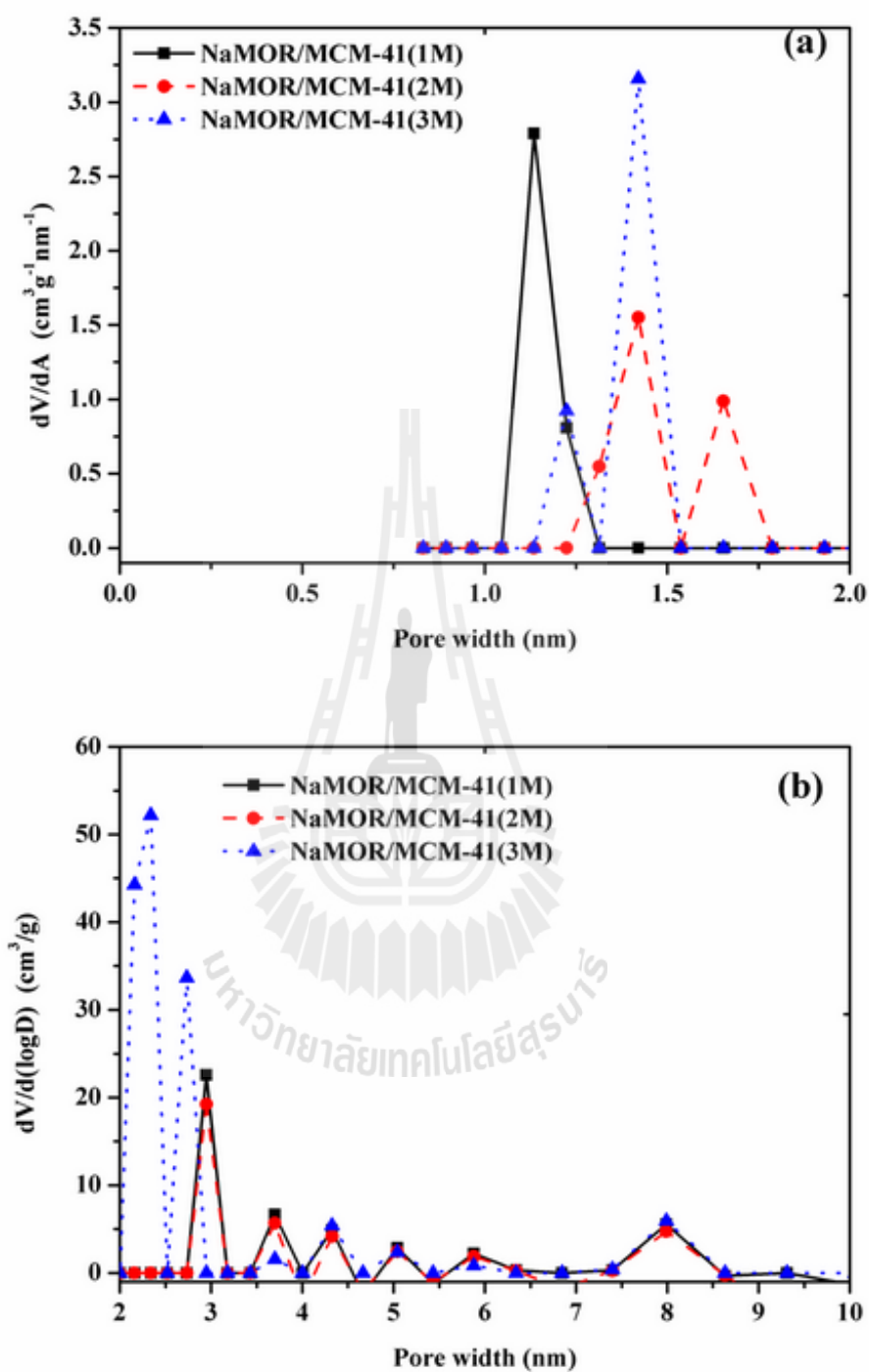size by BJH method (b) of the NaMOR/MCM-41(1M), NaMOR/MCM-
41(2M) and NaMOR/MCM-41(3M) composite zeolites.

TEM micrographs of NaMOR/MCM-41 composites are presented in Figure 5.4. The characteristic of a regular hexagonal array and uniform mesopores structures could be easily found on the images of NaMOR/MCM-41(2M) and NaMOR/MCM-41(3M) (Figure 5.4(b) and (c), respectively). Such pattern was not observed in the images of NaMOR/MCM-41(1M) but some defects likely from desilication could be located (Figure 5.4(a). These results were in a good agreement with the XRD results.

The ^{27}Al MAS NMR profiles of NaMOR and composite zeolites are presented in Figure 5.5. The peak intensities can be used to estimate the amounts of the different Al species and coordination in zeolite framework. All composite samples showed only a single signal at 56 ppm which is a characteristic framework of tetrahedral coordinated Al(Al$_{F-td}$) species (Chen et al., 2005). The Al signal decreased in the following order: NaMOR > NaMOR/MCM-41(1M) > NaMOR/MCM-41(2M) > NaMOR/MCM-41(3M) suggesting dealumination during the composite preparation. Although Al atoms in NaMOR were not dissolved in the base solution during the preparation of composite zeolites, they could be hydrolyzed in hydrothermal after aged in the autoclave. A treatment of MOR by base could generate extra-framework Al (^{27}Al MAS NMR signal appeared at 0 ppm) which could be considered as structure defect. In this study, after mixing the partially dissolved NaMOR with CTAB and treatment under hydrothermal condition, the peak at 0 ppm was not observed. Such Al defect sites could be the origin of formation of the composite structural framework by bonding with silicate species in the alkaline solution to regenerate the framework Al connecting with MCM-41 structure.

NH$_3$-TPD profiles of the NaMOR and NaMOR/MCM-41 composites from 130 to 650 °C are shown in Figure 5.6. All samples showed large two peaks at low temperature region (max at around 250 and 350°C with different peak ratio). These peaks could be from ammonia adsorbed on Na cation and surface silanol groups. A small peak at high temperature could be seen in some samples. The high temperature peaks are often related

to Lewis acid site which are extra-framework Al. These results are consistent with those from NMR which inferred that most Al atoms of the NaMOR/MCM-41 composites were in the framework. The acid amounts (mmol/g_{cat}) calculated from the total peak areas are included in Table 5.1. Because the major peaks were in the low temperature region, they could not represent the acidity of the composites. Thus, the acid and base properties of the composites were investigated further by testing them on decomposition of MBOH.
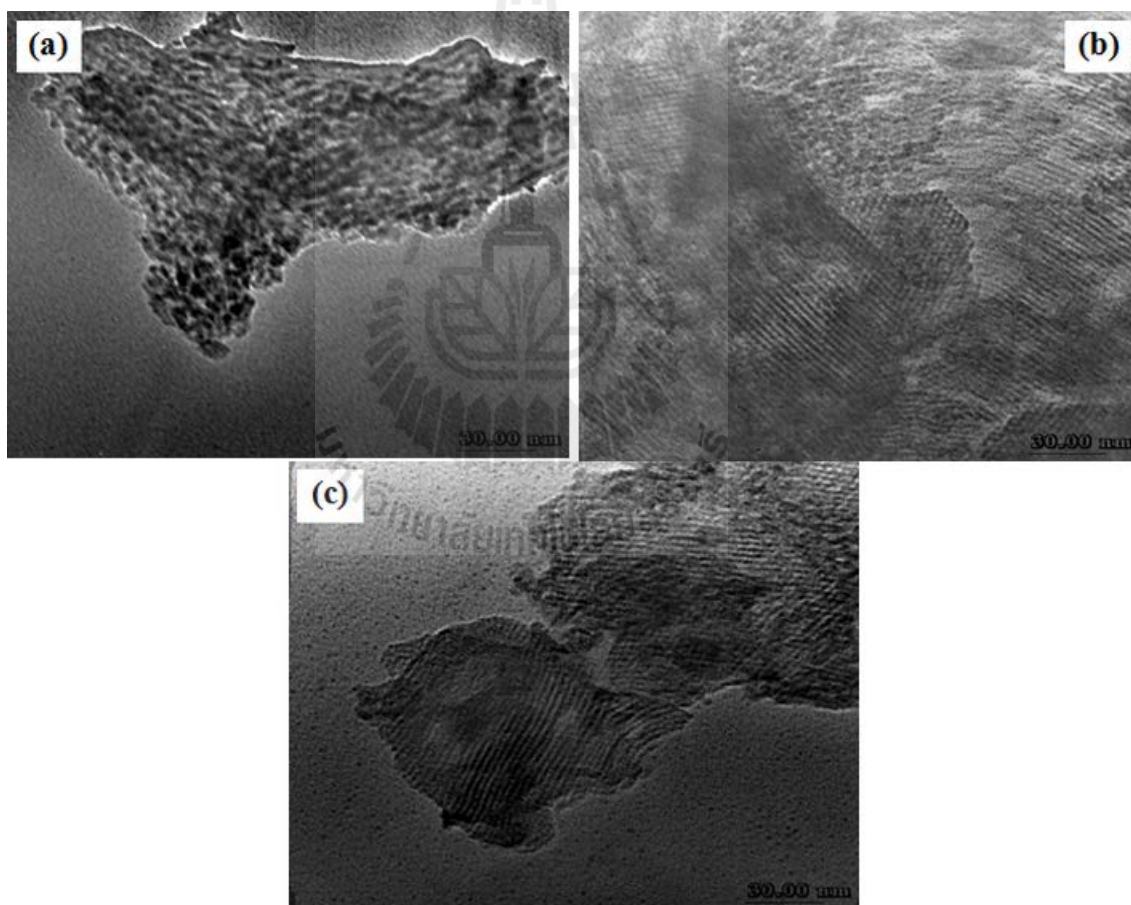

Figure 5.4 TEM of the NaMOR/MCM-41(1M) (a), NaMOR/MCM-41(2M) (b) and NaMOR/MCM-41(3M) (c) composite zeolites.
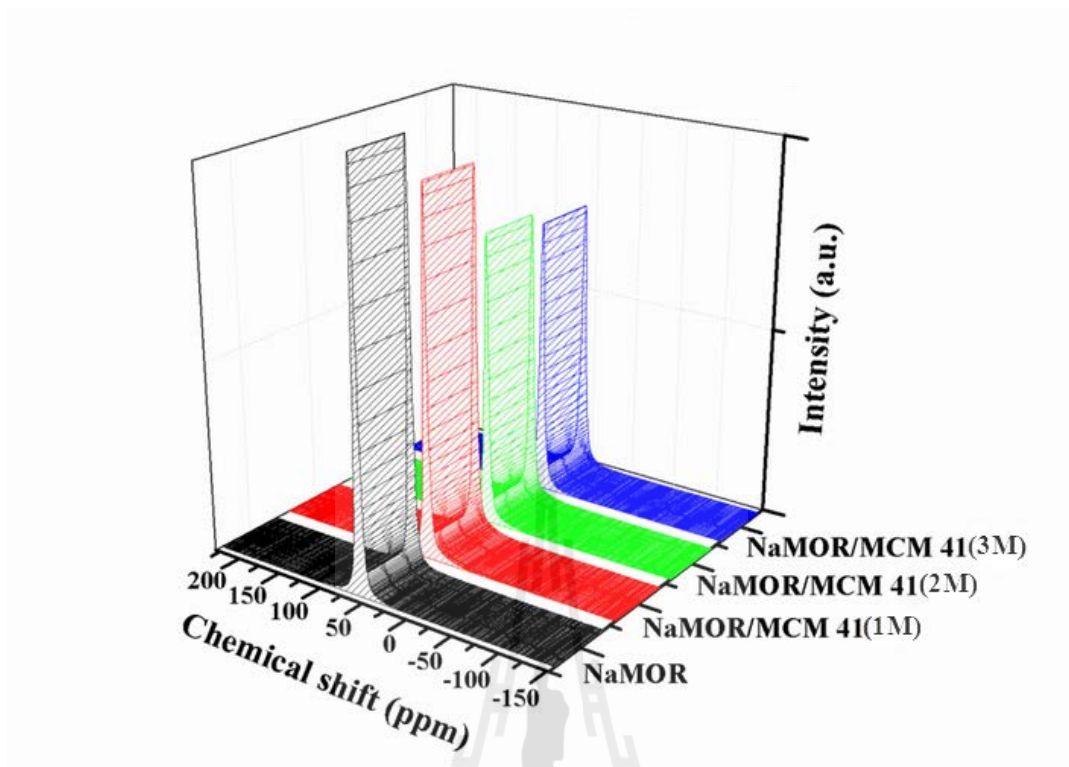
Figure 5.5 ^{27}Al MAS NMR spectra of the parent NaMOR, NaMOR/MCM-41(1M), NaMOR/MCM-41(2M) and NaMOR/MCM-41(3M) composite zeolites.
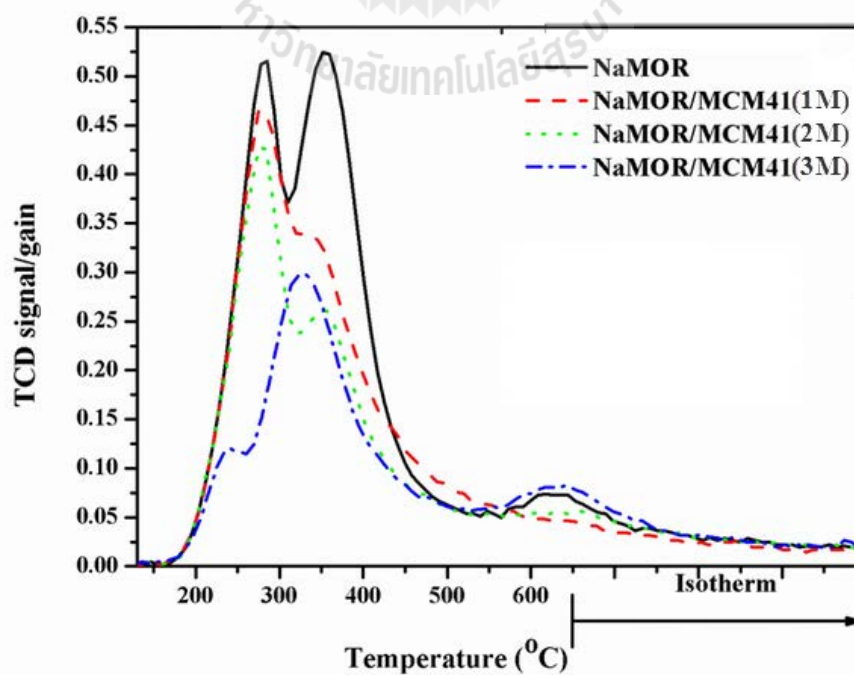
Figure 5.6 NH$_3$-TPD profiles of the NaMOR, NaMOR/MCM-41(1M), NaMOR/MCM-41(2M) and NaMOR/MCM-41(3M) composite zeolites.

Table 5.1 Results from nitrogen adsorption-desorption and NH_3-TPD.

Samples	Surface area[a] (m^2/g)	Microporevolume[b] (cm^3/g)	Mesoporevolume[b] (cm^3/g)	External surface area[b] (m^2/g)	Acid site$_{total}$[c] $(mmol/g)$
Parent NaMOR	414	0.18	-	36	0.27
NaMOR/MCM-41(1M)	526	0.22	0.08	66	0.26
NaMOR/MCM-41(2M)	477	0.15	0.19	164	0.24
NaMOR/MCM-41(3M)	569	0.12	0.28	323	0.29

[a] BET method, [b] t-Plot method and [c] NH_3-TPD.

5.3.2 Decomposition of MBOH on NaMOR and NaMOR/MCM-41 composites

To study the acid and base properties of the NaMOR/MCM-41 composites, the model reaction of MBOH was used on all samples (Lauron-Pemot et al., 1991). The conversion of MBOH on acid sites produces 2-methyl-1-butene-3-yne (MBYNE) by dehydration and 3-methyl-2-butenal (prenal) by intramolecular rearrangements. The conversion on basic sites produces acetone and acetylene by cleavage of C-C bond. Moreover, the reaction on defect sites generates 3-hydroxyl-3methyl-2-butanone (HMB) and 3-methyl-2-butyne-2-one (MIKP) by dehydrated product.

The results from decomposition of MBOH on NaMOR and the composite zeolites are shown in Figure 5.7. The conversions on all samples decreased with time and became nearly constant after two hours. All the composites were more active than the

parent NaMOR and the MBOH conversions were in the following order: NaMOR/MCM-41(3M) > NaMOR/MCM-41(2M) > NaMOR/MCM-41(1M). The results suggested that the active sites were on both NaMOR and MCM-41 components in the composites. The decrease of conversions seemed to vary with the extent of MOR structure which decreased when more NaOH concentration was used. The presence of micropores could cause difficulty in diffusion of starting reagents, intermediates and products from the reactions leading to deactivation by coke formation. With the presence of mesopores, the diffusive properties were improved and the deactivation became slower.

Figure 5.8(a)-(d) shows selectivities of products from the decomposition of MBOH. On the parent NaMOR, the main products were acetone and acetylene with the ratio nearly 1:1. These products were generated from basic sites which were mainly the Na cation. Another product from the parent NaMOR was MBYNE which was generated from acid sites which could be hydroxyl groups on the zeolite surface. The product selectivities on the NaMOR/MCM-41 composites were different from those from the parent NaMOR. MBYNE became the major products which could be generated from silanol groups on MCM-41 surface which were more abundant than the parent zeolite. Among the composites, the amount of MBYNE in the following order: NaMOR/MCM-41(3M) > NaMOR/MCM-41(2M) > NaMOR/MCM-41(1M) suggesting the dependence on the extent of MCM-41 in the composites. The products from basic sites, acetone and acetylene with the ratio 1:1 were also obtained from the composites and the amounts could be range in the following order: NaMOR/MCM-41(1M) > NaMOR/MCM-41(2M) > NaMOR/MCM-41(3M) suggesting the dependence on the extent of NaMOR in the composites.

Figure 5.7 Conversion of the MBOH on the NaMOR, NaMOR/MCM-41(1M), NaMOR/MCM-41(2M) and NaMOR/MCM-41(3M) composite zeolites.
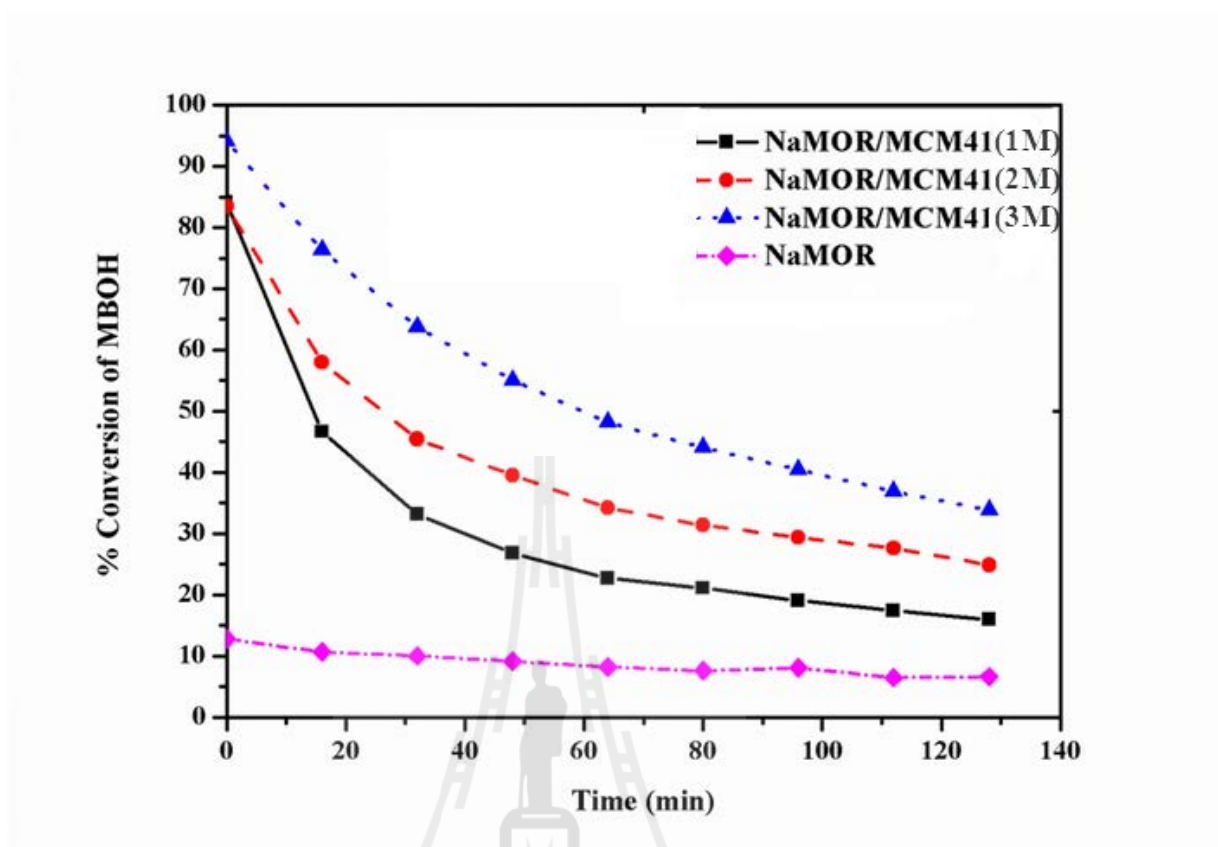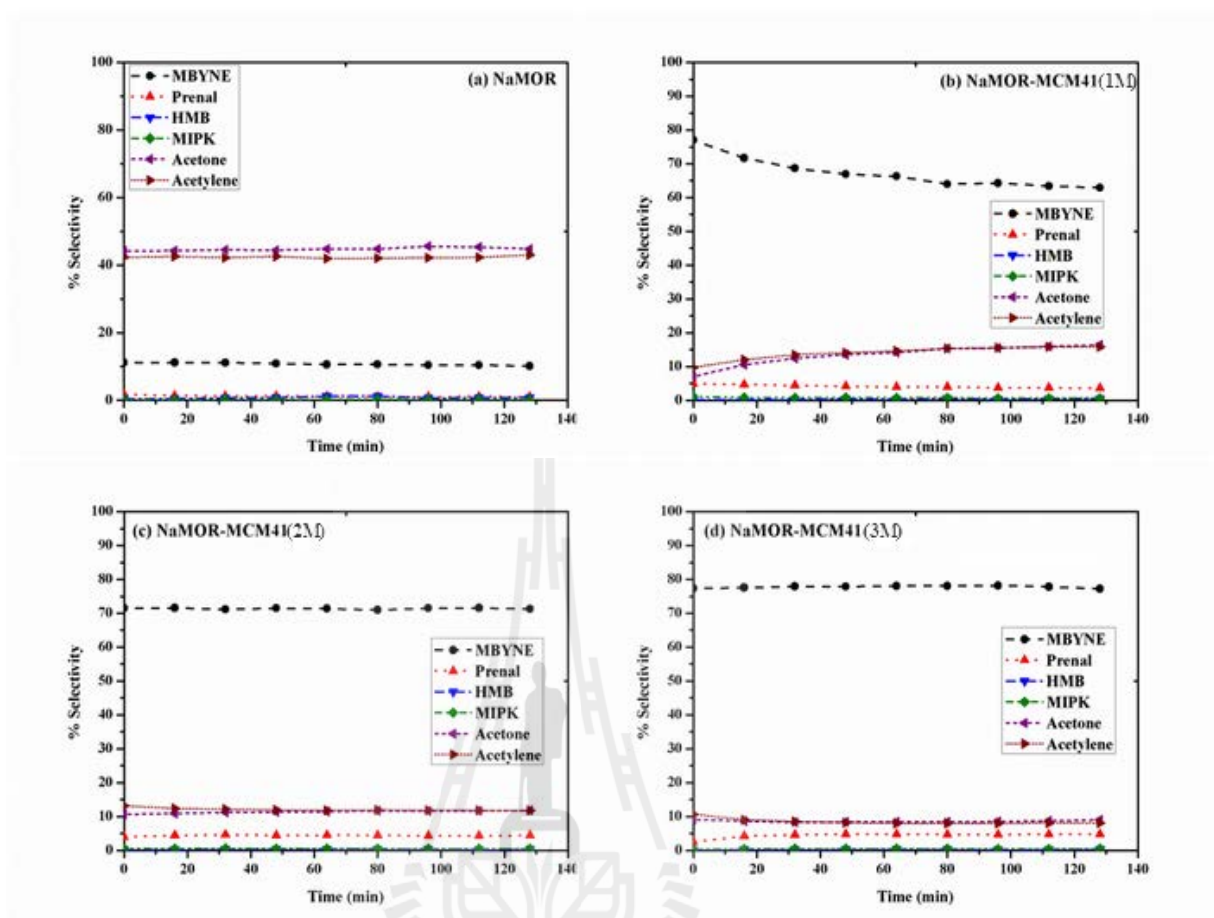
Figure 5.8 Selectivity products from decomposed of MBOH on the NaMOR, NaMOR/MCM-41(1M), NaMOR/MCM-41(2M) and NaMOR/MCM-41(3M) composite zeolites.

5.3.3 Characterization of Fe catalysts supported on NaMOR/MCM-41 composites

For XRD profiles of the ABMOR and Fe/ABMOR IE catalyst did not shown in this report. When the NaMOR was treated with acid-base (ABMOR) and further was transformed to proton form. The diffraction peak positions of ABMOR were similar to that the NaMOR pattern. However, the intensities peak of ABMOR sample is higher than the NaMOR sample. O'Donovan et al. (1995) reported an effect of ion exchange, the sodium ions were removed without affecting the Si/Al ratio during the unit cell was changed resulting different of the intensity peak. Moreover, after ABMOR in ammonium form was ion-exchanged with iron solution, the peaks at 14.5, 24 and 36 degrees were observed. These are peak of Fe_2O_3 (JCPDS, 1998).

The Fe/NaMOR/MCM-41 (2M) IE1 composite catalyst, the batch composition was started from the Fe/HMOR as a catalyst-alumina and the SiO_2 as a silicate source. The characteristic peak of both MCM-41 and MOR regions were observed (Figure 5.9). On the other hand, the Fe/NaMOR/MCM-41 (2M) IE2 composite catalyst, the batch composition was started from only the Fe/HMOR IE as a catalyst and silica-alumina source. The peak of MCM-41 at 3.8 and 4.5 degrees were not observed (Figure 5.9). When used Fe/HMOR IE directly, the silicon atom was blocked by Fe resulting partially of silicate formed structure of MCM-41.
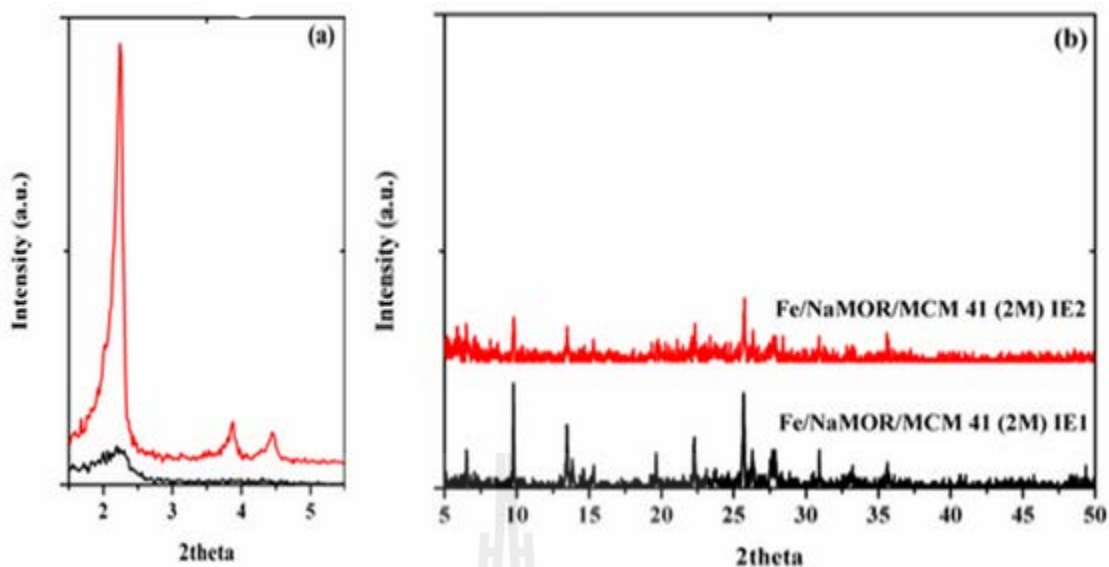
Figure 5.9 XRD profiles of the Fe/NaMOR/MCM-41 (1M) IE1 and Fe/NaMOR/MCM-41
(1M) IE2 catalysts supported Fe by ion-exchanged method at low 2θregion (a)
and high 2θ region (b).

The XRD pattern of Fe catalysts supported on composites zeolites by IMP
method are shown in Figure 5.10. After loading with Fe, the characteristic peaks of
NaMOR structure did not change. In contrast, the characteristic peaks of MCM-41
structure decreased nearly completely on 5Fe/NaMOR/MCM-41(2M) and
5Fe/NaMOR/MCM-41(3M). The absence of MCM-41 peaks from the
5Fe/NaMOR/MCM-41(1M) sample was not surprising because such peaks were not found
at the first place on the bare composites. From XRD patterns, the peaks corresponding to
oxides of Fe such as Fe_2O_3 at 33.5, 36.0, 49.8 and 54.2 degrees (JCPDS, 1998) were not
clearly identified, although the peak at 33.5 degree which was also found on the composites
seemed to be increase in intensity. As a result, it was necessary to confirm the species of Fe
by other technique such as XANES.
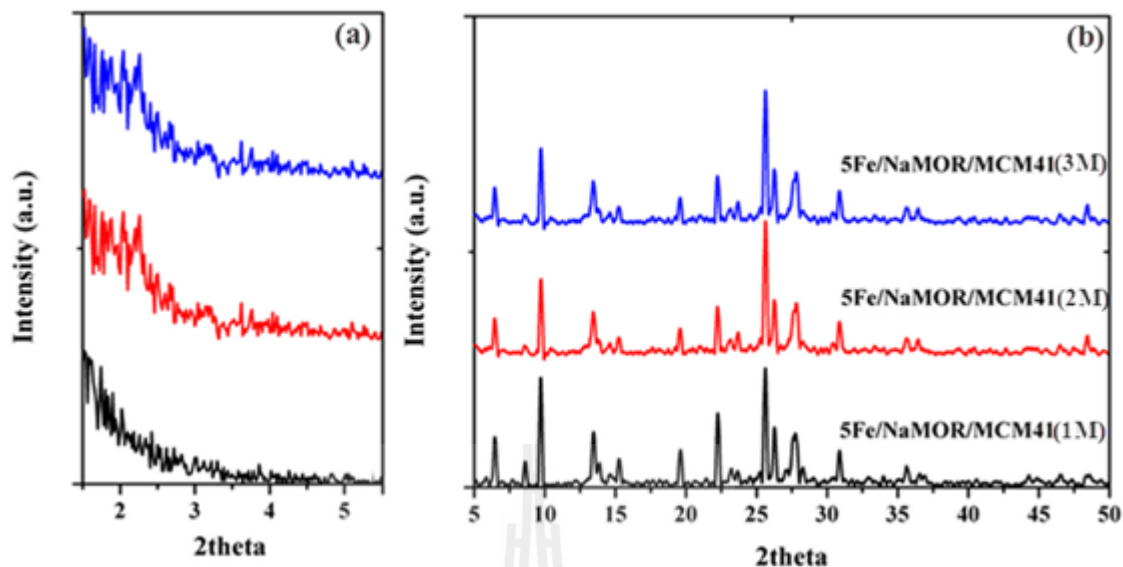
Figure 5.10 XRD profiles of the NaMOR/MCM-41(1M), NaMOR/MCM-41(2M) and NaMOR/MCM-41(3M) composite zeolites supported 5 wt.%Fe catalysts at low 2θ region (a) and high 2θ region (b).

        To check whether the mesoporous structures on supported catalysts collapsed after the catalyst preparation, they were analyzed by TEM again. The TEM images of the Fe catalysts supported on the NaMOR/MCM-41 composites are shown in Figure 5.11. Similar to the composites before impregnation with Fe, mesoporous structures could be observed on 5Fe/MOR/MCM-41(2M) and 5Fe/MOR/MCM-41(3M) but not on 5Fe/MOR/MCM-41(1M).
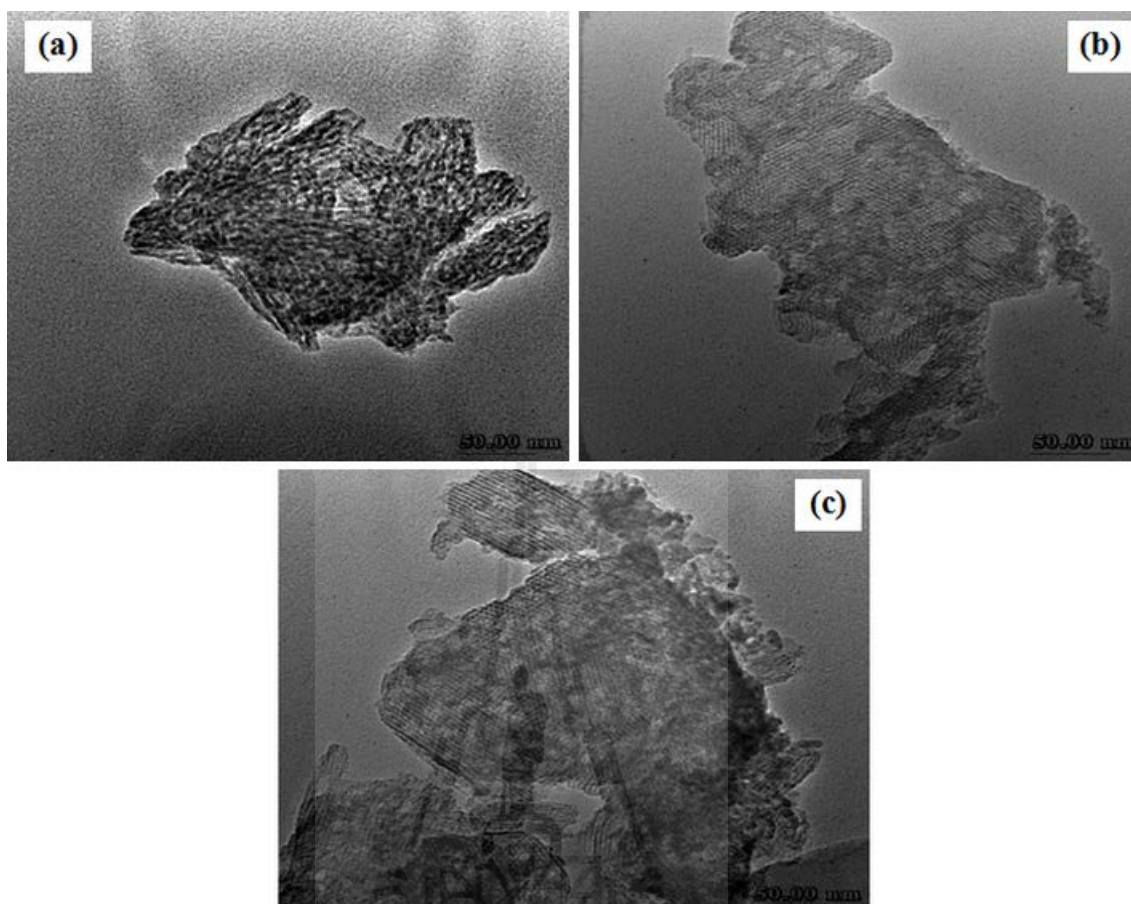
Figure 5.11 TEM of 5 wt.% Fe supported catalyst on the NaMOR/MCM-41(1M) (a), NaMOR/MCM-41(2M) (b) and NaMOR/MCM-41(3M) (c) composite zeolites.

Table 5.2 Results from linear combination fitting of XANES spectra of 5 wt.% Fe supported on the NaMOR/MCM-41(1M), (2M) and (3M) composite zeolites, respectively.

Catalyst	5Fe/NaMOR/MCM 41(1M)	5Fe/NaMOR/MCM 41(2M)	5Fe/NaMOR/MCM 41(3M)
FeO (%)	0.6	0.0	1.4
Fe_2O_3 (%)	99.4	100.0	98.6
Fe_3O_4 (%)	0.0	0.0	0.0

The forms of Fe in the supported catalysts could be confirmed by comparing XANES spectrum of each one with standards containing Fe in various oxidation states including FeO, Fe_2O_3 and Fe_3O_4. As shown in Figure 5.12, the XANES spectra of all supported Fe catalysts were similar to that of the Fe_2O_3 standard indicating that all Fe had oxidation state of +3. Furthermore, the composition of Fe phases in all catalysts could be calculated from the XANES spectra by Linear Combination Fitting tool in ATHENA program. Results from the calculation (Table 5.2) confirmed that the form of Fe in all catalysts was Fe_2O_3.
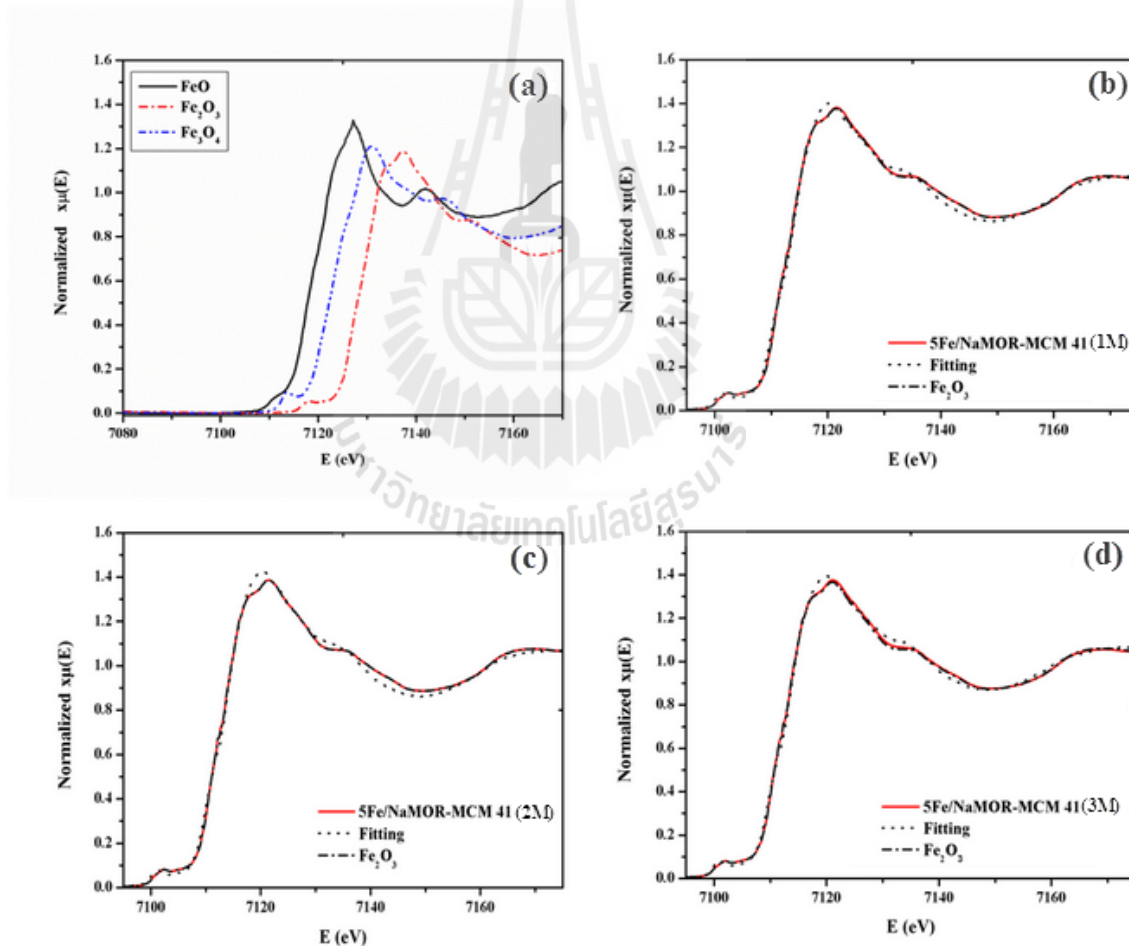
Figure 5.12 XANES spectra of FeO, Fe_2O_3 and Fe_3O_4 standards (a) and linear combination fitting of 5Fe/NaMOR/MCM-41(1M), 5Fe/NaMOR/MCM-41(2M) and 5Fe/NaMOR/MCM-41(3M) composites (b)-(d).

Table 5.3 Catalytic performance of NaMOR-MCM-41 composite zeolites with phenol:H_2O_2 mole ratio = 1:3, solvent = water and temperature = 70 °C.

Sample	Time (min)	% Conversion of phenol	% Selectivity		
			CE	HQ	BQ
NaMOR/MCM-4(1M)	15	9.6	0.0	0.0	100.0
	30	5.3	0.0	0.0	100.0
	60	8.0	0.0	0.0	100.0
	120	6.3	0.0	0.0	100.0
	180	3.1	0.0	0.0	100.0
NaMOR/MCM-4(2M)	15	17.1	0.0	0.0	100.0
	30	16.8	0.0	0.0	100.0
	60	13.7	0.0	0.0	100.0
	120	5.9	0.0	0.0	100.0
	180	8.8	0.0	0.0	100.0
NaMOR/MCM-4(3M)	15	12.5	0.0	0.0	100.0
	30	5.0	0.0	0.0	100.0
	60	6.7	0.0	0.0	100.0
	120	9.3	0.0	0.0	100.0
	180	9.0	0.0	0.0	100.0

5.3.4 Catalytic performance of 5Fe/MOR/MCM-41 for phenol hydroxylation

Both bare NaMOR/MCM-41 composites and 5Fe/NaMOR/MCM-41 catalysts were tested for phenol hydroxylation with the same condition in chapter III. The phenol conversion and product selectivities on the bare NaMOR/MCM-41 composites are shown in Table 5.3. The conversions on all composites were similar, fluctuating around 10% and the only product observed was benzoquinone (BQ).

Table 5.4 Catalytic performance of 5 wt.% Fe supported NaMOR-MCM-41 composite zeolites and with phenol:H_2O_2 mole ratio = 1:3, solvent = water and temperature = 70 °C.

Sample	Time (min)	% Conversion of phenol	% Selectivity		
			CE	HQ	BQ
5Fe/NaMOR/MCM-4(1M)	15	8.2	0.0	0.0	100.0
	30	50.2	36.0	27.5	36.6
	60	67.1	51.0	49.0	0.0
	120	67.0	55.0	45.0	0.0
	180	68.2	52.3	47.7	0.0
5Fe/NaMOR/MCM-4(2M)	15	4.8	0.0	0.0	100.0
	30	7.3	0.0	0.0	100.0
	60	65.1	52.6	47.4	0.0
	120	66.2	51.1	48.9	0.0
	180	68.9	49.3	50.7	0.0
5Fe/NaMOR/MCM-4(3M)	15	6.3	0.0	0.0	100.0
	30	30.6	0.0	0.0	100.0
	60	65.9	48.7	50.7	0.6
	120	70.1	50.8	49.2	0.0
	180	68.7	49.4	50.6	0.0

The phenol conversion and product selectivities on 5Fe/NaMOR/MCM-41 catalysts are shown in Table 5.4. The reaction on all catalysts reached equilibrium within 60 min because both conversions and selectivities became nearly constant. This fast reaction rate was also found when Fe was loaded on MOR modified with both acid and base (Chapter III) because diffusion of reactants was facilitated by the presence of mesopores. For selectivities, only BQ was observed as a major product within the first 30 min on all Fe catalysts. The results suggested that BQ was a kinetic product from over-oxidation of phenol by the excess of H_2O_2. The BQ could be responsible for the tar formation from polymerization reaction. As the time was prolonged, BQ was no longer

observed. The products were only catechol (CE) and hydroquinone (HQ) with the CE:HQ ratio of about 1:1. The conversions on 5Fe/NaMOR/MCM-41 were higher than Fe catalysts on MOR modified with acid, base or both (Chapter III) and the CE and HQ selectivities were also improved; the CE:HQ ratio in the previous work (Chapter III) was about 3:2. The improvement was likely due to the more uniform mesopores generated by using organic template.

To compare position of the Fe on support has effects to the reaction rate and product selectivity of phenol hydroxylation reaction. The Fe/NaMOR-MCM-41(2M) IE composite catalysts were prepared by immobilization of Fe and the Fe/ABMOR IE catalysts was prepared by ion-exchanged method. The catalytic performance of phenol hydroxylation reaction is shown in Table 5.5.

The phenol conversion on Fe/ABMOR IE and catalyst increased with time and the products observed were CE, HQ and BQ. The selectivity for BQ rapidly decreased as the conversion increased. The conversion obtained was considerably low when compared with the 5Fe/ABMOR catalyst which was about 60% at the first hour (Chapter III). However, when took four hour for the conversion to reach about 62% and the ratio selectivity of CE:HQ is similar the 5Fe/ABMOR catalyst. The conversion on Fe/ABMOR IE catalyst was lower than 5Fe/ABMOR catalyst probably because the amount of active metal deposited on the support was lower.

Table 5.5 Catalytic performance of Fe supported on modified MOR zeolites by ion-exchanged method with phenol:H_2O_2 mole ratio = 1:3, solvent = water and temperature = 70 °C.

Sample	Time (min)	% Conversion of phenol	% Selectivity		
			CE	HQ	BQ
Fe/ABMOR IE	15	4.9	0.0	0.0	100.0
	30	2.1	0.0	0.0	100.0
	60	6.6	0.0	0.0	100.0
	120	22.8	16.9	0.0	83.1
	180	62.2	52.5	45.5	2.0
	240	61.6	54.9	44.9	0.2
Fe/NaMOR/MCM-41(2M) IE1	15	6.3	0.0	0.0	100.0
	30	5.5	0.0	0.0	100.0
	60	6.8	0.0	0.0	100.0
	120	6.6	0.0	0.0	100.0
	180	6.9	0.0	0.0	100.0
	240	6.2	0.0	0.0	100.0
Fe/NaMOR/MCM-41(2M) IE2	15	4.5	0.0	0.0	100.0
	30	5.9	0.0	0.0	100.0
	60	5.8	0.0	0.0	100.0
	120	12.9	0.0	0.0	100.0
	180	39.8	37.1	0.0	62.9
	240	62.3	63.2	31.9	4.9

The composite catalysts also tested for phenol hydroxylation. The Fe/NaMOR/MCM-41(2M) IE1 catalyst was prepared by using both Fe/HMOR and SiO_2. The phenol conversion fluctuated around 6.5% and the only product observed was BQ. The results suggested that BQ was from over-oxidation of phenol by the excess of H_2O_2. The BQ was likely responsible for tar formation which could be confirmed by mass balance. On

the other hand, the Fe/NaMOR/MCM-41(2M) IE2 catalyst was prepared by using only Fe-HMOR. The phenol conversion increased with time and the products observed were CE, HQ and BQ. Again, it took four hour for the BQ selectivity to decrease. However, the ratio of CE:HQ is different with Fe-ABMOR IE catalyst. The ratio of CE:HQ on the Fe/NaMOR/MCM-41(2M) IE2 catalyst is 2:1 and on the Fe/ABMOR IE catalyst is 3:2.

The phenol conversion was low on the Fe/NaMOR/MCM-41(2M) IE1 composite catalyst. It was possible that the phenol hydroxylation reaction occurred in mesopores because most Fe ions were in cavities of MOR and some could be immobilized on the wall of MCM-41. In contrast, on the Fe/NaMOR/MCM-41(2M) IE2 composite, the Fe is dispersed in framework of MOR and MCM-41. It can be seen clearly that the rate reaction will increased rapidly when comparing at the same time.
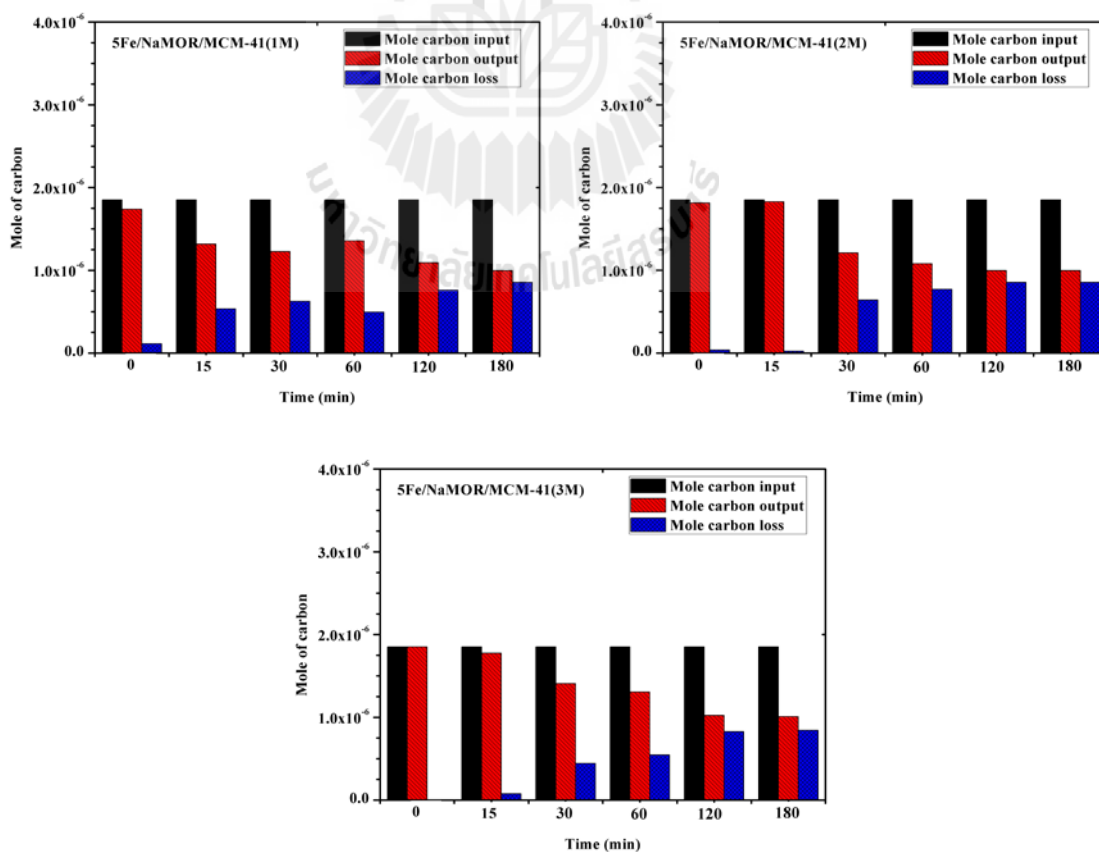

Figure 5.13 Mole carbon balance for phenol hydroxylation of 5Fe supported on the NaMOR/MCM-41(1M), (2M) and (3M) composite zeolites.
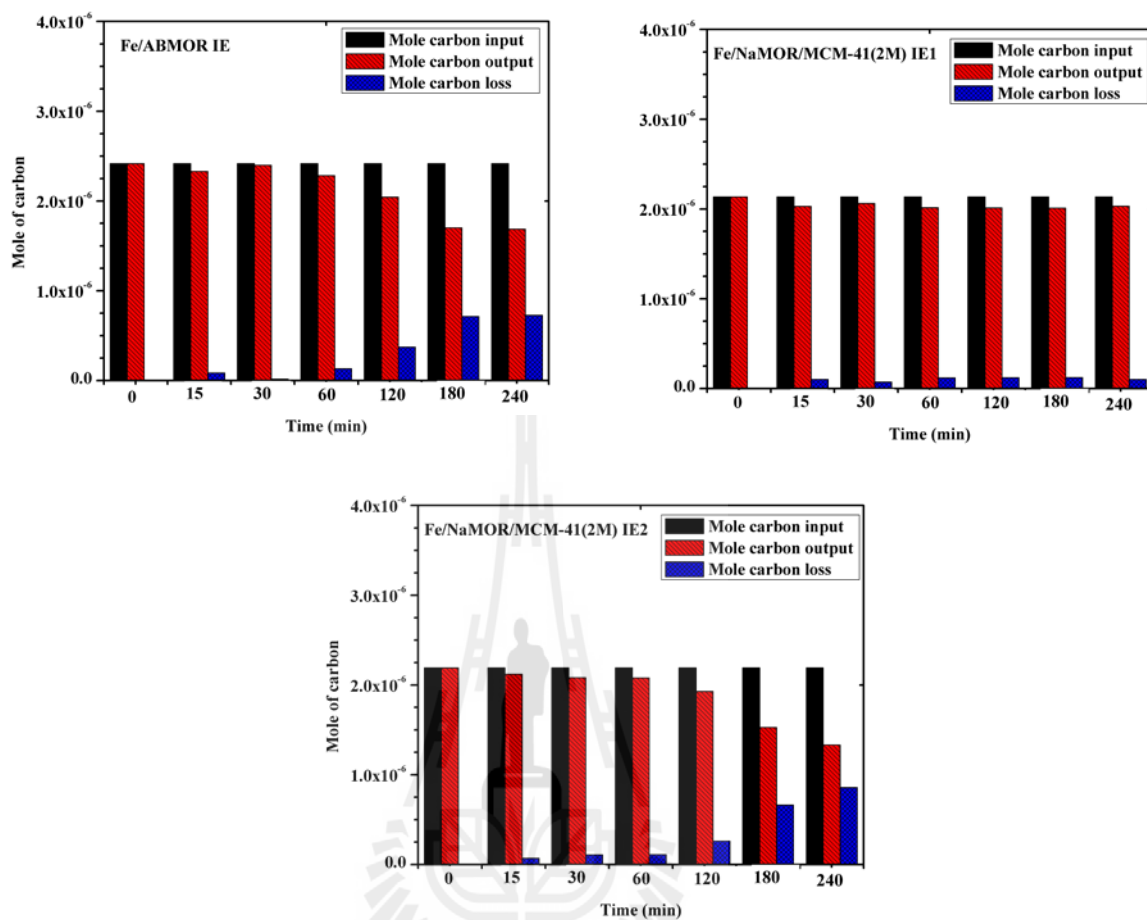
Figure 5.14 Mole carbon balance for phenol hydroxylation of Fe supported on modified MOR zeolites by ion-exchange method.

The mole carbon balancesfrom phenol hydroxylation on 5Fe supported on the NaMOR/MCM-41composite zeolites are shown in Figure 5.13. The amount of carbon loss increased with time and the by-products, black tarry materials are formed. The tar was possibly from polymerization of BQ which was originated at the beginning of the reaction.

Carbon mole balances from phenol hydroxylation on Fe supported on modified MOR zeolites by ion-exchange method are shown in Figure 5.14. The initial products from these catalysts were also BQ which could be responsible for the tar formation. The loss was low on Fe/NaMOR/MCM-41 (2M) IE1 because the phenol conversion was low.

5.4 Conclusions

The NaMOR/MCM-41 composites were synthesized by using silica-alumina source from partially dissolved NaMOR and CTAB as an organic template. The phases of MOR and MCM-41 in the composites were confirmed by XRD. The increase in concentration of NaOH solution to dissolve NaMOR caused the decrease of MOR phase and increase MCM-41 phase. Results of N_2 adsorption-desorption further confirmed the MCM-41 mesoporous properties including an increase in total surface area as well as mesopore surface area and volume. The mesoporous structure was further confirmed by TEM revealing ordered structure. Results from ^{27}Al MAS NMR provided the information of Al atoms that are mainly in the zeolite framework with tetrahedral geometry. NH_3-TPD showed the difference in ammonia desorption temperature from the composites despite similar total acid sites and suggested that weak acid sites were the majority in the NaMOR/MCM-41 composites. When the composites were tested for decomposition of MBOH, they gave the major products generated from acid sites whereas the parent NaMOR gave the major products from basic sites.

When Fe was loaded on NaMOR/MCM-41 composites and characterized by XRD, the MOR phase of the composite did not change but the MCM-4 phase decreased. TEM images still showed mesoporous structure in the composites. The form of Fe in all catalysts analyzed by XANES was mainly Fe_2O_3. When tested for phenol hydroxylation, the reaction reached equilibrium within 60 min. The phenol conversions on all catalysts and products selectivities of CE and HQ were improved from Fe on MOR modified by other method. The conversion were in the range of 65-70% and CE:HQ ratio was about 1:1.

5.5. References

Chen, T.-H., Houthoofd, K. and Grobet, P. J. (2005). Toward the aluminum coordination in dealuminated mordenite and amorphous silica-alumina: a high resolution ^{27}Al MAS and MQ MAS NMR study. **Microporous and Mesoporous Materials**. 86: 31-37.

Choi, J. S., Yoon, S. S., Jang, S. H. and Ahn, W. S. (2006). Phenol hydroxylation using Fe-MCM-41 catalysts. **Catalysis Today**. 111: 280-287.

Groen, J. C., Peffer, L. A. A. and Pérez-Ramrez, J. (2003). Pore size determination in modified micro- and mesoporous materials. Pitfalls and limitations in gas adsorption data analysis. **Microporous and Mesoporous Materials**. 60: 1-17.

Ivanova, I. I., Kuznetsova, A. S., Knyazeva, E. E., Fajula, F., Thibault-Starzyk, F., Fernandez, C. and Gilson, J. -P. (2011). Design of hierarchically structured catalysts by mordenites recrystallization: Application in naphthalene alkylation. **Catalysis Today**. 168: 133-139.

JCPDS, Joint Committee on Powder Diffraction Standards. 1998. International Centre for Diffraction Data, Sets 1-48: 374.

Knözinger, H. and Kochloefl, K. (2003). Heterogeneous catalysis and solid catalysts. Bohnet, et al. (eds.). **Ullmann's encyclopedia of industrial chemistry** (vol. 16). (6th ed., pp. 315-431). Wiley-VCH Verlag GmbH, Weinheim.

Kurdi, J. and Tremblay, A. Y. (2002). The determination of interaction parameters in the characterization of polyetherimide gas separation membranes using the Horvath-Kawazoe model. **Desalination**. 148: 341-346.

Lauron-Pernot, H., Luck, F. and Popa, J. M. (1991). Methylbutynol: a new and simple diagnostic tool for acidic and basic sites of solids. **Applied Catalysis**. 78: 213-225.

Musa, M. A. A., Yin, C. -Y. and Savory, R. M. (2011). Analysis of the textural characteristics and pore size distribution of a commercial zeolite using various adsorption models. **Journal of Applied Sciences**. 11: 3650-3654.

O'Donovan, A. W., O'Connor. C. T. and Koch, K. R. (1995). Effect of acid and steam treatment of Na- and H-mordenite on their structural, acidic and catalytic properties. **Microporous Materials**. 5: 185-202.

Ou, D. L. and Chevalier, P. M. (2002). Organic-inorganic hybrids towards the preparation of nanoporous composite thin films for microelectronic application. **Chemical Research in Chinese Universities**. 18: 178-182.

Park, K. C., Yim, D. and Ihm, S. (2002). Characteristics of Al-MCM-41 supported Pt catalysts: effect of Al distribution in Al-MCM-41 on its catalytic activity in naphthalene hydrogenation. **Catalysis Today**. 74: 281-290.

Preethi, M. E. L., Revathi, S., Sivakumar, T., Manikandan, D., Divakar, D., Rupa, A. V. and Palanichami, M. (2008). Phenol hydroxylation using Fe/Al-MCM-41catalysts. **Catalysis Letters**. 120: 56-64.

Ravel, B. and Newville, M. (2005). ATHENA, ARTEMIS, HEPHAESTUS: data analysis for X-ray absorption spectroscopy using IFEFFIT. **Journal of Synchrotron Radiation**. 12: 537-541.

Roland, E. and Kleinschmit, P. (2003). Zeolites, Bohnet, M., et al. (eds.). **Ullmann's encyclopedia of industrial chemistry** (vol. 39). (6th ed., pp. 625-655). Wiley-VCH Verlag GmbH, Weinheim.

Rouquerol, F., Rouquerol, J. and Sing, K. (eds.). (1999). **Adsorption by powders and porous solids: principles, methodology and application**. London: Harcourt Brace & Company.

Wang, S., Dou, T., Li, Y., Zhang, Y., Li, X. and Yan, Z. (2004). Synthesis, characterization, and catalyticproperties of stable mesoporous molecularsieve MCM-41 prepared from zeolite mordenite. **Journal of Solid State Chemistry**. 177: 4800-4805.

Wang, S., Dou, T., Li, Y., Zhang, Y., Li, X. and Yan, Z. (2005). A novel method for the preparation of MOR/MCM-41 composite molecular sieve. **Catalysis Communications**. 6: 87-91.

Wang, X., Zhang, X., Wang, Y., Liu, H., Qiu, J., Wang, J., Han, W. and Yeung, K. L. (2011). Investigating the role of zeolite nanocrystal seeds in the synthesis of mesoporous catalysts with zeolite wall structure. **Chemistry of Materials**. 23: 4469-4479.

Zhang, H. J. and Li, Y. D. (2008). Preparation and characterization of Beta/MCM-41 composite zeolite with a stepwise-distributed pore structure. **Powder Technology**. 183: 73-78.

Zhao, W., Luo, Y., Deng, P. and Li, Q. (2001). Synthesis of Fe-MCM-48 and its catalytic performance in phenol hydroxylation. **Catalysis Letters**. 73: 199-202.
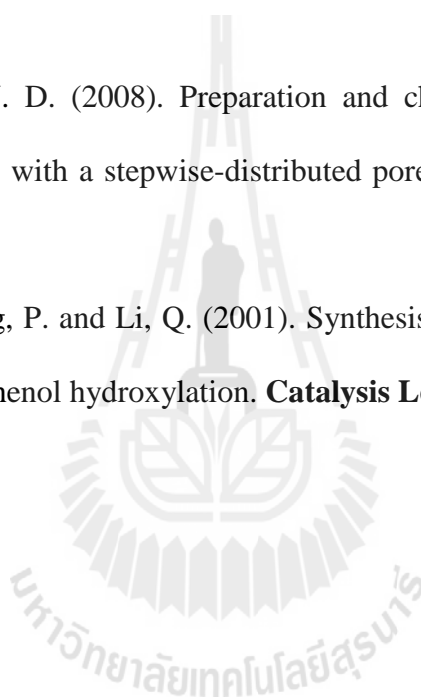
CHAPTER VI

CONCLUSION

Silica from rice husk was used for the synthesis of zeolite mordenite in sodium form (NaMOR) by hydrothermal method. The NaMOR was further transformed to proton form (HMOR), and modified by treatment with acid (AMOR), base (BMOR) and both acid-base (ABMOR). The produced AMOR, BMOR and ABMOR increase of surface area without destroying the MOR crystal structure. Mesopores with average diameter of 2.7 nm were produced on ABMOR. From ^{27}Al MAS NMR, HMOR and BMOR showed similar spectrum and the removal of Al acid sites in AMOR and ABMOR were confirmed. From NH$_3$-TPD, strong acid sites (high temperature band) decreased in the following order: HMOR > BMOR > ABMOR > AMOR. In the MBOH test reaction, the MBOH conversion was in the following order: ABMOR > BMOR > AMOR ≈ HMOR ≈ NaMOR and the highest acidity was suggested on ABMOR. When Fe was loaded on NaMOR, HMOR, AMOR, BMOR and ABMOR, the major form of Fe active in all catalysts was Fe$_2$O$_3$. When the supported catalysts were tested for phenol hydroxylation, the fastest and highest phenol conversion was observed on 5Fe/ABMOR producing CE and HQ.

The NaMOR/MCM-41 composites were synthesized by using silica-alumina source from partially dissolved NaMOR and CTAB as an organic template. When Fe was loaded on NaMOR/MCM-41 composites, the form of Fe in all catalysts analyzed by XANES was mainly Fe$_2$O$_3$. When tested for phenol hydroxylation, the reaction reached equilibrium within 60 min. The phenol conversions on all catalysts and products selectivities of CE and HQ were improved from Fe on MOR modified by other method. The conversion were in the range of 65-70% and CE:HQ ratio was about 1:1.

APPENDICES

APPENDIX A

EXPERIMENTAL SET-UP AND EXPERIMENTAL CONDITION FOR
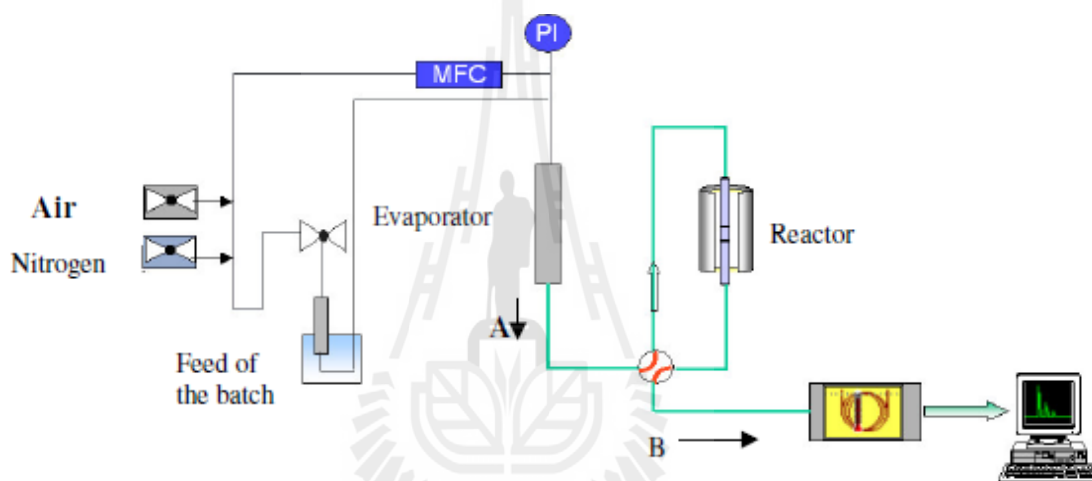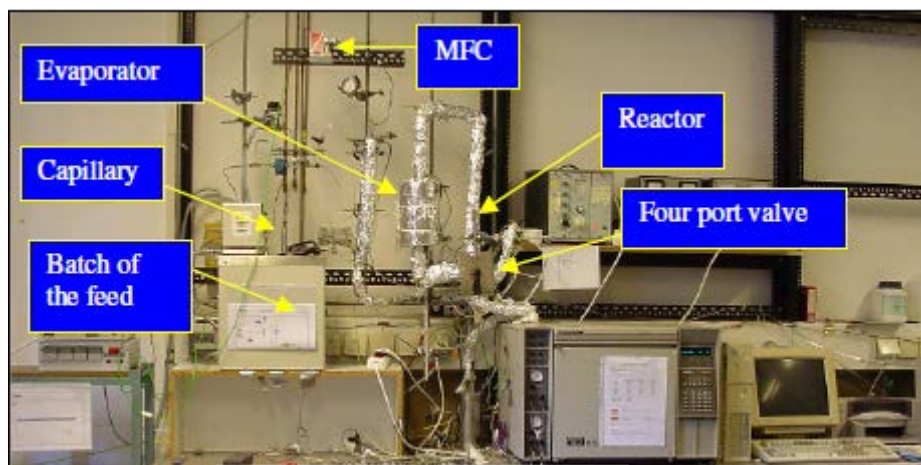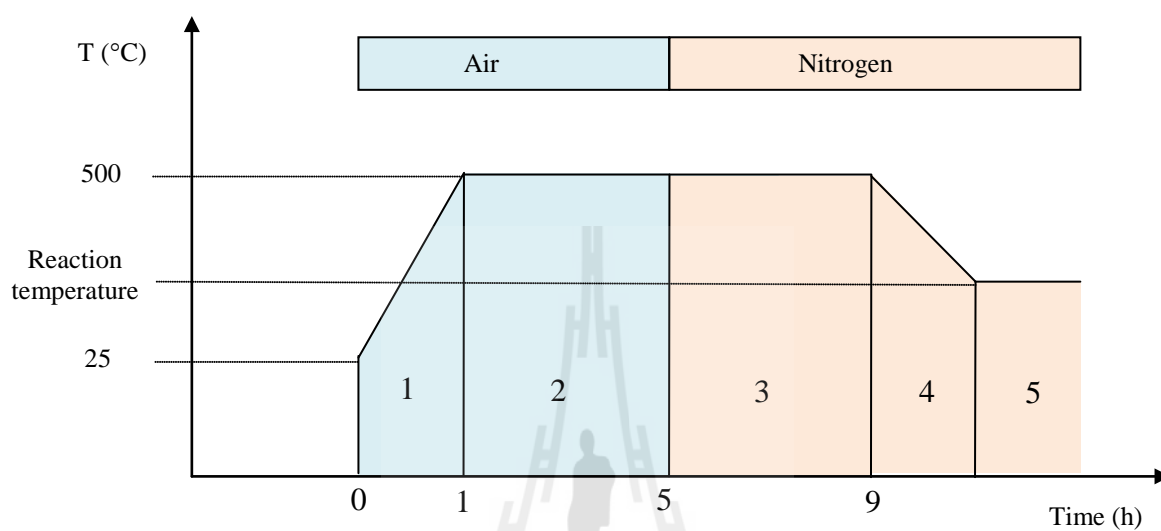
MBOH TEST REACTION

Figure A-1 The apparatus for the MBOH test reaction.

Condition for MBOH test reaction

The conversion of MBOH was carried out in a fixed-bed reactor (**Figure A**-1). The MOR and modified MOR samples were pressed and sieved to 200 - 315 μm mesh size. One hundred milligrams of sample was packed in the center of a quartz tubular reactor, activated under air flow by heating to 400 °C with a rate of 8 °C/min and holding for 4 h to remove water and CO_2 adsorbed on the surface, and kept under to N_2 flow at this temperature for 4 h. After the activation, the reactor was cooled to the reaction temperature (180 °C). N_2 was flowed over a storage vessel containing a mixture of MBOH and toluene (95:5 v/v) cooled at 13 °C before entering the reactor (**Figure A**-2). Toluene was used as

an internal standard because it was not converted over the catalysts. The reaction products were analyzed by a gas chromatograph (Hewlett Packard HP 5890 Series II).

No.	Condition
1	Heating up
2	Oxidation (air)
3	Inertization (N_2)
4	Cool down to reaction temperature
5	Reaction

Figure A-2 Activation procedure.
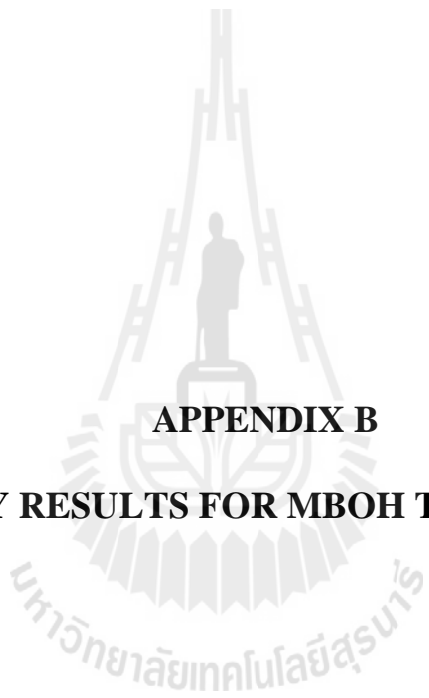
APPENDIX B

SUMMARY RESULTS FOR MBOH TEST REACTION

Table B-1 MBOH conversions and product selectivity over parent NaMOR and modified MOR after activated temperature at 350 °C for 8 h under a N_2-gas and reaction temperature at 180 °C.

. Sample	Time (min)	% Conversion of MBOH	% Selectivity					
			Acidic site		Amphoteric site		Basic site	
			MBYNE	Prenal	HMB	MIPK	Acetone	Acetylene
NaMOR	0	12.78	11.18	1.76	0.40	0.15	44.23	42.28
	16	10.69	11.19	1.37	0.44	0.13	44.29	42.57
	32	10.00	11.15	1.22	0.68	0.17	44.55	42.23
	48	9.16	10.87	1.23	0.75	0.15	44.42	42.59
	64	8.22	10.59	1.15	1.19	0.24	44.82	42.01
	80	7.60	10.62	1.03	1.27	0.26	44.78	42.04
	96	8.07	10.40	1.02	0.63	0.18	45.56	42.22
	112	6.50	10.43	1.04	0.74	0.19	45.33	42.28
	128	6.64	10.14	1.02	0.83	0.13	44.84	43.04
HMOR	0	14.53	33.67	2.98	0.50	0.35	31.94	30.56
	16	12.56	31.49	2.71	0.66	0.32	32.90	31.91
	32	10.98	30.32	2.48	0.54	0.37	34.14	32.16
	48	9.98	29.19	2.30	0.68	0.31	34.47	33.04
	64	8.96	28.98	2.13	0.76	0.30	34.92	32.90
	80	8.65	28.30	2.03	0.60	0.31	35.66	33.11
	96	8.61	26.90	1.96	1.00	0.34	36.52	33.28
	112	6.41	28.93	1.74	0.85	0.30	35.59	32.59
	128	7.59	26.30	1.80	0.97	0.32	37.07	33.54
BMOR	0	34.88	50.76	4.44	0.44	0.66	21.32	22.39
	16	24.54	48.84	3.72	0.46	0.57	23.03	23.38
	32	20.11	46.89	3.47	0.52	0.56	24.35	24.20
	48	16.71	45.64	3.22	0.40	0.49	25.41	24.84
	64	14.86	45.64	3.03	0.40	0.46	25.54	24.92
	80	13.90	44.40	2.90	0.74	0.50	26.28	25.19
	96	12.95	44.52	2.76	0.46	0.48	26.47	25.32
	112	12.17	43.97	2.66	0.50	0.42	26.74	25.71
	128	11.32	44.15	2.60	0.49	0.41	26.59	25.76
AMOR	0	15.74	45.86	3.44	0.63	0.52	18.91	30.64
	16	13.41	42.71	3.28	0.74	0.41	22.39	30.48
	32	11.37	40.68	3.11	0.54	0.35	24.61	30.71
	48	10.39	39.45	2.79	0.56	0.33	26.26	30.61
	64	9.62	37.80	2.46	0.84	0.34	27.83	30.74
	80	9.35	37.86	2.24	0.66	0.34	28.26	30.66
	96	8.22	36.15	2.58	0.93	0.35	29.43	30.57
	112	7.36	35.02	2.63	0.82	0.34	30.45	30.73
	128	7.50	34.99	2.76	1.25	0.30	30.40	30.30
ABMOR	0	90.41	78.94	5.41	0.11	2.08	6.85	6.61
	16	68.71	78.06	6.06	0.22	1.61	7.42	6.62
	32	54.03	77.79	6.04	0.27	1.48	7.68	6.74
	48	45.51	79.10	4.93	0.25	1.27	7.78	6.66
	64	40.24	77.09	5.37	0.20	1.24	8.74	7.37
	80	34.89	76.08	5.01	0.36	1.33	9.52	7.70
	96	33.02	76.97	4.80	0.20	1.15	9.26	7.63
	112	29.76	76.43	4.79	0.20	1.16	9.71	7.71
	128	26.51	76.12	4.48	0.42	1.19	10.01	7.79

Table B-2 MBOH conversions and product selectivity over composite NaMOR-MCM-41
after activated temperature at 350 °C for 8 h under a N2-gas and reaction temperature at
180 °C.

Sample	Time (min)	% Conversion of MBOH	% Selectivity					
			Acidic site		Amphoteric site		Basic site	
			MBYNE	Prenal	HMB	MIPK	Acetone	Acetylene
NaMOR-MCM41-1M	0	84.16	77.06	4.89	0.17	1.12	7.03	9.73
	16	46.63	71.72	4.72	0.15	0.81	10.57	12.02
	32	33.19	68.69	4.40	0.21	0.77	12.43	13.51
	48	26.84	66.95	4.16	0.46	0.79	13.54	14.11
	64	22.72	66.33	3.93	0.28	0.69	14.15	14.61
	80	21.08	64.01	3.99	0.56	0.77	15.36	15.32
	96	19.05	64.31	3.71	0.33	0.63	15.44	15.58
	112	17.44	63.44	3.69	0.50	0.63	15.91	15.84
	128	15.96	62.95	3.64	0.50	0.62	16.40	15.89
NaMOR-MCM41-2M	0	83.50	71.49	3.98	0.17	0.52	10.64	13.20
	16	57.99	71.58	4.40	0.22	0.50	10.91	12.39
	32	45.46	71.17	4.61	0.28	0.55	11.24	12.16
	48	39.54	71.49	4.43	0.30	0.49	11.36	11.94
	64	34.24	71.39	4.50	0.34	0.50	11.48	11.79
	80	31.37	71.00	4.47	0.38	0.51	11.68	11.95
	96	29.40	71.51	4.28	0.30	0.43	11.59	11.88
	112	27.63	71.59	4.26	0.24	0.44	11.69	11.78
	128	24.86	71.29	4.43	0.26	0.45	11.79	11.78
NaMOR-MCM41-3M	0	94.08	77.36	2.50	0.06	0.31	9.10	10.68
	16	76.32	77.59	4.17	0.17	0.36	8.66	9.05
	32	63.78	77.93	4.55	0.21	0.48	8.29	8.53
	48	55.08	77.87	4.84	0.25	0.44	8.39	8.21
	64	48.19	78.08	4.81	0.26	0.43	8.40	8.02
	80	44.06	78.08	4.72	0.28	0.44	8.46	8.01
	96	40.47	78.20	4.72	0.17	0.39	8.52	8.01
	112	36.90	77.85	4.75	0.24	0.40	8.71	8.05
	128	33.85	77.26	4.79	0.36	0.48	9.00	8.11

APPENDIX C

CALCULATION FOR PHENOL HYDROXYLATION

Calculation for phenol conversion

The conversion was calculated as follows;

$$X_{PhOH} (\%) = 100 \times ([PhOH]_i - [PhOH]_f) / [PhOH]_i$$

where

X_{PhOH} is the conversion of phenol

$[PhOH]_i$ is the mole of phenol before reaction

$[PhOH]_f$ is the mole of phenol after sampling

Calculation of product selectivity

The selectivity was calculated as follows:

Product selectivity $(\%) = 100 \times [product]_f/([CAT]_f + [HQ]_f + [BQ]f]_f)$,

where

$[product]_f$ is the molar concentration of catechol, and hydroquinone,

benzoquinone after the reaction.

Calibration curve of standard solution phenol, catechol, hydroquinone, and benzoquinone

The calibration curved was prepared from mixing standard of 0.30 M phenol, 0.12 M catechol, 0.12 M hydroquinone, and 0.12 M benzoquinone. Toluene was used as an internal standard because it was not converted over the catalysts. The mixing standard was diluted with ethanol to 4 concentrations. Then the phenol solutions were analyzed by GC.
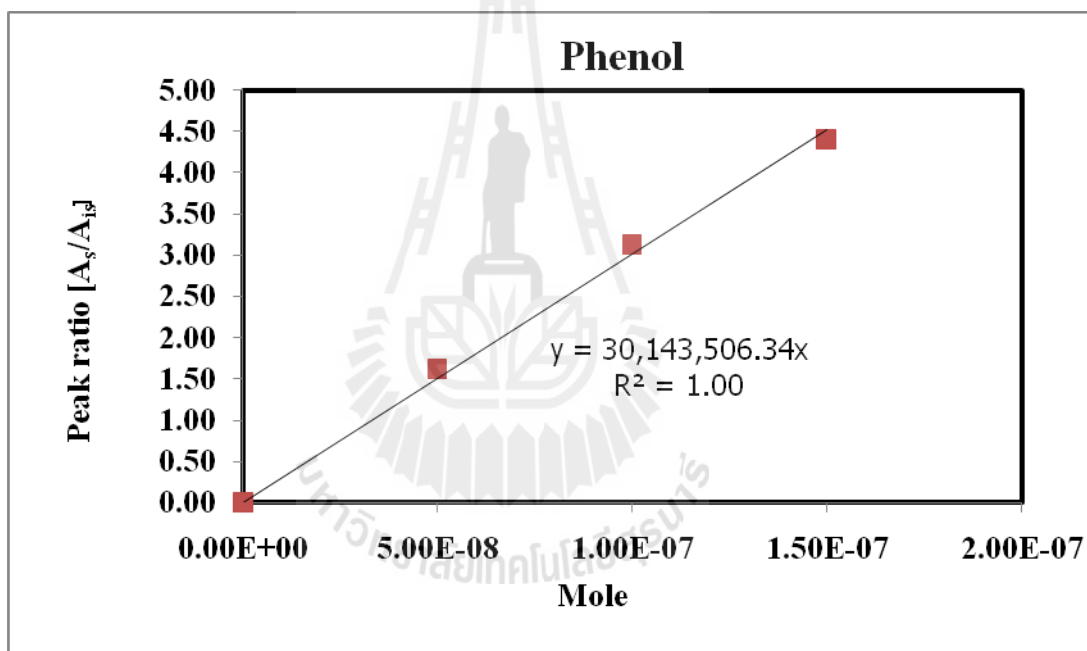
Figure C-1 Calibration curve of phenol for phenol hydroxylation.
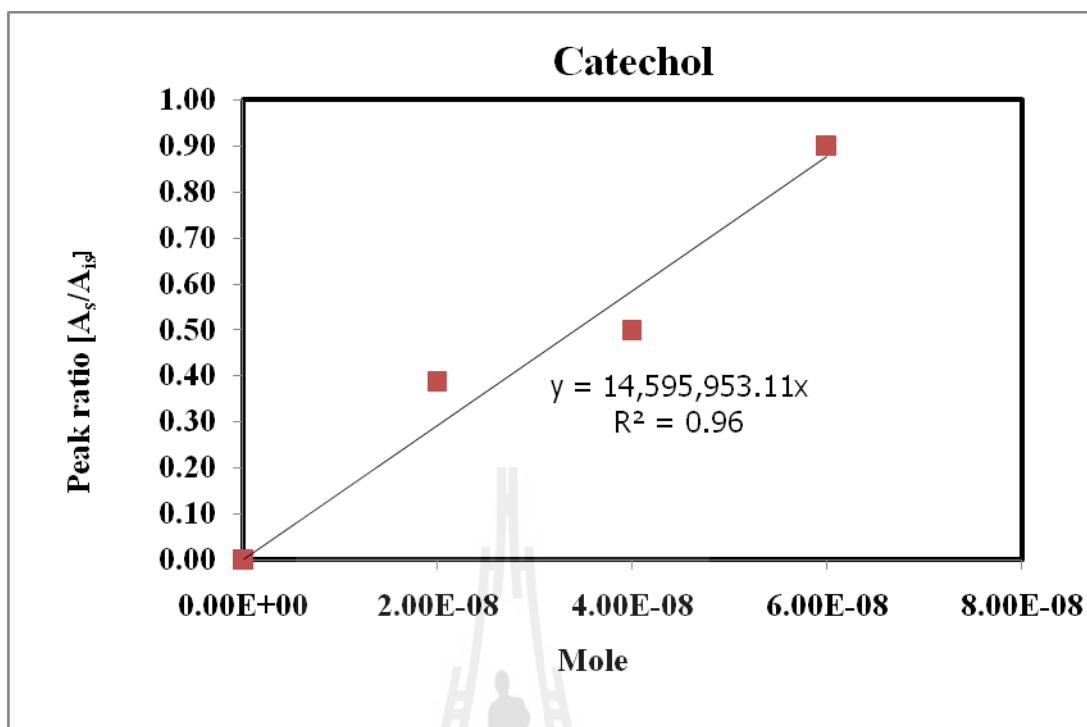
Figure C-2 Calibration curve of catechol for phenol hydroxylation.
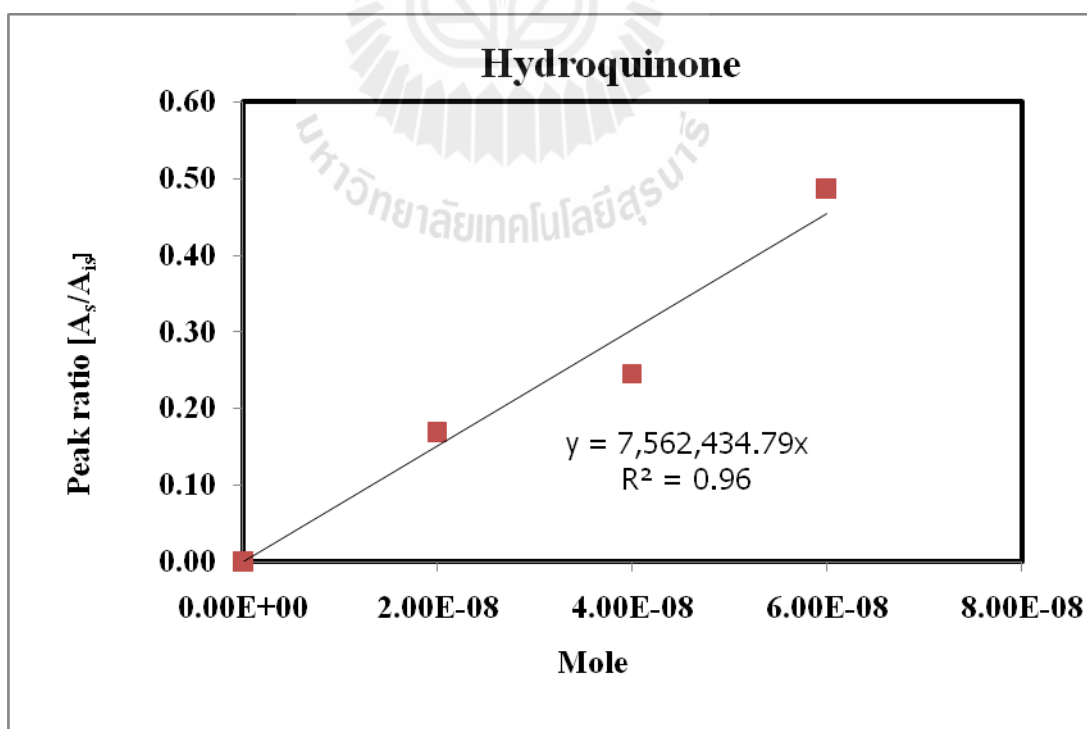
Figure C-3 Calibration curve of hydroquinone for phenol hydroxylation.
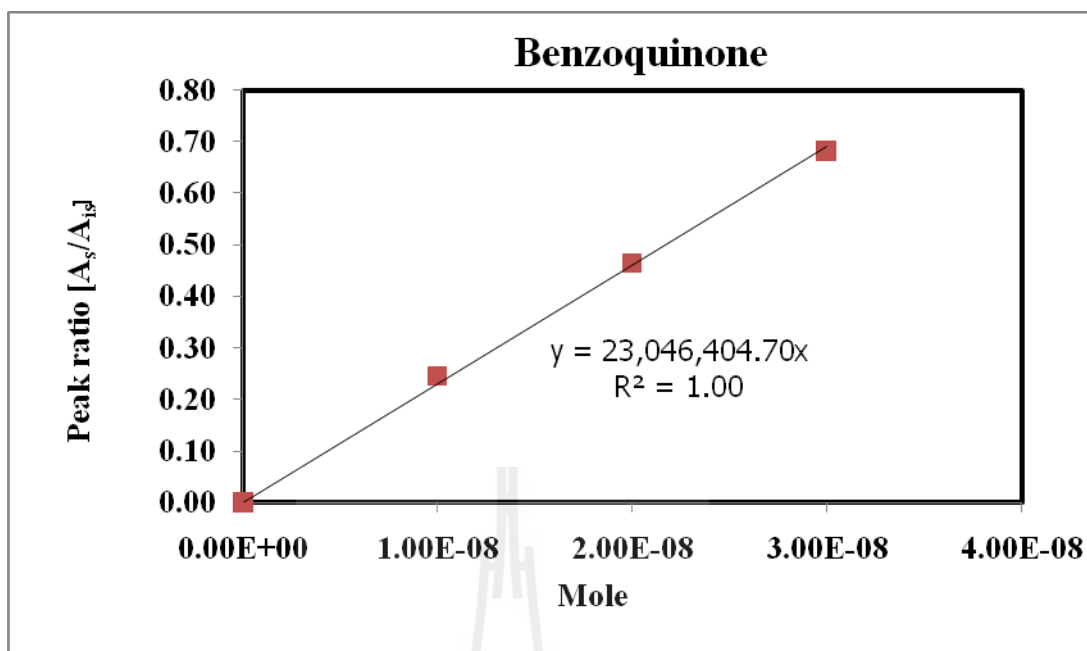
Figure C-4 Calibration curve of benzoquinone for phenol hydroxylation.

APPENDIX D
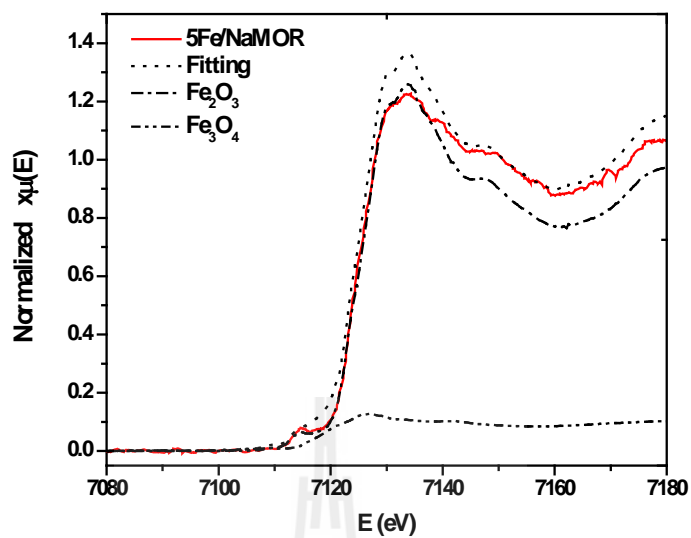
DATA FROM LINEAR COMBINATION FITTING

Figure D-1 XANES spectra and linear combination fitting of 5Fe/NaMOR showing forms
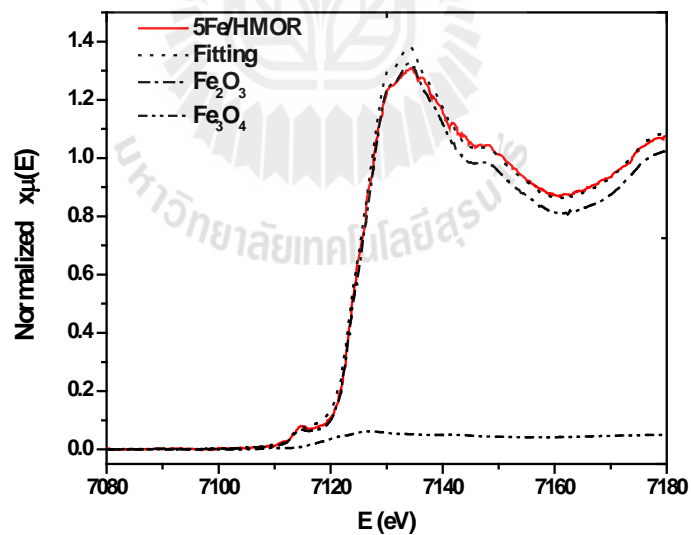
of Fe as Fe_2O_3 and Fe_3O_4.

Figure D-2 XANES spectra and linear combination fitting of 5Fe/HMOR showing forms
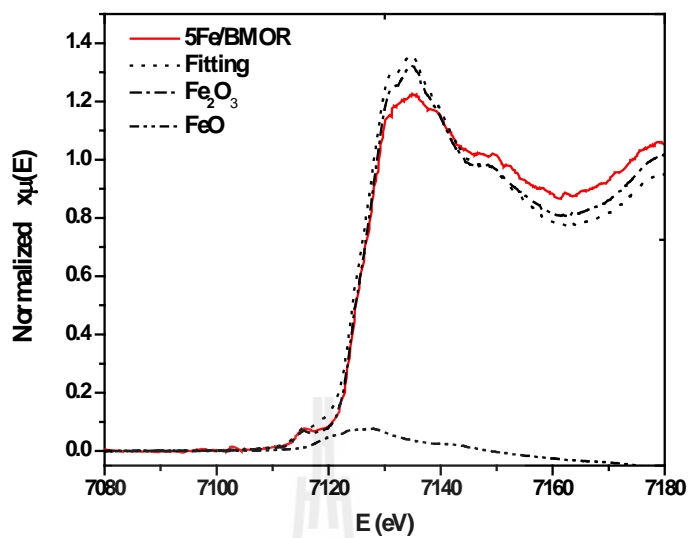
of Fe as Fe_2O_3 and Fe_3O_4.

Figure D-3 XANES spectra and linear combination fitting of 5Fe/BMOR showing forms
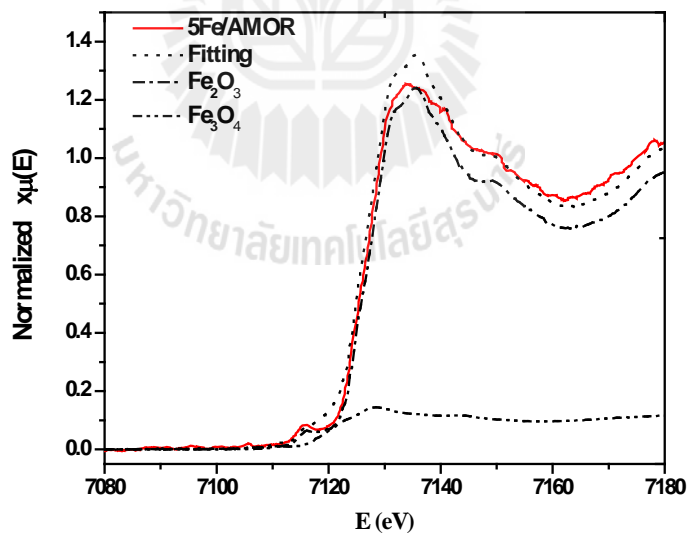
of Fe as Fe_2O_3 and Fe_3O_4.

Figure D-4 XANES spectra and linear combination fitting of 5Fe/AMOR showing forms
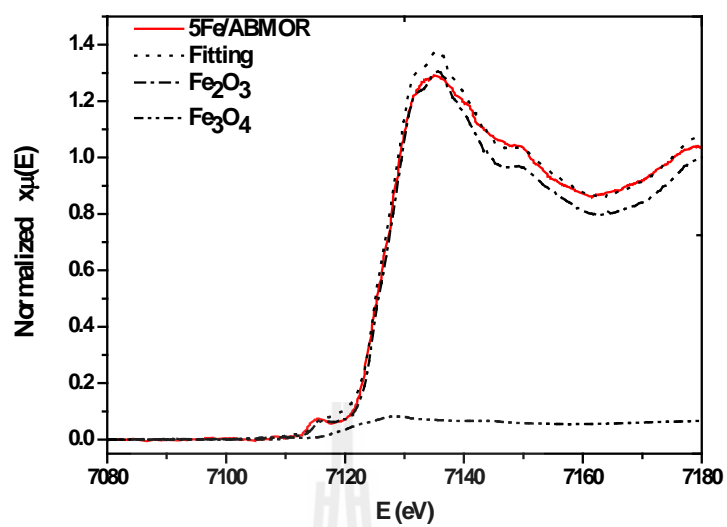
of Fe as Fe_2O_3 and Fe_3O_4.

Figure D-5 XANES spectra and linear combination fitting of 5Fe/ABMOR showing forms

of Fe as Fe_2O_3 and Fe_3O_4.

APPENDIX E

CALIBRATION CURVE OF Si AND Al AND Si/Al RATIOS OF

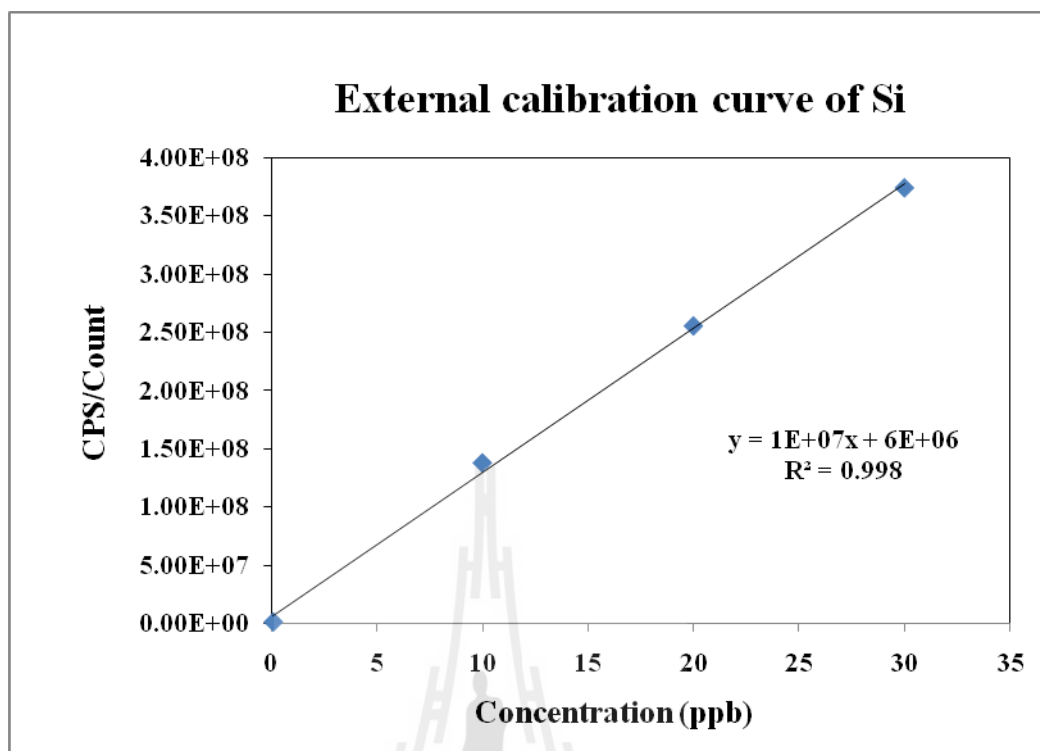**MODIFIED ZEOLITE ANALYZED BY ICP-MS**

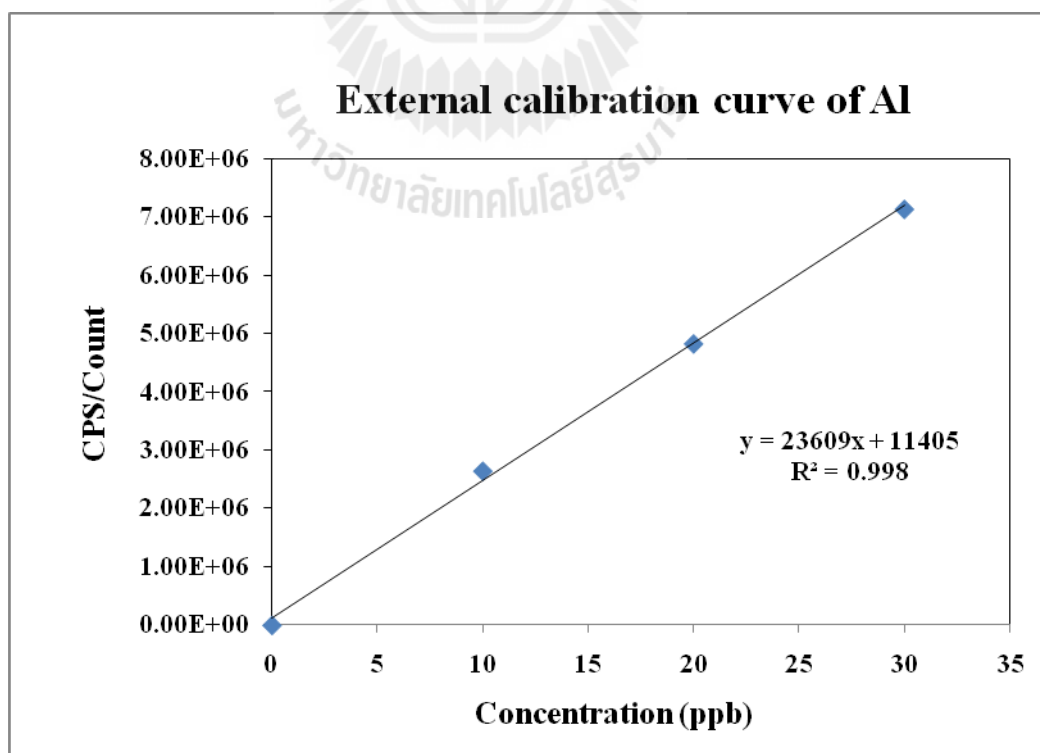**Figure E-1** External calibration curve of Si standard measured by ICP-MS.

Figure E-2 External calibration curve of Al standard measured by ICP-MS.

Table E-1 Data calculation of Si/Al ratios of modified zeolite from ICP-MS.

Samples	Preparation dilution	Amount of samples (g)	Element analysis	Conc. ppb	Amount of elements (ng)	Initial dilution 100 mL (ng)	Element in sample (g)	Mole	Si/Al
NaMOR	100,000	0.125	Si (28)	7.51E-02	7.51E+00	7.51E+03	6.00E-03	2.14E-04	10.95
		0.125	Al (27)	6.61E-03	6.61E-01	6.61E+02	5.29E-04	1.96E-05	
HMOR		0.125	Si (28)	9.08E-02	9.08E+00	9.08E+03	7.26E-03	2.59E-04	10.47
		0.125	Al (27)	8.36E-03	8.36E-01	8.36E+02	6.69E-04	2.48E-05	
BMOR		0.125	Si (28)	8.08E-02	8.08E+00	8.08E+03	6.46E-03	2.31E-04	9.54
		0.125	Al (27)	8.16E-03	8.16E-01	8.16E+02	6.53E-04	2.42E-05	
AMOR		0.125	Si (28)	7.22E-02	7.22E+00	7.22E+03	5.78E-03	2.06E-04	35.51
		0.125	Al (27)	1.96E-03	1.96E-01	1.96E+02	1.57E-04	5.81E-06	
ABMOR		0.125	Si (28)	4.33E-02	4.33E+00	4.33E+03	3.47E-03	1.24E-04	27.83
		0.125	Al (27)	1.50E-03	1.50E-01	1.50E+02	1.20E-04	4.45E-06	

CURRICULUM VITAE

Mr. SITTICHAI KULAWONG

Date of Birth   November 16th, 1981, Ubonratchatanee, Thailand

Education

2010   Research at Carl von Ossietzky University Oldenburg, Germany for 3 months (August - October)

2006 - 2008   M. Sc. Chemistry, Suranaree University of Technology, Thailand

2000 - 2004   B. Sc. Chemistry, Ubonratchatanee University, Thailand

National Presentation

Kulawong, S., Prayoonpokarach, S., Neramittagapong, A. and Wittayakun, J. (2010). Conference Proceeding, Commission on Higher Education Congress IV: University Staff Development Consortium, Pattaya Chonburi, Thailand, 14-16 September 2011 (Poster presentation).

International Presentation

Kulawong, S., Prayoonpokarach, S., Neramittagapong, A. and Wittayakun, J. (2010). Conference Proceeding, Hilton Adelaide, South Australia, 26-29 September 2010 (Poster presentation).

International Publications

Kulawong, S., Prayoonpokarach, S., Neramittagapong, A. and Wittayakun, J. (2011). **Journal of Industrial and Engineering Chemistry**. 17: 346-351.